



# CATÓLICA

UNIVERSIDADE CATÓLICA PORTUGUESA | PORTO

Escola Superior de Biotecnologia

## **A FUNDAMENTAL STUDY ON PHYSICAL PROPERTIES AND STABILITY IN FOOD SYSTEMS – THE RELATIONSHIP WITH MOLECULAR DYNAMICS**

Thesis submitted to the *Universidade Católica Portuguesa* to attain  
the degree of PhD in Biotechnology – with specialisation in Food  
Science and Engineering

By  
Joana de Freitas Salgado do Fundo Pereira

Under the supervision of Prof. Dr. Cristina L.M. Silva and  
Dr. Mafalda A.C. Quintas

**October 2014**



*Aos meus pais, ao Pedro e ao meu filho,*

*Zé Pedro.*



**ABSTRACT**

Food systems physical properties and stability are critical for delivering safe and healthy food to the consumers, and thus this is a theme that attracts food scientists for a long time. Recently, literature suggests that stability can only be fully grasped if food molecular dynamics and structure are taken into consideration, i.e. an appropriate understanding of the behaviour of food products requires knowledge of its composition, structure and molecular dynamics, through the three-dimensional arrangement of the various structural elements and their interactions.

Food systems behaviour is strongly dependent on the water molecular dynamics. Understanding changes in water location and mobility represents a significant step in food stability knowledge, once that water “availability” profoundly affects the chemical, physical and microbiological quality of foods.

Nuclear magnetic resonance (NMR), through the analysis of nuclear magnetisation relaxation times, has been presented as a powerful technique to investigate water dynamics and physical structures of foods. It provides information on molecular dynamics of different components in complex systems. The application of this technique may be very useful in predicting food systems physicochemical changes, namely texture, viscosity or water migration.

The research leading to this thesis focused on two main food systems: i) films from biological sources, for their interest as model matrices and potential for food industry; and ii) fresh-cut fruit, due to its complexity and significance in food markets.

Films from biological sources, particularly chitosan, present several applications including biodegradable packaging and edible coatings for shelf-life extension. As model food systems, films from biological sources are partially crystalline, partially amorphous, and easily reproducible materials. From a fundamental perspective, foods are mainly edible and digestible biopolymers that are also partially crystalline/partially amorphous. Despite of the wealth of information on literature, a systematic approach to understand the contribution of film forming solutions (FFS) on chitosan films physical properties, as well as the knowledge on its molecular dynamics to such properties, are still uncommon. In this thesis, the relevance of FFS composition on films properties is highlighted through the monitoring of solutions with different polymer/plasticiser ratios. Also the molecular dynamics, evaluated through NMR methodology, was analysed and compared with the films physical properties. Results demonstrated the influence of solutions polymer/plasticiser concentrations on both thermo-mechanical and water related properties. Chitosan concentration in solutions affected consistency coefficient, and this was related with differences in films water retention and structure. Plasticiser quantities used in FFS are responsible for films compositions, while polymer/plasticiser ratio determined the thickness and thus the structure of the films. NMR allows understanding the films molecular rearrangement, demonstrating that water is also an

important component in these matrices and performs differently when compared with the plasticiser. A relationship between water and plasticiser dynamics and films macroscopic properties was also observed.

Fruits are high water content products with a complex cellular structure, where water can be present in both intra and extra cellular spaces. Fresh-cut fruit, due to processing, has high metabolic rates with faster physiological and biochemical changes and microbial degradation, which results in product's colour and texture alterations. The second part of this thesis focused on fresh-cut fruits, pear and melon, which were chosen for their significantly different composition and structure. Fresh-cut fruit was monitored during 7 days of refrigerated storage conditions. Relevant quality parameters, such as colour and firmness, were analysed. Water activity ( $a_w$ ) and water molecular dynamics ( $T_2$ ), measured by a NMR technique, were also assessed throughout storage. Results demonstrated that processing and storage affected quality parameters, as was expected, but also system's water molecular dynamics. Throughout storage, it was possible to find relationships between the molecular dynamics and the quality parameters. These relationships were different for the two studied fruits, and the role of microstructure on food stability could be observed.

These studies highlight the significance and impact of molecular dynamics on physical properties and stability of foods, and also the usefulness of NMR methodology as a tool to evaluate food physical properties and stability. Therefore, NMR could provide a novel instrument to improve the knowledge of food systems, even when complex.

**Keywords**

Edible films; Fresh-cut fruit; Quality parameters; Physical properties; Microstructure; Molecular dynamics; Storage stability; NMR studies

## RESUMO

O controlo das propriedades físicas e da estabilidade dos alimentos é requisito essencial para o fornecimento de produtos seguros e saudáveis aos consumidores. Por este motivo, desde há muito tempo que o tema tem despertado a atenção e a curiosidade dos cientistas que trabalham na área alimentar.

A literatura tem vindo a sugerir que as propriedades físicas e a estabilidade só podem ser plenamente compreendidas se a dinâmica molecular e a estrutura dos alimentos for tida em consideração; ou seja, é necessário um conhecimento da composição, da estrutura e da dinâmica molecular dos sistemas alimentares, entendendo o arranjo tridimensional dos vários elementos estruturais e das suas interações.

No caso particular dos alimentos, a dinâmica molecular da água desempenha um papel fundamental no seu comportamento. A “disponibilidade” da água influencia profundamente a qualidade química, física e microbiológica dos sistemas alimentares. A compreensão das alterações na localização e mobilidade da água do sistema representa um passo significativo no conhecimento dos mecanismos que estão associados às reacções de degradação dos alimentos.

A ressonância magnética nuclear (RMN), através da análise dos tempos de relaxação da magnetização nuclear, tem sido considerada uma poderosa técnica para investigar a dinâmica da água e avaliar estruturas físicas em sistemas complexos como os alimentos. A aplicação desta técnica pode ser muito útil na previsão de alterações físico-químicas como a textura, a viscosidade ou a migração da água na matriz.

Esta tese considerou dois sistemas alimentares distintos: (i) filmes de origem biológica, pelo seu interesse como matrizes modelo e potencial para a indústria alimentar; e (ii) fruta minimamente processada, pela sua complexidade e reconhecida importância económica nos mercados de alimentos.

Os filmes com origem biológica, neste caso específico provenientes do quitosano, possuem várias aplicações industriais como é o caso das embalagens ou revestimentos comestíveis, que têm como objectivo prolongar a vida útil dos produtos. Como modelo para sistemas alimentares mais complexos têm as vantagens de: serem facilmente reprodutíveis; e tal como os alimentos, de um ponto de vista fundamental podem ser considerados biopolímeros comestíveis parcialmente cristalinos, e parcialmente amorfos. Apesar da vasta informação que existe na literatura sobre as propriedades físicas dos filmes de quitosano, uma abordagem sistemática para a identificação da contribuição das soluções formadoras do filme, assim como a influência da dinâmica molecular nessas propriedades, revela-se ainda necessária. Nesta tese, a importância da composição das soluções formadoras nas propriedades dos filmes é realçada através da monitorização de soluções formadoras com diferentes proporções polímero/plasticizante. A importância destas soluções foi avaliada

também nas alterações das propriedades termomecânicas dos filmes assim como a sua influência na dinâmica molecular dos mesmos (através de técnicas de RMN).

Os resultados demonstram que a composição das soluções formadoras influenciou as propriedades mecânicas e térmicas dos filmes, bem como as propriedades relacionadas com a água (atividade, solubilidade, permeabilidade e a dinâmica molecular). A concentração de quitosano afetou o coeficiente de consistência das soluções formadoras, o que pode ser relacionado com diferenças na estrutura e na retenção de água dos filmes. Por outro lado, a quantidade de plasticizante usado na preparação das soluções formadoras é responsável pela composição dos filmes, enquanto a razão polímero/plasticizante determinou a espessura, logo a estrutura dos filmes. Através dos estudos de RMN foi possível compreender o rearranjo molecular dos filmes, demonstrando o papel importante que a água, como componente, desempenha neste tipo de matrizes, revelando diferenças de comportamento entre esta e o plasticizante. Estes resultados revelaram ainda que existe uma relação entre a dinâmica molecular quer da água quer do plasticizante nos filmes com as propriedades macroscópicas dos mesmos.

As frutas são alimentos com uma estrutura celular muito complexa, ricos em água que pode estar presente quer nos espaços intracelulares, quer nos extracelulares. As frutas, minimamente processadas, devido ao fermento a que são sujeitas, tem altas taxas metabólicas que provocam rápidas alterações fisiológicas, bioquímicas e de degradação microbianas, resultando, por exemplo, em perda de cor e textura. A segunda parte desta tese dedica-se ao estudo de pêra e melão minimamente processados. Estas frutas são muito diferentes no que diz respeito à estrutura. As amostras foram estudadas durante 7 dias de armazenamento em condições de refrigeração. Foram avaliados alguns dos parâmetros de qualidade mais relevantes, como é o caso da cor e da textura. A atividade da água ( $a_w$ ) e a dinâmica molecular da água ( $T_2$ ), analisada através de uma técnica de RMN, foram também monitorizadas durante o tempo de armazenamento. Os resultados mostram que quer o processamento quer o tempo de armazenamento afetaram os parâmetros de qualidade, bem como a dinâmica da água nos sistemas. Observou-se ainda uma relação entre os parâmetros de qualidade e os valores da dinâmica da água. Esta relação foi diferente para os dois frutos estudados, realçando o papel da estrutura na estabilidade dos alimentos.

Nesta tese evidencia-se o interesse e a utilidade dos estudos de dinâmica molecular, utilizando a técnica de RMN como ferramenta na avaliação das propriedades físicas e da estabilidade de sistemas alimentares e complexos.

### **Palavras-chave**

Biofilmes; Fruta minimamente processada; Parâmetros de qualidade; Propriedades físicas; Microestrutura; Dinâmica molecular; Estabilidade durante armazenamento; Estudos de NMR



## ACKNOWLEDGMENTS

This PhD program and dissertation were made possible due to the contribution of institutions and special persons, to whom I would like to express my gratitude:

To Fundação para a Ciência e a Tecnologia (Portugal) for my PhD grant (SFRH/ BD / 62176 / 2009);

To Escola Superior de Biotecnologia of Universidade Católica Portuguesa for the opportunity and excellent research conditions made available for me as a PhD student;

My word of appreciation goes to my supervisor Professor Cristina L.M. Silva. She accepted to support me during this journey and accompanied me all the way. She also provided the opportunity, and encouraged me, to contact with the scientific community, through meetings attendance and collaborations, contributing for my growth as a person and researcher;

To my co-supervisor Mafalda A.C. Quintas for believing in my capabilities and in this project, for her guidance, availability, motivation, help and support over the years. Her knowledge and commitment to science were essential to my research, enriching it greatly. She sets an example of excellence and perseverance;

To Professor Gabriel Feio and Dr. Alexandra Carvalho, at Universidade Nova de Lisboa, for the opportunity to work at their laboratory, for the knowledge transfer, technical assistance, encouragement, suggestions and valuable discussions throughout the years;

To my good friends Ana Amaro and Manuela Amorim, for their invaluable friendship, for their help and company during the research experiments, for their affection, support and encouragement;

To Teresa Brandão for her friendship, affection, support and guidance during my research journey;

To my friends and research group colleagues Fátima Miller, Sara Oliveira, Inês Ramos and Bárbara Ramos. I also thank to Andrea Galvis, Lígia Pimentel and Raquel Madureira;

Thank you to Telma Delgado, Maria do Céu Selbourne, Fátima Poças, Orlanda Martins, Marta Guimarães, and Paulo Filipe: your will in helping others is an example;

My last words go to my family. This thesis is the result of their love and support. To my husband Pedro and my son Zé Pedro. Pedro sharing my life with you makes me better and stronger every day. Thank you Zé, for all the smiles that you gave in every return home from work, inspiring me to do more and better every day.

**LIST OF CONTENTS**

Abstract	V
Resumo	VII
Acknowledgments	IX
Scope and outline	XVII
List of symbols and abbreviations	XXV
List of tables	XXVII
List of figures	XXVIII

**PART I**

<b>CHAPTER 1 State of the art</b>	<b>3</b>
1.1. Overall molecular dynamics concept	5
1.2. Aspects of water molecular dynamics	7
1.2.1. Water activity concept shortcomings	9
1.2.2. Glass transition temperature	11
1.2.3. Water proton relaxation time and NMR as a powerful technique for assessing proton relaxation time	13
1.3. Food structure/ microstructure	15
1.4. Practical applications of NMR to assess molecular dynamics and structure	17
1.4.1. Edible films as food systems models	17
1.4.2. Real food matrices	18
1.5. Conclusions	22

**PART II**

<b>CHAPTER 2 Film forming solutions polymer/plasticiser ratio effect on the films properties</b>	<b>25</b>
Abstract	27
2.1. Introduction	28
2.2. Materials and methods	29
2.2.1. Chitosan film forming solution (FFS) preparation	29
2.2.2. Characterisation of FFS	30
2.2.2.1. Rheological behaviour	30
2.2.2.2. Water activity	30
2.2.3. Chitosan films preparation	30
2.2.4. Characterisation of chitosan films	31
2.2.4.1. Water activity, moisture content and solubility	31
2.2.4.2. Films barrier properties	31
2.2.4.3. Films thickness	32
2.2.4.4. Films mechanical properties	32
2.2.4.5. Films thermal properties	33
2.2.4.6. FTIR-ATR spectroscopy	33
2.2.4.7. Data analysis	34
2.3. Results and discussion	35
2.3.1. Characterisation of the FFS	35
2.3.2. Characterisation of chitosan films	38
2.3.2.1. Water and barrier properties	38
2.3.2.2. Mechanical and thermal properties	41
2.3.2.3. FTIR-ATR spectroscopy results	45
2.4. Conclusions	49

<b>CHAPTER 3 Molecular dynamics, composition and structure analysis</b>	<b>51</b>
Abstract	53
3.1. Introduction	54
3.2. Materials and methods	56
3.2.1. Chitosan films preparation	56
3.2.2. Characterisation of the chitosan films	56
3.2.2.1. Chemical composition	56
3.2.2.2. Thickness	57
3.2.2.3. Water activity	57
3.2.2.4. Nuclear magnetic relaxation	57
3.2.2.5. Microstructure	58
3.3. Results and discussion	58
3.3.1. Composition of the films	58
3.3.2. Molecular mobility	61
3.3.3. Microstructure	67
3.4. Conclusions	70
<b>CHAPTER 4 Molecular dynamics and functional properties</b>	<b>71</b>
Abstract	73
4.1. Introduction	74
4.2. Materials and methods	75
4.3. Results and Discussion	75
4.3.1. Molecular mobility versus thermal properties	76
4.3.2. Molecular mobility versus mechanical properties	79
4.3.3. Molecular mobility versus water vapour permeability	81
4.4. Conclusions	83

**PART III**

<b>CHAPTER 5 Studies on fresh-cut fruit</b>	<b>87</b>
Abstract	89
5.1. Introduction	90
5.2. Materials and methods	91
5.2.1. Fruit material, processing, packaging and storage conditions	91
5.2.2. Transverse relaxation times measurement	92
5.2.3. Microscopic techniques	92
5.2.4. Quality parameters evaluation	93
<u>Section A - Fresh-cut melon</u>	95
5A.3. Results and discussion	97
5A.3.1. Transverse relaxation times	97
5A.3.2. Microstructure analysis	99
5A.3.3. Quality parameters	101
5A.3.4. Relaxation time versus quality parameters	104
<u>Section B - Fresh-cut pear</u>	107
5B.3. Results and discussion	109
5B.3.1. Transverse relaxation times	109
5B.3.2. Microstructure analysis	111
5B.3.3. Quality parameters	113
5B.3.4. Relaxation time versus quality parameters	116
5.4. Conclusions	118

**PART IV**

**CHAPTER 6 General discussion** **121**

6.1. General conclusions 123

6.2. Future prospects 126

**REFERENCES** **127**

**APPENDICES**

Appendix A A1

Appendix B B1

Appendix C C1





## **SCOPE AND OUTLINE**

Food physical properties are critical for product and process design, safety and sensorial attributes and contribute to food stability. Stability is a critical parameter for both consumers and industry. Concerning consumers, it assures safety, nutritional and sensorial quality of food products. For industry, stability allows maximising shelf-life: minimising waste along the distribution chain, increasing profit and reducing the environmental impact.

For a long time scientists believed that  $a_w$  was the determinant parameter in food stability and physical properties. This concept was challenged with the revolutionary approach to the study of food systems using the glass transition concept. Recently, scientific research suggests that water molecular dynamics is a fundamental approach to fully attain food physical properties and stability. Food water content, location and interactions with other components are critical in microbial growth, degradation reactions and sensorial aspects.

This dissertation aims to contribute at clarifying the influence of systems molecular dynamics, with particular relevance on water molecular dynamics. Thus, this project addresses studies on matrices with different complexities, i.e. films from biological sources, and fruits as more complex high water content products. Micro and macroscopic behaviour will be analysed, by means of assessing texture, dynamic linear viscoelastic behaviour and thermodynamic transitions. Molecular mobility will be evaluated by means of NMR.

### **Outline of dissertation structure**

This dissertation is divided into 4 main parts, each with a variable number of chapters. Figure 0.1 presents schematically the dissertation structure, illustrating the relationships between each subject.

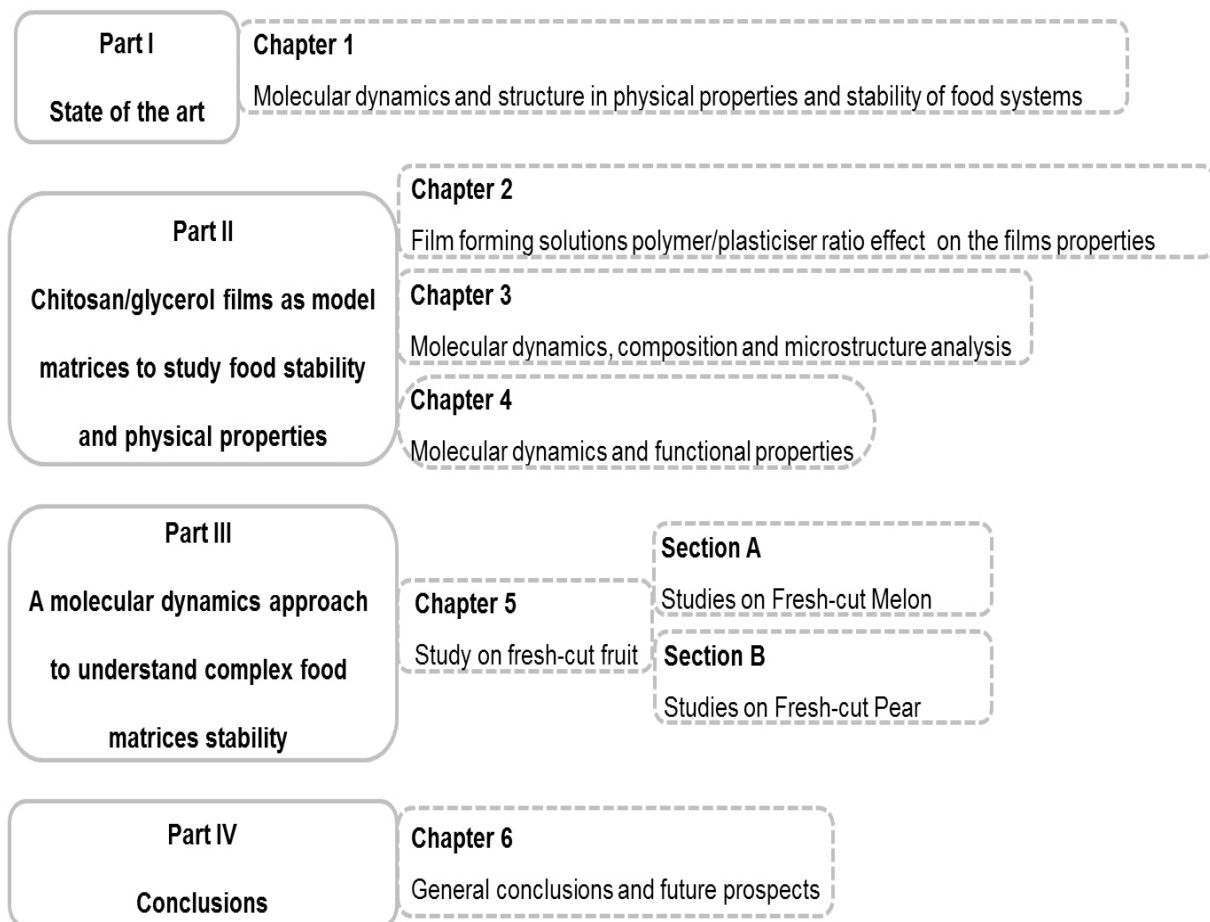


**Figure 0.1** Schematic structure of the dissertation.

Part I, the introductory section, is composed by chapter 1 dedicated to a review of the critical factors affecting the physical properties and stability of food systems, identifying water as a critical component, considered as the main factor in systems dynamics.

In Part II, studies on the relationship between composition, microstructure, functional properties and molecular dynamics of simple food matrices were developed. This part was divided into 3 chapters. Films from biological sources were chosen, in particular chitosan films. Chitosan, a natural polysaccharide obtained by deacetylation of chitin, is an excellent edible film component due to its film-forming capacity, good mechanical and barrier properties and antimicrobial activity. Physical behaviour is vital for proper film functionality and is also critical for product and process design. Critical physical properties are water, gas and other molecules diffusion through the film and thermal-mechanical properties. Studies on the formulation and processing effects on chitosan films physical behaviour have been long presented in the literature. However, results on molecular mobility in films are less common. The novelty of this work is that gathering such data was carried using a systematic approach, linking physical properties with NMR results on molecular mobility. In chapter 2, the FFS polymer/plasticisant ratio was analysed in order to describe its effect on films properties. In both chapters 3 and 4, data on molecular mobility of the films, previously characterised, was measured, by means of NMR. Water related properties, in chapter 3, and physical properties, in chapter 4, were compared with the molecular dynamics measurements.

Part III is dedicated to the study of fresh-cut fruit, along refrigerated storage time. Fruits are high water content products. Due to their cellular structure, water can be presented in both intra and extra cellular spaces. This influences the water

dynamics. Specifically, fresh-cut fruits are interesting matrices for these studies, since it is well known that fruits processing promotes a faster physiological deterioration, biochemical changes and microbial degradation, which may result in degradation of overall perceived quality. The observed chemical and physical changes could certainly be clarified by systems molecular dynamics and structure alterations, and monitoring with the support of NMR techniques. The purpose of this part of the thesis was to relate, for fresh-cut melon and pear, NMR parameters with some of the most important quality parameters, i.e. colour, softening rate and  $a_w$ . Chapter 5 - section A focuses on fresh-cut melon, while chapter 5 - section B is about fresh-cut pear. Melon and pear represent important segments in the world of fruit market. However, the biochemical bases for colour and firmness changes, for example, are completely different, as well as their structures.

Finally, conclusions and suggestions for further work, based on critical questions arising from this dissertation, are presented in chapter 6 (Part IV).

### **Scientific outputs of dissertation**

The work reported in this dissertation has been already subjected to international peer reviewing via publication in international referred journals as indicated by the list below. Furthermore, the research work has been presented to the scientific community in both national and international meetings.

## Publications

### Refereed in international scientific publications

Joana F. **Fundo**, Rui Fernandes, Pedro M. Almeida, Alexandra Carvalho, Gabriel Feio, Cristina L.M. Silva, Mafalda A.C. Quintas (2014). Molecular mobility, composition and structure analysis in glycerol plasticised chitosan films, *Food Chemistry*, 144, 2-8.

Joana F. **Fundo**, Ana L. Amaro, Ana Raquel Madureira, Alexandra Carvalho, Gabriel Feio, Cristina L.M. Silva, Mafalda A.C. Quintas. Fresh-cut melon quality during storage: a NMR study of water transverse relaxation time. *Journal of Food Engineering*. Accepted with minor revisions.

Joana F. **Fundo**, Cristina L.M. Silva, Mafalda A.C. Quintas. Molecular dynamics and structure in physical properties and stability of food systems. *Food Engineering Reviews*, Submitted (FERE-D-14-00068, 01 August 2014).

Joana F. **Fundo**, Andrea C. Galvis-Sanchez, Ivonne Delgadillo, Cristina L.M. Silva, Mafalda A.C. Quintas. The effect of polymer/plasticiser ratio in film forming solutions on the properties of chitosan films. *Food Biophysics*, Submitted (FOBI-D-14-00104, 30 June 2014).

Joana F. **Fundo**, Alexandra Carvalho, Gabriel Feio, Cristina L.M. Silva, Mafalda A.C. Quintas. Relationship between molecular mobility, microstructure and functional

properties in chitosan/glycerol films. Innovative Food Science and Emerging Technologies, Submitted (IFSET-D-14-00315, 02 July 2014).

Joana F. **Fundo**, Andrea C. Galvis-Sanchez, Ana Raquel Madureira, Alexandra Carvalho, Gabriel Feio, Cristina L.M. Silva, Mafalda A.C. Quintas. A NMR water transverse relaxation time approach to understand storage stability of fresh-cut pear. Innovative Food Biophysics, Submitted (FOBI-D-14-00129, 02 October 2014).

*Non-Refereed in conference proceedings*

Joana F. **Fundo**, Mafalda A.C. Quintas, Cristina L.M. Silva (2011). Influence of film forming solutions on properties of chitosan/glycerol films. Conference proceedings of 11<sup>th</sup> International Congress on Engineering and Food, Athens, 22-26 May.

**Communications**

*Oral communications*

Joana F. **Fundo**, Mafalda A.C. Quintas, Cristina L.M. Silva (2012). Molecular mobility and the thermomechanical properties of chitosan films. Presented orally at 7<sup>th</sup> International Conference on Water in Food, Helsinki, 3-5 June.

*Poster Communications*

Joana F. **Fundo**, Mafalda A.C. Quintas, Cristina L.M. Silva (2011). Influence of film forming solutions on properties of chitosan/glycerol films. Poster presented at 11<sup>th</sup> International Congress on Engineering and Food, Athens, 22-26 May.

Joana F. **Fundo**, Pedro M. Almeida, Alexandra Carvalho, Mafalda A.C. Quintas, Gabriel Feio, Cristina L.M. Silva (2011). A NMR approach to understand water behaviour on chitosan/ glycerol films. Poster presented at 2<sup>nd</sup> International ISEKI\_Food Conference, Milan, 31 August - 3 September.

Joana F. **Fundo**, Cristina L.M. Silva, Mafalda A.C. Quintas (2013). Molecular mobility, crystallinity and barrier properties of chitosan film. Poster presented at 1<sup>st</sup> Sao Paulo School of Advanced Sciences on Advances in Molecular Structuring of Food Material, Pirassununga, 3-5 April.

Joana F. **Fundo**, Pedro M. Almeida, Alexandra Carvalho, Gabriel Feio, Cristina L.M. Silva, Mafalda A.C. Quintas (2014). A NMR contribute to understand fresh-cut melon behaviour during storage. Poster presented at 3<sup>rd</sup> International ISEKI\_Food Conference, Athens, 20-23 May. Received "Elsevier Award"





**LIST OF SYMBOLS AND ABBREVIATIONS***Symbols*

$a^*$	colour space co-coordinate (degree of greenness/redness)
$A$	area ( $\text{m}^2$ )
$A_1$	water population
$A_2$	glycerol population
$a_w$	water activity
$b^*$	colour space co-coordinate (degree of blueness/yellowness)
EB	elongation at break (%)
$K$	consistency coefficient ( $\text{Pa s}^n$ )
$L^*$	colour space co-coordinate (degree of lightness)
MC	moisture content (%)
$n$	flow index (dimensionless)
$O_2P$	oxygen permeability ( $\text{g Pa}^{-1} \text{m}^{-1} \text{s}^{-1}$ )
SOL	solubility in water (%)
$t$	time (s)
$T_2$	relaxation time (ms)
$T_g$	glass transition temperature ( $^{\circ}\text{C}$ )
$T_m$	melting temperature ( $^{\circ}\text{C}$ )
TS	tensile strength (MPa)
$w$	weight loss (g)
WVP	water vapour permeability ( $\text{g Pa}^{-1} \text{s}^{-1} \text{m}^{-1}$ )
$x$	thickness (mm)
$\Delta h$	melting enthalpy ( $\text{J g}^{-1}$ )
$\Delta P$	difference of partial vapour pressure (Pa)

$\sigma$  shear stress (Pa)

$\dot{\gamma}$  shear rate ( $s^{-1}$ )

*Abbreviations*

a.u. arbitrary units

Chit chitosan

FFS film forming solutions

Gly glycerol

TCD total colour difference

**LIST OF TABLES**

<b>Table 2.1</b>	Experimental results for the characterization of film forming solutions	<b>36</b>
<b>Table 2.2</b>	Experimental results for chitosan films water related properties	<b>39</b>
<b>Table 2.3</b>	Experimental values for films mechanical and thermal characterisation	<b>42</b>
<b>Table 3.1</b>	Composition and thickness of the films obtained using different polymer/plasticiser percentages in film forming solution	<b>60</b>
<b>Table 4.1</b>	Polymer/plasticiser/water composition and thickness of films produced with different formulations	<b>76</b>

## LIST OF FIGURES

<b>Figure 0.1</b>	Schematic structure of the dissertation.	<b>XVIII</b>
<b>Figure 1.1</b>	Schematic representation of molecular dynamics as a key factor for food physical properties and stability assessment.	<b>6</b>
<b>Figure 1.2</b>	Viscosity versus water activity ( $a_w$ ) of model solutions produced with different solutes (Anese et al., 1996).	<b>11</b>
<b>Figure 1.3</b>	Representation of glass transition temperature ( $T_g$ ) effects on structural transformation and diffusion-controlled changes in biological food systems (Roos, 1998).	<b>12</b>
<b>Figure 1.4</b>	Distribution of transverse water proton relaxation times in fresh and freeze-thawed apple tissues (Hills and Remigereau, 1997).	<b>19</b>
<b>Figure 1.5</b>	Banana proton transverse relaxation time, during seven days of storage (Raffo et al., 2005).	<b>21</b>
<b>Figure 2.1</b>	Oxygen permeability of films prepared with different chitosan and glycerol concentrations (■ 1%, □ 2%; ● 3% chitosan).	<b>41</b>
<b>Figure 2.2</b>	Glass transition temperature ( $T_g$ ) (a) and melting temperature ( $T_m$ ) (b) of the chitosan films prepared with different chitosan/glycerol concentrations (■ 1%, □ 2%; ● 3% chitosan).	<b>44</b>
<b>Figure 2.3</b>	Results obtained from FTIR measurements: a) FTIR measurements with different chitosan/glycerol percentage, b) representation of the scores resulting from PCA model applied to the films with different chitosan/glycerol percentages (1-1%, 2-2% and 3-3% of chitosan) and c) PC1 and d) PC2 loading profiles plots of films according their chitosan/glycerol composition.	<b>46</b>

- Figure 3.1** Proton multi-echo acquisition of a chitosan/glycerol sample with a CPMG multi-pulse sequence. The echo envelope is bi-exponential, with a fast and a slow decay of the transverse nuclear magnetism. **62**
- Figure 3.2** Films relaxation time ( $T_2$ ) for water molecules as function of different chitosan and glycerol concentrations (a) and for the ratio chitosan/glycerol in the films (b). Results grouped films of the same final thickness: produced with ■ 1%, □ 2% and ● 3% chitosan in the film forming solutions. **63**
- Figure 3.3** Films relaxation time ( $T_2$ ) for water molecules as a function of water content (a) and *water activity* (b). Results grouped by films of same final composition: produced with 10 % glycerol solution (white bullets) and 90 % glycerol solution (black bullets). Samples prepared with 50% of glycerol are not shown because of the deviant behaviour (antiplasticisation), which impairs the data analysis. **65**
- Figure 3.4** Films relaxation time ( $T_2$ ) for glycerol molecules of: a) different chitosan and glycerol concentration, and b) glycerol content ( $\text{mg g}^{-1}\text{film}$ ). Films produced with ■ 1%, □ 2% and ● 3% chitosan in the film forming solutions, each group corresponding to thickness of the obtained film. Again, antiplasticised samples are not shown. **66**
- Figure 3.5** TEM micrographs of the films produced with different polymer/plasticiser concentrations. **68**
- Figure 4.1** Films water (a) and glycerol (b) relaxation time ( $T_2$ ), at room temperature, as a function of glass transition temperature ( $T_g$ ). Empty symbols correspond to thinnest films (range between 0.0556 and 0.0642 mm); fill symbols correspond to thickest films (range between 0.2348 and 0.2844 mm). Different data points symbols indicate the different compositions (see Table 4.1) ○/●- 388.13 Chit and 13.10Gly; □/■- 188.88 Chit and 38.93Gly; △/▲ -176.96 Chit and 50.60Gly **77**

**Figure 4.2** Films water (a) and glycerol (b) relaxation time ( $T_2$ ), as a function of films melting enthalpy ( $\Delta h$ ). Empty symbols correspond to thinnest films (range between 0.0556 and 0.0642 mm); fill symbols correspond to thickest films (range between 0.2348 and 0.2844 mm). Different data points symbols indicate the different compositions (see Table 4.1). **78**

○/●- 388.13 Chit and 13.10Gly; □/■- 188.88 Chit and 38.93Gly; △/▲ -176.96 Chit and 50.60Gly

**Figure 4.3** Films water and glycerol relaxation time ( $T_2$ ) as a function of EB (respectively Figure 4.3a and b) and TS (respectively Figure 4.3c and d). Empty symbols correspond to thinnest films (range between 0.0556 and 0.0642 mm); fill symbols correspond to thickest films (range between 0.2348 and 0.2844 mm). Different data points symbols indicate the different compositions (see Table 4.1). **80**

○/●- 388.13 Chit and 13.10Gly; □/■- 188.88 Chit and 38.93Gly; △/▲ -176.96 Chit and 50.60Gly

**Figure 4.4** Films water (a) and glycerol (b) relaxation time ( $T_2$ ) as a function of water vapour permeability (WVP). Empty symbols correspond to thinnest films (range between 0.0556 and 0.0642 mm); fill symbols correspond to thickest films (range between 0.2348 and 0.2844 mm). Different data points symbols indicate the different compositions (see Table 4.1). **81**

○/●- 388.13 Chit and 13.10Gly; □/■- 188.88 Chit and 38.93Gly; △/▲ -176.96 Chit and 50.60Gly

**Figure 4.5** Samples crystallinity ( $\Delta h$ ) as function as water vapour permeability (WVP). Empty symbols correspond to thinnest films (range between 0.0556 and 0.0642 mm); fill symbols correspond to thickest films (range between 0.2348 and 0.2844 mm). Different data points symbols indicate the different compositions (see table 4.1.). **82**

○/●- 388.13 Chit and 13.10Gly; □/■- 188.88 Chit and 38.93Gly; △/▲ -176.96 Chit and 50.60Gly

**Figure 5A.1** Distribution of water relaxation time ( $T_2$ ) in fresh-cut melon measured at 300 MHz and room temperature. **98**

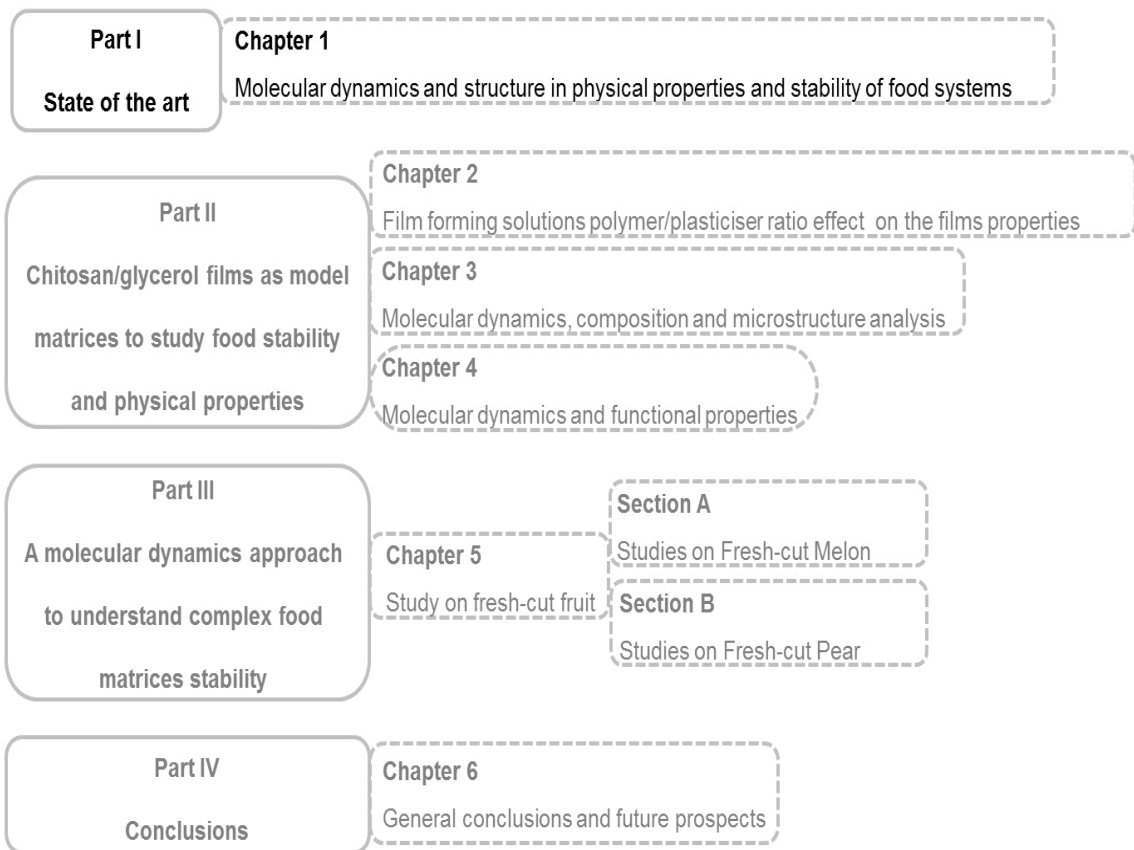
- 
- Figure 5A.2** Light and scanning electron microscope images of fresh-cut melon, at different days of storage. (A-cellular wall; B-cellular organelles; C-chloroplasts; D-plasmalemma). **101**
- Figure 5A.3** Fresh-melon quality parameters: a) total colour difference (TCD), b) firmness, and c) water activity ( $a_w$ ), during 7 days of storage. Vertical bars present the mean standard error. **102**
- Figure 5A.4** Fresh-cut melon relaxation time ( $T_2$ ) as function of a) total colour difference (TCD), b) firmness, and c) water activity ( $a_w$ ) **105**
- Figure 5B.1** Distribution of transverse water proton relaxation times ( $T_2$ ) in fresh-cut pear measured at 300 MHz and room temperature **111**
- Figure 5B.2** Light and scanning electron microscope images of fresh-cut pear, at different days of storage. (A-cellular wall; B-sclereids; C-cellular organelles; D-plasmalemma) **112**
- Figure 5B.3** Fresh-pear quality parameters: a) total colour difference (TCD), b) firmness, and c) water activity ( $a_w$ ), during 7 days of storage. Vertical bars present the mean standard error **115**
- Figure 5B.4** Fresh-cut pear relaxation time ( $T_2$ ) as function of a) total colour difference (TCD), b) firmness, and c) water activity ( $a_w$ ) **117**





# PART I

---





# **CHAPTER 1**

State of the art

---



### **1.1. Overall molecular dynamics concept**

Molecular dynamics has been pointed as the actual most promising parameter for characterising multi-component systems. Analysis of systems at a molecular scale has been demonstrated to be an useful methodology for investigating complex geometries and molecules, as well as study structural and dynamic properties (Wang and Liapis, 2012).

Molecular dynamics involves, at a microscopic level, the displacement of reactants towards with other within the food matrix, which promote chemical reactions. Macroscopically, molecular dynamics can be related to the viscosity of the material, which in turn controls the flow properties, structure collapse, mechanical properties, and thus the product texture (Roudaut et al., 2004).

It is generally accepted that the knowledge of molecular dynamics is determinant for assessing physico-chemical and microbiological stability of food systems (Lin et al., 2006; Roudaut et al., 2004), and is quite dependent on composition and matrices microstructure.

Food stability is a critical parameter for different stakeholders. Concerning consumers, stability assures safety, nutritional and sensorial quality of food products and answers to the increasing demand for a diversity of ready-to-eat food with fresh appearance and health-promoting properties (Olsen et al., 2010). For industry, stability allows maximizing shelf-life: minimising waste along the distribution chain, increasing profit, and reducing the environmental impact (Labuza et al., 1972; Rahman, 2006, 2010; Ubbink and Kruger, 2006).

Food physical stability is assessed by shelf-life changes of mechanical, thermal, or surface properties, which are often related with food product's quality, processing behaviour or development of novel food products and processes (Berk, 2013; Lewicki, 2004). Physicall state is directly affected and responsible for the molecular dynamics of a matrix (Ludescher et al., 2001; Quintas et al., 2010).

It is possible to observe in Figure 1.1 a simplified scheme of how molecular dynamics covers several concepts related to food properties and stability, being a key and linking factor between all aspects involved in food systems assessment, including food structure/microstructure. The better understanding of these factors and relationship between them are essential for controlling degradation reaction rates and maintaining food integrity (Rahman, 2006).

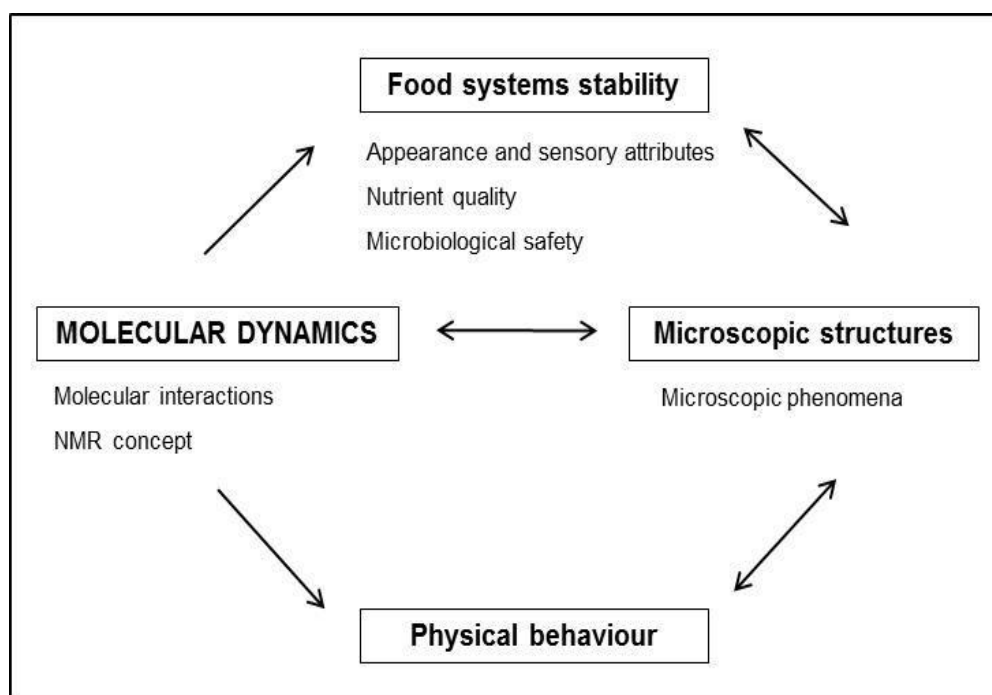


**Figure 1.1** Schematic representation of molecular dynamics as a key factor for food physical properties and stability assessment.

Food systems are complex mixtures of water, biopolymers (proteins and polysaccharides), low-molecular weight ingredients (minerals, sugars, surfactants, etc.), and colloid particles (oil droplets or air bubbles). The molecular dynamics between these different components reflects on the stability of such systems, determining the physical state, microstructure and composition, which impacts on food characteristics (Roos, 1995). Water, as one of the most important food constituents

and its interactions with other food ingredients, controls both thermodynamic and dynamic properties of all aqueous elements (Roudaut et al., 2004). These interactions affect mainly appearance and sensory attributes (texture/firmness) (Palzer, 2010; Toivonen and Brummel, 2008; Watada and Qi, 1999), nutrient quality (Watada and Qi, 1999), and the microbiological load (Kou et al., 1999). The extensions of the reactions between food constituents, usually associated with metabolic processes, are responsible for the degradation of quality, safety and nutritional attributes.

Although molecular dynamics has been considered an useful methodology for investigating complex systems (geometries and molecules) (Wang and Liapis, 2012) and the degradation reactions extension, a high number of studies have been focused on chemically pure or homogeneous materials, such as proteins or polysaccharides, instead of food systems. The data for “pure and simple” systems cannot be extrapolated when considering food systems, since it is necessary to take into account the heterogeneity of the systems, as well as their interactions with water (Roudaut et al., 2004). Moreover, it is important to consider the system’s microstructure, to understand the spatial and molecular distribution of water within its food matrix environment and determine if water is already bound or free for metabolic reactions.

## **1.2. Aspects of water molecular dynamics**

Water is the most important solvent, dispersion medium and plasticiser in biological and food systems (Matveeva et al., 2000). It affects reactions, can be a substrate and a product of reactions, and is involved in nutrient transport and dissolution of salts and other solutes. It establishes pH, acts as a polymer plasticiser and modulates viscosity, osmotic pressure, etc. (Vittadini et al., 2005). Specifically,

the state of water in food influences physical properties, such as rheological, electrical, optical, thermal or mass transfer (Lewicki, 2004).

For long, water has been considered as one of the most important food components in impacting food physicochemical and microbiological attributes, shelf-life and deteriorative changes (Hills et al., 1996a; Labuza, 1977; Labuza et al., 1972; Lewicki, 2004; Mathlouthi, 2001; Pittia and Sacchetti, 2008; Rahman, 2010; Sablani et al., 2007; Slade and Levine, 1991). Therefore, determination of water content is one of the most frequent analyses in the food industry laboratories (Mathlouthi, 2001). Water content of food systems normally ranges from 80-95%, for high moisture foods, to a percentage close to zero in semi-dry and dry foods (Anese et al., 1996; Pittia and Sacchetti, 2008). However, various foods with the same water content differ in stability (Kou et al., 1999), which demonstrates that the sole value of “water content” in a food does not inform about the nature of water (Fennema, 1996; Kou et al., 1999; Mathlouthi, 2001). In fact, in a food matrix, water molecules can be “bound” to other constituents or “free” to participate in degradation reactions (Mathlouthi, 2001).

The knowledge of each of these fractions is important, specifically because available water, its location, and the interactions with the other food components (like proteins and polysaccharides) are responsible for the physicochemical and microbiological properties and stability of foods (Matveeva et al., 2000; Sablani et al., 2007). As such, besides water content in a food material, it is important to understand the water state and dynamics for a proper comprehension of properties and stability of food products.

Water mobility/dynamics can thus be described as a manifesto of how “freely” water molecules can participate in reactions or how easily water molecules diffuse to the reaction sites to participate in reactions (Ruan and Chen, 1998). Presence of molecules of different molecular weight and solubility in water can have a profound influence on water mobility/dynamics, as this is dependent on the physicochemical



properties of other nonaqueous food constituents and their interactions with water and among themselves (Ruan and Chen, 1998; Vittadini et al., 2003).

Different parameters have been used in the literature to describe water dynamics in the food systems and its repercussion in stability: like water activity ( $a_w$ ), glass transition temperature ( $T_g$ ) or water relaxation time ( $T_2$ ). These concepts are detailed in the next sub-sections.

### ***1.2.1. Water activity concept and shortcomings***

Water activity concept was introduced in middle of 20<sup>th</sup> century as a critical parameter for estimating food stability (Rahman, 2010), and has been one of the most widely used to determine food's water availability (Kou et al., 1999). For a long time,  $a_w$  was regarded as the most important parameter controlling the behaviour of foods during processing and storage, with particular emphasis on its effects on reaction degradation rates (Anese et al., 1996; Labuza, 1977; Maltini et al., 2003; Sablani et al., 2007). This parameter has been used thoroughly as the indicator for microbial growth and microbial stability of a food system (Vittadini and Chinachoti, 2003). Also, with respect to most of degradation reactions of a chemical, enzymatic, or physical nature, such as lipid oxidation, non-enzymatic and enzymatic activities, and the texture/mouthfeel of foods following production, water activity is currently used as an important parameter (Maltini et al., 2003; Sablani et al., 2007; Slade and Levine, 1991).

Despite of the irrefutable significance of  $a_w$  for food science and engineering, the limitations of this analysis are, actually, evident. Water activity is a thermodynamic measure of the chemical potential of water in the system, assuming that food is in equilibrium with the surrounding atmosphere (Lewicki, 2004). However, it is well known that most foods are not in the state of equilibrium (Hills et al., 1996a; Rahman, 2006). Water activity measurements may not provide, for example, the relationship of

the evolution of the structural changes of the food material with the changes of the water-macromolecules and water-water interactions that occur during food shelf-life (Wang and Liapis, 2012). Studies have stressed that under many common circumstances, the thermodynamics activity of water is far less relevant to processing and storage than structure-related properties, which can restrict the mobility and diffusion of the reactants (Anese et al., 1996; Slade and Levine, 1991).

Moreover, the  $a_w$  analysis does not consider microstructure nor the possibility that there may be local regions differing in water content and presumably in water availability (Hills et al., 1996a). This can be important for microbiological stability, since some authors (Hills et al., 1996b; Hills et al., 1997; Vittadini et al., 2005) demonstrated that microorganisms are sensitive to the local properties of the system, i.e. local water activity, translational motions and microstructure, and not to the bulk water activity. Some authors also showed that microbial response in a solution is more dependent on the solute used to control  $a_w$  values than on  $a_w$  itself (Chirife and Buera, 1994; Vittadini and Chinachoti, 2003), showing the importance of solute interaction. Water activity defined as a relative vapour pressure, reflects only the surface properties of a system and not necessarily the molecular dynamics that takes place in its interior (Vittadini et al., 2005). Furthermore, it has been reported that solutions with the same water activity can present dramatic differences in the system's "kinetics" (here assessed by viscosity) (Anese et al., 1996; Maltini et al., 2003) (see Figure 1.2).

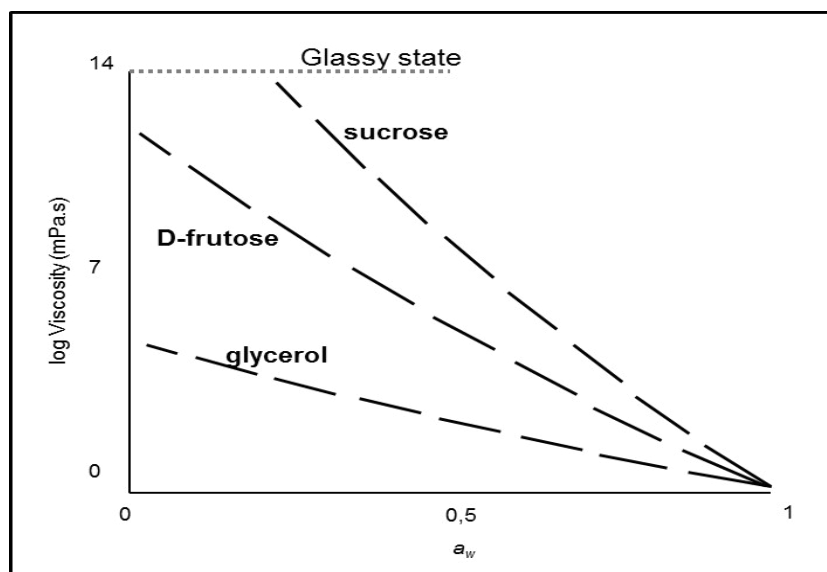


**Figure 1.2** Viscosity versus water activity ( $a_w$ ) of model solutions produced with different solutes (Anese et al., 1996).

### 1.2.2. Glass transition temperature

The glass transition temperature ( $T_g$ ) was introduced in the early 1980's aiming at finding a new parameter that would be able to assess food stability and overcome the limitations of  $a_w$ . This concept has been extensively applied, giving way to a new important area of research and application: food material science (Angel, 1996; Rahman, 2006; Roos, 1995; Slade and Levine, 1995). Essentially, this approach "simplifies" the foods as partially crystalline partially amorphous materials. The amorphous part is in a metastable state, which is very sensitive to changes in moisture content and temperature. Such amorphous matrix may exist either as a very viscous glass or a more liquid-like "rubbery" amorphous structure. The characteristic temperature,  $T_g$ , at which the glass-rubber transition occurs, is the physicochemical parameter that is nowadays a basis for product properties, stability and safety of foods (Chirife and Buera, 1995; Roos, 1998; Slade and Levine, 1991) (Figure 1.3).

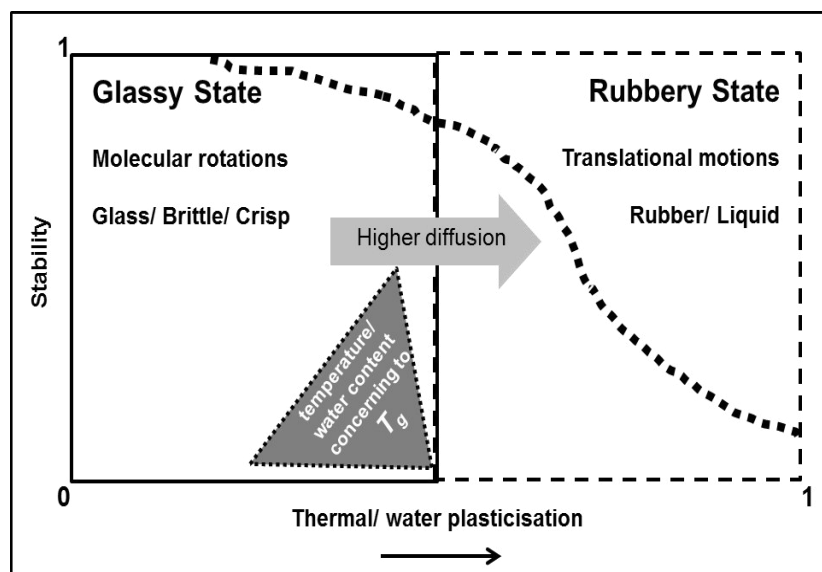


**Figure 1.3** Representation of glass transition temperature ( $T_g$ ) effects on structural transformation and diffusion-controlled changes in biological food systems (Roos, 1998).

The transition observed at  $T_g$  is a second order thermodynamics transition, in which the material undergoes a change in state but not in phase (Rahman, 2006), and is dependent on both composition and solid content of a material (Ferry, 1980).  $T_g$  greatly influences food stability, as the water in the concentrated phase becomes kinetically immobilised and therefore does not support or participate in reactions (Rahman, 2006; Slade and Levine, 1991). Below  $T_g$ , the food is expected to be stable; and above this temperature the difference ( $T - T_g$ ) between  $T_g$  and the storage temperature  $T$ , is assumed to control the rate of physical, chemical and biological changes. As discussed already, these physical and chemical reactions, which are dependent on the diffusion of reactant molecules would be quite slow in the supercooled liquid or rubber, in the vicinity of the  $T_g$ , and kinetically controlled by mobility or viscosity (Champion et al., 2000).

$T_g$  is therefore a very promising and innovative concept for food science, and is considered as a future challenge when associated with other food mechanisms (Rahman, 2006). Despite of this, experimental evidences demonstrate some fragility

(Chirife and Buera, 1994; Hills et al., 1996c; Lin et al., 2006; Vittadini et al., 2003).  $T_g$  considers mobility at a macromolecular level and, therefore, is a parameter descriptive of the physical state and overall mobility of macromolecules, which differs from the molecular mobility of smaller molecules such as water (Lin et al., 2006; Vittadini et al., 2005).

Moreover, some experimental evidence does not support a clear correlation between  $T_g$  and microbial activity (Chirife and Buera, 1994; Vittadini et al., 2003). Similarly, many investigations demonstrate that glass transition alone cannot explain enzymatic and nonenzymatic activities below  $T_g$ . In some cases, reactions occur slower in the rubbery state than in the glassy state (e.g. ascorbic acid oxidation, because the structural collapse in the rubbery state does not allow  $O_2$  diffusion through the system, which results in slower ascorbic acid degradation rates) (Lin et al., 2006).

Moreover,  $T_g$  is not as easy to measure as, for example, water activity, and may not be a representative parameter in multicomponent, multidomain complex foods (Maltini et al., 2003).

### ***1.2.3. Water proton relaxation time and NMR as a powerful technique for assessing proton relaxation time***

Biological systems, and particularly foods, consist largely of water and macromolecules, both rich in protons. Proton relaxation time ( $T_2$ ) is a characteristic of proton dynamics/mobility (Champion et al., 2000), and is a function of physical and chemical characteristics of individual chemical compounds, as well as interactions among them (Marcone et al., 2013; Ruan and Chen, 1998). Water protons are one of the most important contributors to the proton relaxation in biological systems, and the interactions between water and macromolecules is the most important factor affecting proton relaxation process (Ruan and Chen, 1998).

Nuclear magnetic resonance (NMR) spectroscopy is one of the most common investigated techniques used to evaluate systems molecular dynamics, by identifying molecular structures and evaluating the progress of chemical reactions (Marccone et al., 2013). This technique provides information on different food components, that are considered as dense complex systems (Domjan et al., 2009; Hills et al., 1991; Ruan and Chen, 1998), both in solution and solid state (Claridge, 2009; Keeler, 2002; Yan et al., 1996). It also allows to study independently the dynamics of water and food solids (Kou et al., 1999).

Water dynamics/mobility can be analysed by NMR, through proton ( $^1H$ ), deuterium ( $^2H$ ) and oxygen-17 ( $^{17}O$ ) (Vittadini et al., 2003).  $^1H$  NMR, as the most used NMR technique, has been used to investigate water dynamics and physical structures through analysis of proton nuclear magnetisation relaxation times (Li et al., 2000). Many researchers have found that the mobility of water, as measured by NMR, is related to the dynamics and “availability” of water in complex system (Hills et al., 1991; Ruan and Chen, 1998), i.e. the higher mobility of water, the higher the availability of water and very mobile water molecules take a long time to reach their equilibrium state, or relax very slowly, thus having a small relaxation rate or long relaxation time (Ruan and Chen, 1998).

In these measurements the samples are submitted to a static magnetic field and the protons are excited by means of a radiofrequency pulse. The analysis of the signal emitted while the samples return to equilibrium (FID) allows determining the spin-lattice ( $T_1$ ) and spin-spin ( $T_2$ ) relaxation. This latter variable is related with the mobility of the protons in the sample matrix.

For example, in plant tissues different compartments can be discriminated, where water molecules or protons are in exchange. These exchange rates between compartments are controlled by the proton permeability of the membranes separating

the compartments, and/or by the diffusion process by which water molecules reach the membranes (Snaar and Van As, 1992).

NMR can be applied in complex food systems to do quantitative and conformational analysis (nutritional or functional aspects), quality control of packaging materials, process control (Marcone et al., 2013), and also to evaluate food quality during storage period. In the last case, the degradation changes that occur along storage promote changes both in water and solutes bounding and structure, which results in differences in NMR properties of the food (Ludescher et al., 2001; Ruan and Chen, 1998).

Literature reports diverse studies applying this technique to different foods and with different purposes. Some examples are discussed below (section 1.4).

### **1.3. Food structure/microstructure**

Food “matrices” (systems) physical behaviour and stability depend strongly on their molecular mobility, but also on microstructure. Food microstructure recognises that foods are highly structured and heterogeneous materials, composed of architectural elements. The types of such structural units and their interactions are decisive in the food physical behaviour and functional properties, such as texture or sensorial attributes, and also physical and chemical stability during storage. They influence the water/solute interactions and hence the water availability to participate in microbial growth and degradation reactions (Aguilera, 2000). In fact, these intermolecular interactions in which the water molecules play a very important role, can determine the structure of the food material at the beginning of a given process and during processing (Wang and Liapis, 2012).

Also, the effective water diffusivity in foods, as well as free water content, highly depends on pore structure or particle size distribution (Peppas and Brannon-Peppas, 1994; Pittia and Sacchetti, 2008; Xiong et al., 1992).

In addition to water, other structural elements can be identified in foods, such as oil droplets, gas cells, fat crystals, strands, granules, micelles, and interfaces (Aguilera, 2000). These structural elements, composed of proteins, carbohydrates, and lipids (in various combinations and proportions), can exist in different states (glassy/rubbery/crystalline) even at uniform temperatures and water activity. This structural heterogeneity will necessarily affect the molecular dynamics in the system and consequently the macroscopic food quality attributes (Ludescher et al., 2001) and their behaviour along storage.

Designing the food structure during processing can also affect its behaviour during shelf life. For example, physically separating the reactants in microstructural locations can control the biochemical activity by avoiding the reactants to be in contact, thus minimizing the development of off-flavours and browning reactions (Aguilera, 2000). Food microstructure can also be altered by controlling various intermolecular and inter particle interactions among the different ingredients during processing and storage (Lesmes and McClements, 2009). Engineering structures requires knowledge on the molecular organisation of the ingredients (short and long range molecule assemblies) and physical properties, such as charge density, hydrophobicity, molecular size and conformation under different environmental conditions (Scholten et al., 2014). The expression “structure-function”, nowadays widely used, describes basically the way in which physicochemical and functional properties of foods are related with their structure (Aguilera et al., 2000).



## **1.4. Practical applications of NMR to assess molecular dynamics and structure**

As previously referred, molecular mobility/dynamics has been identified as one of the actual most promising parameters for assessing physicochemical properties in multi-component systems. This fact justifies the significant number and type of experimental works performed in food systems. This section briefly discusses examples of  $^1\text{H}$  NMR practical applications on food systems, considering matrices of different complexities.

### ***1.4.1. Edible films as food systems models***

Edible films have been studied for a long time for their potential to improve shelf-life and safety of food products (Aider, 2010; Epure et al., 2011). The literature is extensive in characterisation of such materials, and particularly in reporting the thermo mechanical behaviour and barrier properties of glassy biopolymers and polymers (Butler et al., 1996; Lazaridou and Biliaderis, 2002). These systems are partially crystalline/partially amorphous and easily reproducible materials. From a fundamental perspective, foods are mainly edible and digestible biopolymers that are partially crystalline/partially amorphous (Wang and Liapis, 2012), and thus edible films can be very interesting food model systems for mobility and microstructure studies. Also, in these films, water is one of the most important components, i.e. is used significantly as a plasticiser, creating hydrogen bonds with the polymeric chains present in the system and influencing its physical properties, e.g. relaxation (Hasegawa et al., 1992).

However, it is evident the lack of systematic information about the relationship between the effect of films composition on the microstructure and molecular dynamics of polymeric systems behaviour. A few published papers take advantage of these techniques.  $^1\text{H}$  NMR has been used to characterise starch-chitosan films with different levels of glycerol (Liu et al., 2013). This technique proved to be useful in clarifying the interactions between films components. It was showed that the addition of glycerol

promoted the interactions among chitosan, starch and glycerol through hydrogen bonding. The stronger glycerol/starch/chitosan interactions in samples containing higher glycerol concentration were confirmed by an observed decrease of glycerol mobility.  $^1\text{H}$  NMR experiments have also allowed understanding the differences on ascorbic acid stability observed in different films (León et al., 2008). This study proved that the water dynamics influences the ascorbic acid stability and recognises which of the compounds added to film forming solutions (e.g. calcium) interacted with this dynamics.

#### **1.4.2. Real food matrices**

Fruits are high water content products with a complex cellular structure, where water can be present in both intra and extra cellular spaces. The general fruit constitution may be described as a watery solution of low molecular weight species, mainly sugars, salts and organic acids, and high molecular weight hydrocolloids, contained in a water insoluble cellular matrix of macromolecules, mostly carbohydrates including insoluble pectic substances, hemicelluloses, proteins and, sometimes, lignins. Intracellular air spaces are present in parenchymous tissue and these may be considered as true structural elements, having a very characteristic influence on the perceived texture. This complexity makes these systems of special interest for mobility studies.

Many studies have been performed on the application of  $^1\text{H}$  NMR techniques for evolution of quality in fruits. This technique allows using the changes in the distribution of water proton transverse relaxation times to monitor the subcellular compartmentation of water.

$^1\text{H}$  NMR has been a tool used for purposes as diverse as study the effect of preservation processes (Hills and Remigereau, 1997; Panarese et al., 2012; Tylewicz et al., 2011), monitoring food quality changes during storage (Zhang and McCarthy,

2013), analysing food quality characteristics (Hernández-Sánchez et al., 2007; Marigheto et al., 2008; Tu et al., 2007), or just monitoring ripening (Raffo et al., 2005).

The work of Hills and co-workers (1991) was an important milestone in the use of this technique. The group first identified the signals of water in the cellular wall, cytoplasm and vacuole (Hills et al., 1991; Hills et al., 1996a; Hills et al., 1996c) and applied the methodology for studying the effect of preservation processes on foods. An example is the study on changes in subcellular water compartmentation in parenchyma apple tissues during freezing/thawing (Hills and Remigereau, 1997). Figure 1.4 shows the differences in water proton transverse relaxation time profile for fresh and freezing/thawing apple tissues. For the fresh apple tissue, behaviour presents a proton distribution following three peaks that can be assigned to water located in the vacuolar, cytoplasm and cell wall compartments. After thawing the absence of the three peaks indicate membrane rupture and loss of turgor in the tissue, the cellular structure was broken and the vacuole, cytoplasm and cellular wall lost their integrity and become just one compartment.

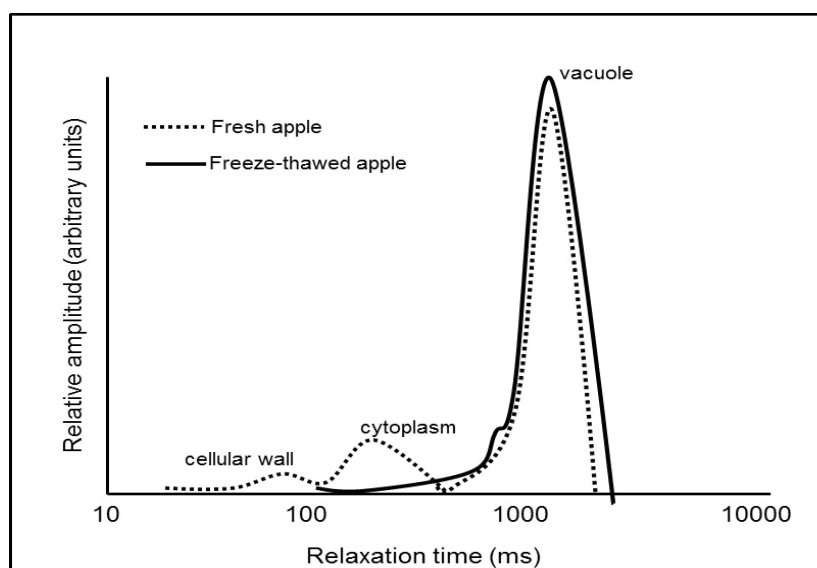


**Figure 1.4** Distribution of transverse water proton relaxation times in fresh and freeze-thawed apple tissues (Hills and Remigereau, 1997).

As discussed, another example on the use of NMR is to understand the response of fruit's quality parameters to different storage conditions, such as on pomegranate fruit (Zhang and McCarthy, 2013). In this case, NMR measurements allow analysing the microscopic structure changes during storage and confirm the water environment in each component. The authors found that water was redistributed between subcellular compartments of the pomegranate aril tissues during controlled atmosphere storage.

Another study has addressed the water proton relaxation times in different pear varieties with two different levels of internal damage (sound tissue and disordered tissue) and tried to find a relationship with the internal browning process and complement the observations with image techniques (Hernández-Sánchez et al., 2007). It was possible to conclude that, at least for one pear variety, internal browning (postharvest disorder) may be identified and correlated with the NMR parameters. Moreover, it was also possible to infer that the cell decompartmentation facilitates the accessibility of enzymes and substrates (responsible for browning reactions). The analysis of firmness and soluble solids content were performed and no correlation between internal browning was found, evidencing once again the relevance of NMR to support the internal inspection of the fruit.

One last example is a study aiming at understanding the banana ripening phenomenon (Raffo et al., 2005), showing the relationship between changes in water dynamics and variations in chemical composition. Results from NMR allow explaining the ripening process that happens for a period of seven days, and where membrane-bound starch granules are almost converted to soluble sugars. Shortly, three components were determined, attributed to vacuole, cytoplasm and cell wall.  $T_2$  values attributed to cytoplasmic and vacuolar water show a gradual increase, correlated with the disappearance of starch that acts as a relaxation sink (Figure 1.5). The disappearance of these granules during ripening increases the cytoplasm and

vacuolar water fractions, that can be influenced by the chemical diffusive exchange effect, increasing cytoplasm and vacuole  $T_2$ .

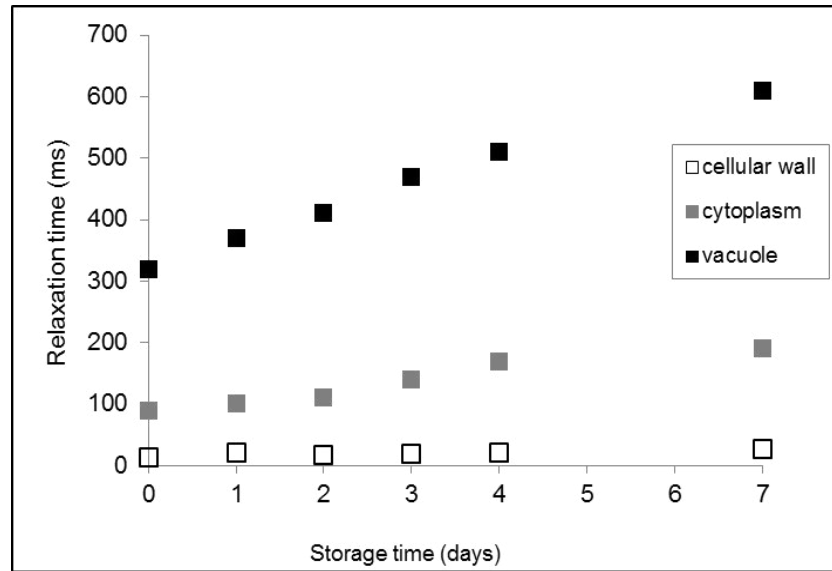


**Figure 1.5** Banana proton transverse relaxation time, during seven days of storage (Raffo et al., 2005).

## 1.5. Conclusions

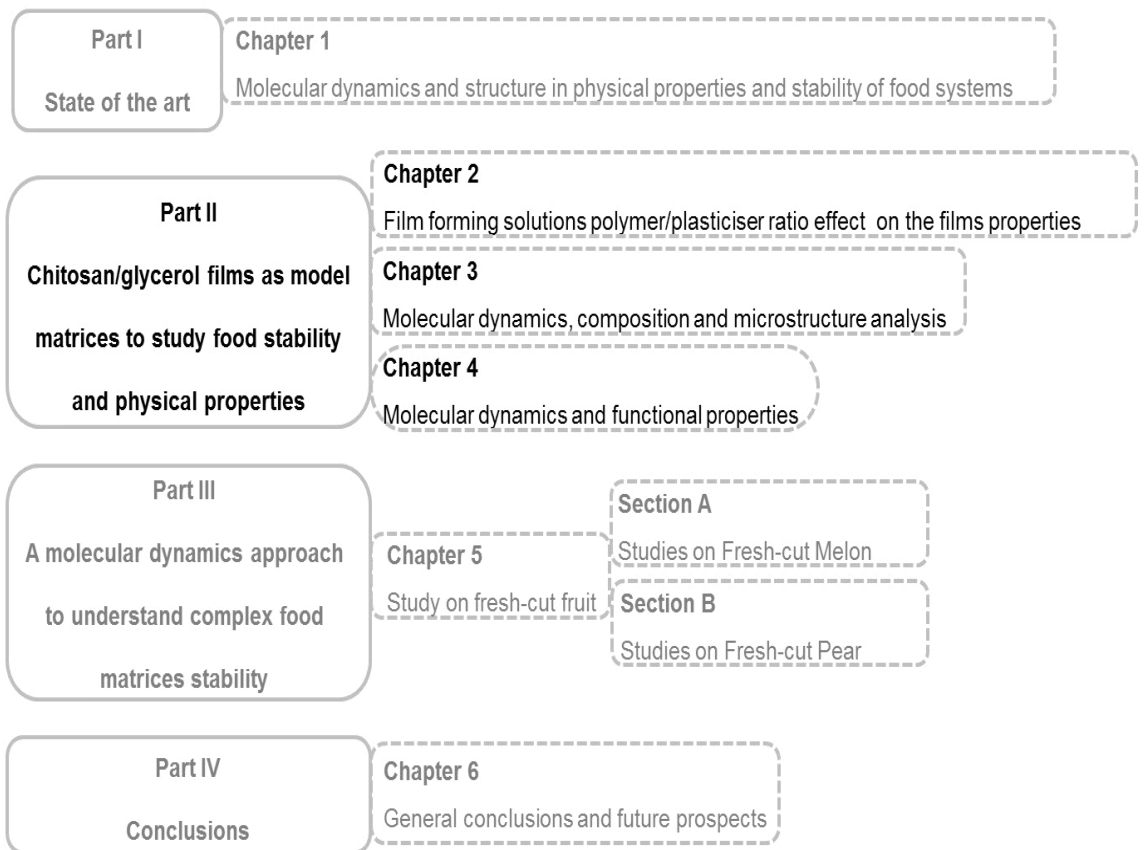
This section reviewed some critical issues and highlighted works in food systems molecular dynamics assessment. Molecular dynamics together with structure/ microstructure are important approaches to study food systems properties and stability. Water is one of the most important food components and is a key factor in biological systems performance. Water activity, glass transition temperature and water proton relaxation time are three concepts that have been used to determine the water performance. Water proton relaxation time, assessed by NMR techniques, is one of the broadest methods to understand dynamics, even in complex biological systems like foods. Dynamic properties play an important role in complementing the information provided by methods based on systems equilibrium and global kinetics. However, it is evident the lack of systematic information, even in straightforward model food matrices.

Further work on relationships between water and solids mobility and glass transition or water activity in food systems is a fundamental and necessary approach to fully attain food physical properties and stability. The absence of studies on the relationship between degradation of quality factors and molecular mobility along shelf-life is also evident.

These studies may be extremely useful for food product and process design, safety and sensorial attributes and also for better understanding and predicting, for example, food storage stability conditions.

# PART II

---







## **CHAPTER 2**

**Film forming solutions polymer/plasticiser ratio effect on the films  
properties**

---



**Abstract**

In this chapter the physico-chemical properties of chitosan/glycerol film forming solutions (FFS) and resulting films were analysed. Solutions were prepared using different concentrations of plasticising agent (glycerol) and chitosan. Films were produced by solvent casting and equilibrated in a controlled atmosphere. FFS water activity and rheological behaviour were determined. Films water content, solubility, water vapour and oxygen permeabilities, thickness, and mechanical and thermal properties were determined. Fourier transform infrared (FTIR) spectroscopy was also used to study the chitosan/glycerol interactions.

Results demonstrate that FFS chitosan concentration influenced solutions consistency coefficient and that this was related with differences in films water retention and structure. Plasticiser addition led to an increase in films moisture content, solubility and water vapour permeability, water affinity and structural changes. Films thermo-mechanical properties were significantly affected by both chitosan and glycerol addition. FTIR experiments confirmed these results.

This chapter highlights the importance of glycerol and water plasticisation in films properties.

## 2.1. Introduction

Edible films technology presents several challenges, especially on the relationship between the composition and properties of FFS and the properties of the obtained films. The viscosity and molecular entanglement of the FFS are of great importance since it may affect the obtained film properties, such as thickness, mechanical and thermal properties, water retention capacity, water affinity and oxygen permeability.

Natural polymers are inherently brittle due to their complex branched primary structure and weak intermolecular forces (Srinivasa et al., 2007). The primary role of plasticisers is to improve the flexibility and processability of polymers, by reducing the intermolecular forces, softening the rigidity of the film structure and rising the mobility of the biopolymeric chains (Melissa Gurgel Adeodato Vieira, 2011; Srinivasa et al., 2007). These additives reduce the tension of deformation, hardness, density, viscosity and electrostatic charge of a polymer, simultaneously increasing chain flexibility, resistance and the dielectric constant (Ferry, 1980).

Glycerol is the most widely used plasticiser due to its good efficiency, large availability and low exudation (Epure et al., 2011). Moreover, this plasticiser has a boiling point and hydrogen bond ability causing high retention in the polymer. Glycerol has also been used to modify natural macromolecules like proteins (Quijada-Garrido et al., 2007; Zhang et al., 2005) and carbohydrates.

Water is also one of the most important plasticisers of biological systems, such as foods (Neto et al., 2005; Roos, 1995), since water molecules create hydrogen bonds with the polymeric chains present in the system.

Chitosan is a semicrystalline biopolymer, having a great potential for chemical and mechanical modifications, to create novel properties, functions and applications in different areas (Pillai et al., 2009). Due to its properties, the use of chitosan in edible films development has been long studied (Neto et al., 2005; Pillai et al., 2009). These

studies have shown that chitosan films properties depend on several parameters, such as chitosan molecular weight and degree of deacetylation, organic acid used and the possible presence of plasticiser (Epure et al., 2011; Suyatma et al., 2005).

The film structure is one of the main responsible for its properties. This is reported to be related with the polymer free volume, which affects molecular mobility of the polymeric matrix (Dlubek et al., 2005; Slade and Levine, 1991). The structure of the film is strongly affected by the composition, specially the amounts of polymer and plasticiser in the FFS and the ratio between these compounds.

This chapter aims at systematically investigating how the properties and structure of chitosan films are influenced by the properties and composition of the FFS. To achieve that, film forming solutions were prepared with 3 different chitosan concentrations and with three chitosan/glycerol ratios, and the rheological behaviour was characterised. The water, barrier, mechanical and thermal properties and FTIR spectra of the obtained films were characterised.

## **2.2. Material and methods**

### **2.2.1. Chitosan FFS preparation**

FFS were prepared by dissolving different chitosan (90% deacetylation, Aqua Premier Co., Thailand) concentrations (1%, 2% and 3% w/v) in a 1% lactic acid solution (Acros Organics, Belgium), and adding to different levels (10%, 50% and 90% w/w) of plasticising agent, (glycerol - Panreac, Spain). These conditions allow the achievement of the same ratio chitosan/glycerol (see Table 2.1). It was decided not to consider films without glycerol, since these films are too brittle, making impossible to perform most of the analysis. To promote a good homogenisation an Ultra-Turrax was used (IKA T18 basic, Wilmington, NC, USA). To allow significant comparisons, two

replicates (samples) were made for each experimental condition (chitosan/plasticiser ratio).

## **2.2.2 Characterisation of FFS**

### *2.2.2.1. Rheological behaviour*

Rheology of FFS was studied by viscometry tests, using a controlled stress rheometer Bohlin VOR (Bohlin Instruments Ltd, Cirencester UK) at 23 °C and a cone-plate configuration. For each sample three measurements were carried out.

### *2.2.2.2. Water activity*

Measurements were performed with a dew point hygrometer (Aqualab - Series 3, Decagon Devices Inc., USA.), at  $23 \pm 1$  °C. The sensitivity of the equipment was 0.001. Calibration was carried out before experiments with distilled water and saturated saline solutions. Water activity value of each sample resulted from the average of nine readings.

## **2.2.3. Chitosan films preparation**

A constant amount (300 mL) of the chitosan solutions was casted in 32 X 40 cm plates and dried in an incubator at 40 °C, for three days. Prior to any characterisation, films were stored at 22 °C and 53% RH, until equilibrium was reached. Once again, to allow significant comparisons, two replicates of films (samples) were produced for each experimental condition (chitosan/plasticiser ratio). All measurements were performed at controlled temperature (22 °C) and humidity (53%) room.

### **2.2.4. Characterisation of films**

#### *2.2.4.1. Water activity, moisture content and solubility*

Films  $a_w$  were determined using the same methodology described under point 2.2.2.2.

To determine the films moisture content (MC), approximately 50 mg of film were dried at 105 °C, until weight equilibrium was attained. The weight loss of the sample was determined, and MC was calculated as the percentage of water removed from the system. Three measurements were obtained for each sample.

Solubility (SOL) was determined as the content of dry matter solubilised after 24 hours of immersion in distilled water. Two pieces of each sample, previously dried until constant weight, were immersed in 50 mL of water (at 23 °C). After 24 hours of immersion with agitation, the pieces of film were withdrawn and dried until constant weight in an oven at 105 °C, to determine the weight of dry matter not solubilised in water. SOL of films in water was determined as the percentage of soluble material. Three measurements were obtained for each sample.

#### *2.2.4.2. Films barrier properties*

Water vapour permeability (WVP) was evaluated gravimetrically based on ASTM E96-92 method (Bourbon et al., 2011; V. Guillard, 2003). The film was sealed on the top of a permeation cell containing distilled water (100% RH; 2337 Pa vapour pressure at room temperature), placed in a desiccator at 22 °C and 0% RH (0 Pa water vapour pressure) containing silica. The cells were weighed at 2 h intervals for 10 h using an analytical balance (McHugh et al., 1993). Two measurements were made for each sample.

Oxygen permeability (O<sub>2</sub>P) was determined based on the ASTM D 3985-02 (2002) method (Martins et al., 2010). Briefly, the films were sealed between two

chambers, having each one two channels. In the lower chamber,  $O_2$  was supplied at a controlled flow rate (J & W Scientific, ADM 2000, USA) to maintain its pressure constant in that compartment. The other chamber was purged with a nitrogen stream, also at controlled flow rate. Nitrogen acted as a carrier for the  $O_2$ . To determine  $O_2$  concentration, 1 mL of sample was injected in a gas chromatograph (Chrompack 9001, Middelburg, The Netherlands) at 110 °C, equipped with a column Porapak Q 80/100 mesh 2 m x 1/8" x 2 mm SS, and a thermal conductivity detector at 110 °C. Helium at 23 mL min<sup>-1</sup> was used as carrier gas. A standard mixture containing 10%  $CO_2$ , 20%  $O_2$  and 70%  $N_2$  was used for calibration. The flows of the two chambers were connected to a manometer to ensure the equality of pressures (both at 1 atm) between both compartments. As the  $O_2$  was carried continuously by the nitrogen flow, it was considered that partial pressure of  $O_2$  in the upper compartment is null, therefore  $\Delta P$  is equal to 1 atm. Three measurements were taken for each sample.

#### *2.2.4.3. Films thickness*

The thickness of the produced films was measured using a digital micrometer (Mitutoyo, Japan). From each sample a minimum of 8 stripes (15 × 170 mm) were cut, and at least 2 readings were randomly performed at different positions.

#### *2.2.4.4. Films mechanical properties*

Films mechanical properties, namely elongation at break (EB) and tensile strength (TS), were determined in extension with an Instron Universal Testing Machine (Model 4500, Instron Corporation, U.S.A.), following the ASTM D 882-91 (1991). The initial grip separation and the crosshead speed were set at 100 mm and 50 mm min<sup>-1</sup>, respectively. EB was calculated as the ratio of the final length at the point of sample rupture to the initial length of a specimen (100 mm), and expressed as a percentage. TS was expressed in MPa and calculated dividing the maximum load



(N) by the initial cross-sectional area of the specimen. EB and TS tests were replicated nine times for each sample.

#### *2.2.4.5. Films thermal properties*

The films thermal profiles, glass transition temperature ( $T_g$ ), melting enthalpy ( $\Delta h$ ) and melting temperature ( $T_m$ ), were determined using differential scanning calorimetry (DSC). DSC was performed using a TA-60WS, Shimadzu Corporation, Japan, with a cooling accessory, under  $N_2$  atmosphere ( $20 \text{ mL min}^{-1}$ ).

Film samples of approximately 5 mg were weighed into aluminium cups and sealed hermetically. An empty cup was used as reference and the temperature was increased at  $20 \text{ }^\circ\text{C min}^{-1}$ , from  $-150$  to  $200 \text{ }^\circ\text{C}$ . The maximum temperature of  $200 \text{ }^\circ\text{C}$  was selected in order to avoid possible chitosan degradation (Bourbon et al., 2011). Thermograms were analysed using the Universal Analyses Software TA-60WS (Shimadzu Corporation, Japan). Two measurements were made for each sample.

#### *2.2.4.6. FTIR-ATR spectroscopy*

All spectra were acquired using a spectrometer Perkin-Elmer (Spectrum BX, Germany) set up for mid-infrared measurements equipped with a horizontal one single reflection ATR Golden Gate (Specac, Germany). The software OPUS v. 5.0 (Brüker, Germany) was programmed to record each spectrum between  $4000$  and  $600 \text{ cm}^{-1}$ , at a resolution of  $4 \text{ cm}^{-1}$ . Samples and background measurements were made by coadding 128 scans for each spectrum before Fourier transformation. The interferometer was operated at a laser frequency of  $10 \text{ kHz}$  and in the single-sided directional mode. Fourier transformation was done with a Mertz phase correction, a triangular apodisation function, with a zero-filling factor of 2. At least three spectrum replicates were recorded for each film composition.

#### 2.2.4.7. Data analysis

To conclude on the isolated effect of chitosan addition in film forming solutions and obtained films ( $p < 0.05$ ), experimental results were analysed by one-way ANOVA and post hoc multiple comparison tests (Tukey's test), for a fixed glycerol concentration. To evaluate glycerol addition, statistical analysis of the data was performed fixing the chitosan concentration.

To assess samples rheological behaviour a power law model (Eq. 2.1) was fitted to the experimental data of shear stress ( $\sigma$ ) as a function of shear rate ( $\dot{\gamma}$ ):

$$\sigma = k(\dot{\gamma})^n \quad (2.1)$$

where  $n$  is the flow behaviour index, and  $K$  the consistency coefficient.

WVP was estimated using regression analysis from equation 2.2; adapted from literature (Sobral et al., 2001) and corresponding 95% confidence intervals were calculated:

$$\frac{w \times x}{A \times \Delta P} = \text{WVP} \times t \quad (2.2)$$

where  $x$  is the average thickness of edible films,  $A$  the permeation area ( $0.005524 \text{ m}^2$ ),  $\Delta P$  the difference of partial vapour pressure of the atmosphere ( $2337 \text{ Pa}$  at  $20 \text{ }^\circ\text{C}$ ),  $w$  the weight loss, and  $t$  the experimental time.

Spectra analysis was performed using the CATS 97 program (Barros, 1999). Principal component analysis (PCA) was used to reduce the dimensionality of the data and to extract the main sources of variability.

## 2.3. Results and discussion

### ***2.3.1. Characterisation of the FFS***

The rheological behaviour and  $a_w$  of the FFS used in this study are presented in Table 2.1 (results are included in Appendix A, Tables A.1.1 and A.1.2).

For all the tested FFS, results show a shear thinning behaviour, which is commonly used for describing the polymer melt behaviour (Steffe, 1996). The Power Law Model (Eq. 2.1) successfully described the obtained rheograms. Flow index ( $n$ ) and consistency coefficient ( $K$ ) were estimated and the corresponding 95% confidence limits calculated (Table 2.1) (Chillo et al., 2008; Garcia et al., 2004) (data in Appendix A, Table A.1.1).

**Table 2.1**

Experimental results for the characterisation of film forming solutions.

			Viscosity Parameters				
Chit (w/v %)	Gly (w/v %)	Chit/ Gly Ratio (w/w)	$K$ (Pa s <sup>n</sup> ) (± 95% Confidence Error)	$n$ (± 95% Confidence Error)	$a_w$ (± Standard Deviation)	Gly *	Chit *
1	10	7.92	0.198±0.010	0.810±0.018	1.002±0.001	a	a
1	50	1.59	0.254±0.021	0.803±0.006	1.000±0.001	a	a
1	90	0.88	0.219±0.013	0.814±0.004	0.999±0.002	a	a
2	10	7.94	2.132±0.430	0.656±0.018	1.001±0.001	a	a
2	50	1.58	1.450±0.104	0.682±0.001	1.001±0.001	a	a
2	90	0.88	1.591±0.135	0.683±0.008	0.997±0.001	a	a
3	10	7.94	3.371±0.260	0.620±0.005	1.002±0.001	a	a
3	50	1.59	3.221±0.095	0.623±0.003	0.999±0.001	ab	a
3	90	0.88	3.034±0.130	0.635±0.002	0.995±0.002	b	a

\*Mean values followed by the same letter are not significantly different at 0.05 by the Tukey HSD test; Letters from Gly column concern to differences between glycerol concentrations (for the same chitosan concentration); Letters from Chit column refer to analysis of the effect of chitosan concentration (for the same glycerol content).

$K$ : consistency coefficient;  $n$ : flow index;  $a_w$ : water activity

Glycerol addition showed no significant effect on FFS rheological behaviour, assessed by  $n$  and  $K$  estimates. On the other hand, chitosan concentration affected significantly FFS rheological behaviour, ranging from close to Newtonian (low chitosan concentrations,  $n \rightarrow 1$ ) to a pseudoplastic behaviour (with increasing chitosan concentration,  $n$  decreasing). Also,  $K$  significantly increased with chitosan addition. These results can be related with the lower amounts of water present in the solutions with higher polymer/plasticiser concentration.

As discussed before, although different chitosan and glycerol concentrations were used to prepare the FFS, for each chitosan level studied (1, 2 and 3%), the same ratios chitosan/glycerol were tested (see Table 2.1). However, the observed rheological behaviour showed that the amount of polymer in the solution has a higher impact on FFS viscoelastic properties than the ratio between polymer and plasticiser.

Regarding  $a_w$ , a significant effect of chitosan and glycerol addition was observed, while no differences were found between replicates ( $p > 0.05$ , Main Effects ANOVA, data in Appendix A, Table A.1.2). To conclude on the significance ( $p < 0.05$ ) of the isolated effect of glycerol concentration on the  $a_w$  of the FFS (for the same chitosan concentration), results were analysed using the glycerol concentration as the categorical predictor factor (Gly column on Table 2.1.). For testing significance of the effect of chitosan concentration (for the same glycerol concentration), results were analysed using chitosan concentration as the factor (Chit column on Table 2.1).

Results show that there is no significant effect of the amount of the polymer present on the  $a_w$  of the solutions. However, the addition of glycerol as a plasticiser showed a different effect depending on chitosan concentration: for lower chitosan concentration (1%), the addition of glycerol did not affect  $a_w$ . While, with increasing chitosan concentration, glycerol addition decreased solutions  $a_w$ . This effect would be even more evident for higher chitosan concentrations. Statistical analyses show that solutions with 3% chitosan concentration and different levels of glycerol are

significantly different, while at lower chitosan concentration (1%) glycerol additions lead to no significant differences between samples (Gly column on Table 2.1).

These results may indicate that interaction of the plasticiser and water molecules with the polymeric chain plays a critical role not only in films, but also in the FFS and may influence the water evaporation during films drying.

### **2.3.2. Characterisation of chitosan films**

#### *2.3.2.1. Water and barrier properties*

Experimental results for  $a_w$ , MC, SOL and WVP of chitosan films are presented in Table 2.2 (data in Appendix A, Tables A.2.1, A.2.2 and A.2.3). No differences between replicates were observed ( $p > 0.05$ , Main Effects ANOVA, data in Appendix A Section A.3). Again, to conclude on the significance of glycerol and chitosan concentrations effects on the different film's properties, experimental results were analysed first using the glycerol concentration as categorical predictor factor (Gly column on Table 2.2). For testing significance of the effect of chitosan concentration (for the same glycerol concentration), results were analysed using chitosan concentration as the factor (Chit column on Table 2.2).

The  $a_w$  results show that chitosan concentration has a significant effect on this parameter (Table 2.2). However, glycerol only has a significant effect for films produced with higher chitosan content (3%). In this case, higher glycerol content led to higher  $a_w$  values. These results may be related with the polymer, plasticiser and/or water ratios and bindings.

**Table 2.2**

Experimental results for chitosan films water related properties.

Chit (w/v %)	Gly (w/v %)	$a_w$ ( $\pm$ Standard Deviation)	Gly *	Chit *	MC (%) ( $\pm$ Standard Deviation)	Gly *	Chit *	SOL (%) ( $\pm$ Standard Deviation)	Gly *	Chit *	WVP (g Pa <sup>-1</sup> s <sup>-1</sup> m <sup>-1</sup> ) ( $\pm$ 95% Confidence Error)
1	10	0.5543 $\pm$ 0.0179	a	a	28.87 $\pm$ 5.91	a	a	48.91 $\pm$ 2.11	a	a	6.768E-08 $\pm$ 2.332E-08
1	50	0.5561 $\pm$ 0.0305	a	a	36.64 $\pm$ 8.57	ab	a	54.09 $\pm$ 4.56	a	a	9.111E-08 $\pm$ 4.118E-09
1	90	0.5658 $\pm$ 0.0170	a	a	51.1 $\pm$ 3.03	b	a	67.52 $\pm$ 7.31	b	a	8.657E-08 $\pm$ 4.210E-09
2	10	0.5195 $\pm$ 0.0123	a	b	17.83 $\pm$ 1.28	a	b	36.06 $\pm$ 0.95	a	b	1.029E-07 $\pm$ 5.244E-08
2	50	0.5031 $\pm$ 0.0140	a	b	38.32 $\pm$ 4.67	b	a	51.02 $\pm$ 3.78	b	a	6.011E-08 $\pm$ 8.235E-08
2	90	0.5011 $\pm$ 0.0067	a	b	51.92 $\pm$ 4.52	c	a	61.40 $\pm$ 4.22	c	a	1.872E-07 $\pm$ 1.182E-08
3	10	0.5072 $\pm$ 0.0029	a	b	16.36 $\pm$ 0.88	a	b	29.73 $\pm$ 1.06	a	c	1.601E-07 $\pm$ 9.046E-08
3	50	0.5116 $\pm$ 0.0062	ab	b	38.87 $\pm$ 1.36	b	a	49.77 $\pm$ 0.89	b	a	1.668E-07 $\pm$ 7.924E-08
3	90	0.5296 $\pm$ 0.0091	b	c	55.06 $\pm$ 0.83	c	a	63.45 $\pm$ 0.65	c	a	2.885E-07 $\pm$ 9.259E-08

\*Mean values followed by the same letter are not significantly different at 0.05 by the Tukey HSD test; Letters from Gly column concern to differences between glycerol concentrations (for the same chitosan concentration); Letters from Chit column refer to analysis of the effect of chitosan concentration (for the same glycerol content).

$a_w$ : water activity; MC: moisture content; SOL: water solubility; WVP: water vapour permeability

Regarding MC, it was observed that higher glycerol concentration solutions produced films with significantly higher MC. For every chitosan concentration, increasing FFS plasticiser content produced a significant increase on film's MC (Table 2.2).

SOL was significantly higher in films produced with higher glycerol concentrations (Table 2.2). However, chitosan content only had a significant effect on solubility of films produced with low glycerol content (10%). These results may be related with high solubility of glycerol in water (and its hygroscopic nature), due to the three hydrophilic hydroxyl groups present (Chillo et al., 2008).

For the results of chitosan films WVP, it is observed that there are significant differences for different chitosan concentrations (Table 2.2): higher chitosan concentrations led to higher values of WVP. This tendency could be explained by an increase of amino groups present and consequent higher hydrophilicity of the biodegradable blend films when increasing the chitosan content (Bourtoom, 2008). Also, samples with higher plasticiser concentration show higher WVP values. These results are probably due to an increase in the free volume between the polymer chains - when hydrophilic plasticisers are incorporated into polysaccharide films, there is a decrease of the intermolecular forces, making the polymer network less dense and hence more permeable (Cuq et al., 1997; Lavorgna et al., 2010).

With respect to samples  $O_2P$ , no significant differences were observed nor between chitosan neither between glycerol concentrations. Nevertheless, Figure 2.1 demonstrates a general tendency with respect to polymer and plasticiser proportions: higher chitosan concentrations in the FFS led to higher values of  $O_2P$ ; and higher plasticiser concentrations led to lower values of  $O_2$  permeability. The exception is samples produced with 1% chitosan, where  $O_2P$  values were almost constant for different glycerol concentrations (results are included in Appendix A, Table A.2.3).



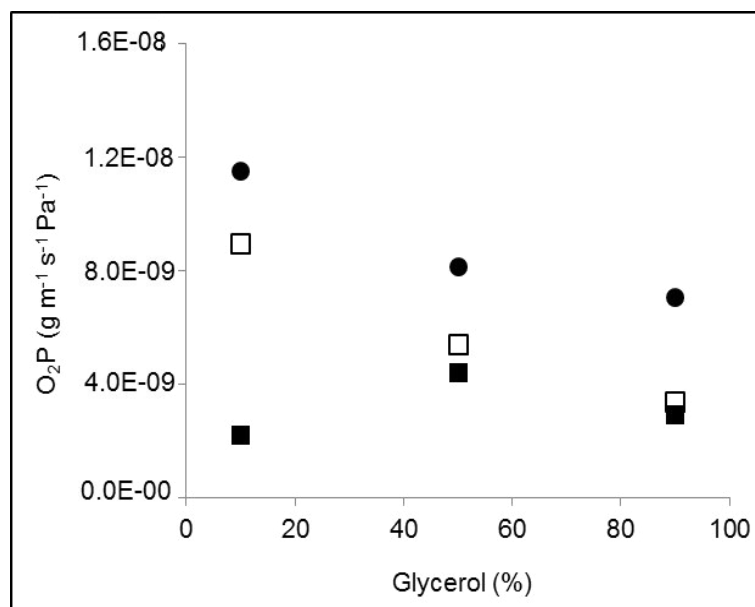


**Figure 2.1** Oxygen permeability of films prepared with different chitosan and glycerol concentrations (■ 1%, □ 2%; ● 3% chitosan).

These results are supported by a direct relationship between decreasing crystallinity of the films (see Table 2.3 of the section below) and the decrease in  $O_2P$ , and may indicate that structural changes should be investigated in the future.

Overall, the addition of plasticiser led to an increase in MC, SOL and WVP of the films, showing increased water affinity and structural changes. This was also reflected on  $O_2P$  decrease with glycerol addition. Chitosan concentration did not significantly affect such properties.

### *2.3.2.2. Mechanical and thermal properties*

The experimental results for the mechanical and thermal analysis of chitosan films are presented in Table 2.3 (results included in Appendix A, Tables A.2.5 and A.2.6).

**Table 2.3**

Experimental values for films mechanical and thermal characterisation.

Chit (w/v %)	Gly (w/v %)	Thickness (mm) (± Standard Deviation)	Gly *	Chit *	EB (%) (± Standard Deviation)	Gly *	Chit *	TS (MPa) (± Standard Deviation)	Gly *	Chit *	$T_g$ (°C) (± Standard Deviation)	Gly *	Chit *	$\Delta h$ (J g <sup>-1</sup> ) (± Standard Deviation)	Gly *	Chit *
1	10	0.0642±0.0292	a	a	46.10±9.29	a	a	8.25±2.97	a	a	-20.02±12.74	a	a	-70.00±26.47	a	a
1	50	0.0556±0.0117	a	a	62.17±21.40	ab	a	4.50±2.09	a	a	-60.81±14.10	b	a	-151.63±14.69	a	a
1	90	0.0605±0.0132	a	a	66.51±28.84	b	a	1.82±0.89	a	a	-72.34±1.43	b	a	-184.25±76.87	a	a
2	10	0.1343±0.0144	a	a	20.00±10.64	a	b	12.15±4.79	a	a	-5.12±8.88	a	a	-165.22±48.92	a	b
2	50	0.1357±0.0227	a	b	34.48±5.05	a	b	0.95±0.38	b	b	-51.54±12.35	b	a	-203.86±23.16	a	b
2	90	0.1527±0.0158	a	b	32.02±7.55	a	b	0.28±0.07	b	b	-65.08±3.31	b	a	-203.75±52.55	a	a
3	10	0.2844±0.0896	a	b	9.19±7.64	a	b	6.03±2.04	a	a	26.39±9.81	a	b	-175.87±37.96	a	b
3	50	0.2348±0.0100	a	c	25.58±3.11	a	b	1.47±0.31	b	b	-64.62±2.09	b	a	-249.20±19.36	ab	c
3	90	0.2452±0.0216	a	c	19.96±7.09	a	b	0.47±0.11	b	b	-82.92±3.29	c	b	-313.12±63.31	b	a

\*Mean values followed by the same letter are not significantly different at 0.05 by the Tukey HSD test; Letters from Gly column concern to differences between glycerol concentrations (for the same chitosan concentration); Letters from Chit column refer to analysis of the effect of chitosan concentration (for the same glycerol content).

EB: elongation at break; TS: tensile strength;  $T_g$ : glass transition temperature;  $\Delta h$ : melting enthalpy

The films thickness was only significantly affected by the chitosan content, showing that possible structural changes due to plasticisation, e.g. increase in free volume, are not reflected on this property (data included in Appendix A, Table A.2.4). Also, the MC (Table 2.2) showed no relationship with the thickness of the obtained film. This may indicate that chitosan is the main contributor to film thickness.

Regarding the films mechanical properties, both chitosan and glycerol addition led to significant differences in EB and TS. At 1% chitosan, the amount of glycerol added shows a conventional action of plasticisers, increasing EB and decreasing the TS. This effect is due to chitosan chains interactions, decreasing intermolecular attraction and increasing polymer mobility, which facilitates film elongation (Suyatma et al., 2005; Ziani et al., 2008). However, films produced with solutions with higher chitosan content (2 and 3 w/v %) and 50% glycerol had a deviant behaviour: showing higher EB than films with 90% of glycerol. This behaviour has been previously observed and may occur due to the relationship between polymer/plasticiser concentrations, corresponding to an antiplasticisation phenomenon: a stronger interaction might be occurring between the polymer and the plasticiser, producing a “cross-linker” effect, which decreases the free volume and the molecular mobility of the polymer (Lourdin et al., 1997; Suyatma et al., 2005; Ziani et al., 2008).

$T_g$  is associated with a change in the physical properties and state of materials, and can be related with the plasticisation of amorphous regions within semi-crystalline materials (Roudaut et al., 2004).  $T_g$  is considered a second order phase transition and occurs over the temperature range at which a glassy material enters the rubbery domain (Lazaridou and Biliaderis, 2002). At temperatures above  $T_g$  various physical properties are significantly affected (Lazaridou and Biliaderis, 2002; Slade and Levine, 1991). Table 2.3 shows the  $T_g$  for the different films analysed. Results

demonstrate that glycerol significantly affected films  $T_g$ . As expected, plasticiser (glycerol) lowered  $T_g$  (Rivero et al., 2010; Suyatma et al., 2005), which also correlated well with MC (Table 2.2), since water acts as plasticiser itself (Arvanitoyannisa et al., 1998; Dai et al., 2006; Rivero et al., 2010). The chitosan/glycerol ratio also affected  $T_g$  (Figure 2.2a): increasing ratio lead to a  $T_g$  decrease. This may be related with the free volume in the films (as was discussed above). Higher plasticiser content increases free volume, and higher polymer content decreases this variable (Lourdin et al., 1997; Rivero et al., 2010; Roudaut et al., 2004).

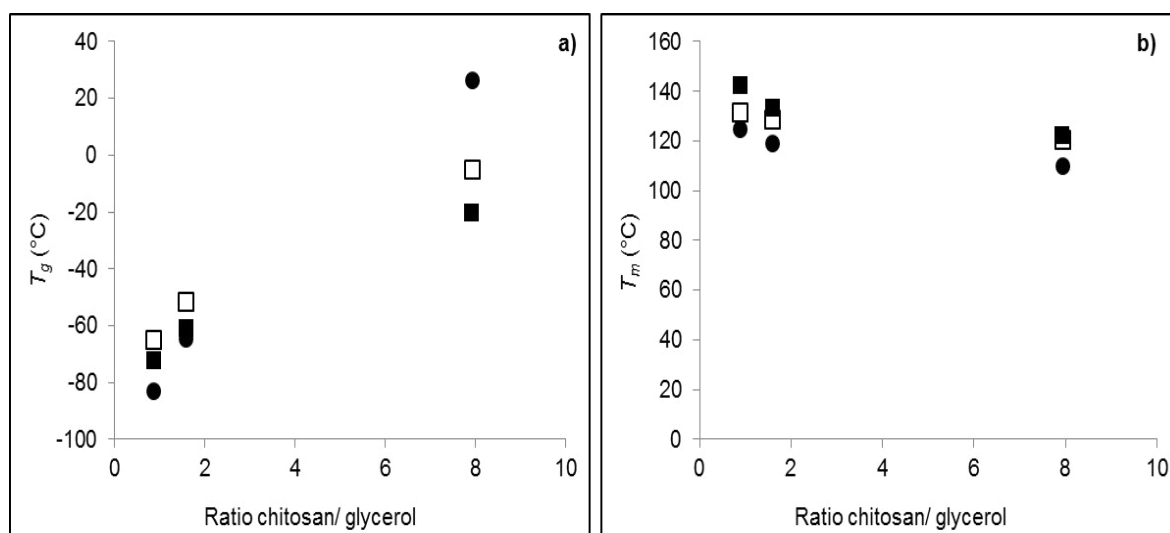


**Figure 2.2** Glass transition temperature ( $T_g$ ) (a) and melting temperature ( $T_m$ ) (b) of the chitosan films prepared with different chitosan/glycerol concentrations (■ 1%, □ 2%; ● 3% chitosan).

The crystalline component of the films was evaluated by the melting enthalpy ( $\Delta h$ ) and melting temperature ( $T_m$ ). Table 2.3 shows that  $\Delta h$  increased with increasing chitosan concentrations, particularly for samples produced with lower glycerol concentrations. This result was expected once that chitosan, as a polymer, is responsible for the formation of crystals in the system. Also, plasticiser addition

increased the  $\Delta h$ , i.e. increases the samples crystallinity, and this may be due to glycerol interaction with chitosan chains: the H-bonds stabilised the chitosan crystals (Okuyama et al., 1997).

In Figure 2.2b the values of the  $T_m$  ranged from 110 to 140 °C. Despite the fact that these values were not significantly different between formulations, a tendency in values depending on the FFS composition is observed. Higher concentrations of chitosan presented lower  $T_m$  values. On the other hand, temperature of the main peak shifted to higher melting temperatures when increasing plasticiser concentration (decreasing ratio), as referred in previously published results (Rivero et al., 2010), and may be also related with an increase of the strength of the H-bonds stabilising the chitosan crystals in the presence of plasticiser (Okuyama et al., 1997).

Overall, thermal and mechanical characterisation showed a significant effect on the properties of films produced with FFS of different compositions. Once again, the observed effect on these properties reflects changes in the films structure.

### 2.3.2.3. FTIR-ATR spectroscopy results

FTIR has been extensively applied for the characterisation of biopolymers, as this technique reveals specific information about the molecular structure of chemical compounds (Gao et al., 2006; Lawrie et al., 2007). Also, important information about specific interactions between the different constituents of the biopolymers can be extracted from the infrared spectrum.

Figure 2.3 presents the results obtained from FTIR measurements. Figure 2.3a presents typical spectra of the different films with different compositions. In order to better understand the possible interaction of the different constituents of the films, a band assignment was performed by comparing the films' spectrum with the spectra of their pure compounds and comparison with literature results.

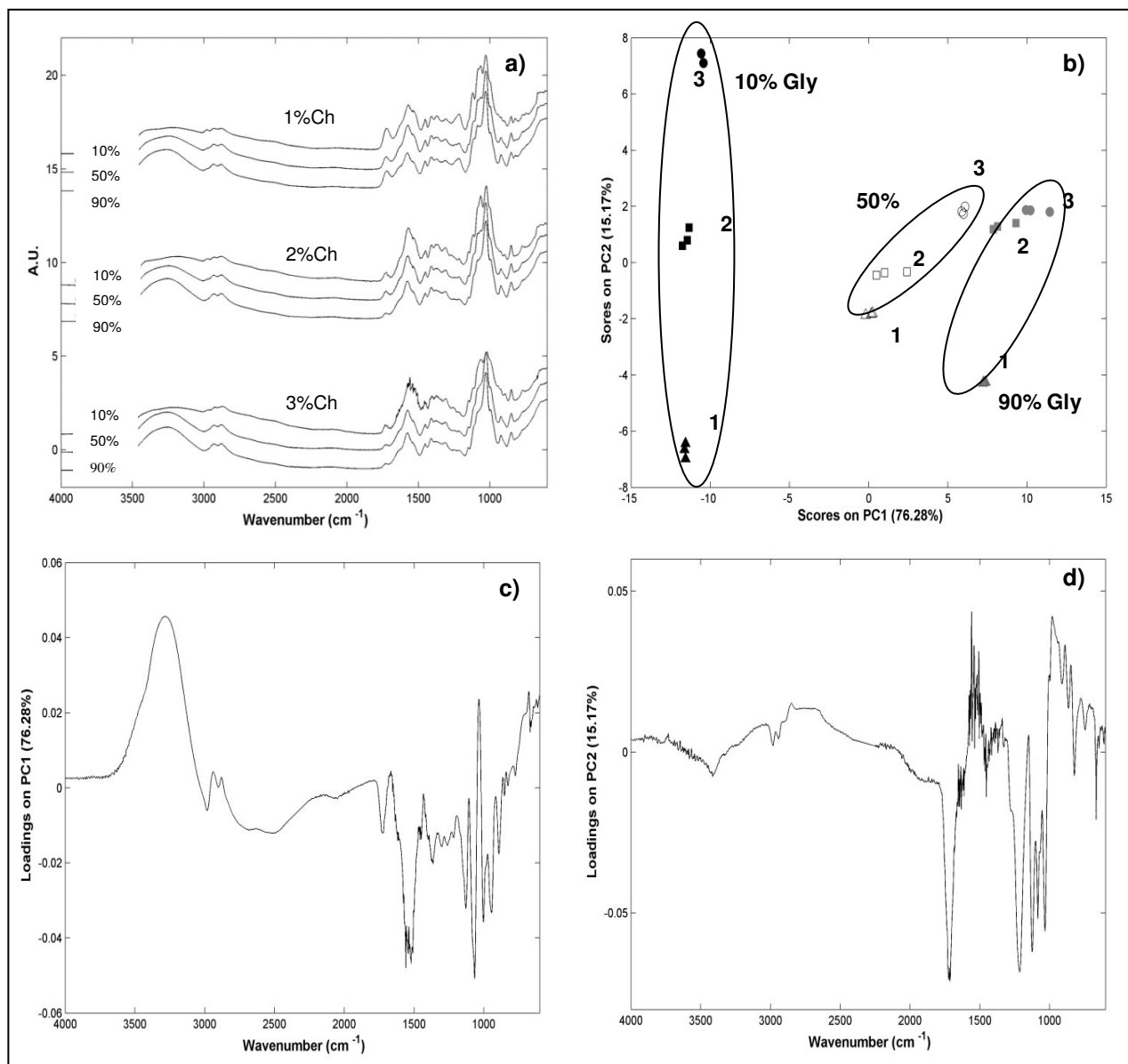


**Figure 2.3** Results obtained from FTIR measurements: a) FTIR measurements with different chitosan/glycerol percentage, b) representation of the scores resulting from PCA model applied to the films with different chitosan/ glycerol percentages (1-1%, 2-2% and 3-3% of chitosan) and c) PC1 and d) PC2 loading profiles plots of films according their chitosan/glycerol composition.

The residual lactic acid is evident in all films, as confirmed by a band arising at  $1715\text{ cm}^{-1}$  (Figure 2.3a) corresponding to the C=O from the carboxylic acid stretching (Lawrie et al., 2007).

Analysis of the whole spectra shows differences in the regions between  $3400$  and  $2815\text{ cm}^{-1}$ , refining the band with increasing glycerol content. This region corresponds to the stretching vibrations of the –O–H and –C–H groups, present in glycerol ( $\text{C}_3\text{H}_8\text{O}_3$ ).

Literature reports that chitosan with 85% of degree of deacetylation displayed two strong vibration bands at  $1645$  and  $1584\text{ cm}^{-1}$ ; those bands were assigned to amide I and amide II vibrations, respectively. It is also reported that amine deformation vibrations usually produce strong to very strong bands in the  $1638$ - $1575\text{ cm}^{-1}$  region (Lawrie et al., 2007).

In a chitosan spectrum, bands arise at  $1638\text{ cm}^{-1}$  and  $1583\text{ cm}^{-1}$  corresponding to the amide I, amine II and to the amine deformation. In Figure 2.3a a big band at  $1569\text{ cm}^{-1}$ , in between of two shoulders at  $1631\text{ cm}^{-1}$  and  $1529\text{ cm}^{-1}$ , are observed. The shift of those bands when compared with the pure chitosan spectrum could be due to the NH bending vibration at  $1583\text{ cm}^{-1}$ , which overlaps the amide II. Also, considering the protonation of the amines, which can cause an anti-symmetric deformation in the  $1625$ - $1560\text{ cm}^{-1}$  range and a symmetric deformation in the  $1550$ - $1505\text{ cm}^{-1}$  range, and the amide and amine moieties present in the films, the two represented bands must embody an envelope of at least five bands in close proximity (Lawrie et al., 2007).

Previous works have observed that the intensity of the amide II band was significantly affected by the level of plasticiser in a protein based film-films, without glycerol presenting a broader band's shape when compared with those with 40% of plasticiser in its composition (Gao et al., 2006). This observation is in agreement with the results presented in Figure 2.3a, where films with lower concentration of glycerol

(10%) in their composition presented a untidy band at  $1569\text{ cm}^{-1}$ , when compared with the films with higher plasticiser (50% and 90% of glycerol) in their composition. This indicates higher molecular vibration in the films with higher plasticiser content, which may be correlated by an increase of molecular mobility in these samples. Such hypothesis is supported by the increase of crystallinity in these samples (Table 2.3), with consequent increased free volume.

Figure 2.3b represents the PCA analysis of the films with different compositions; this figure confirms the previous results showing that the films form three homogenous clusters along the PC1 (reflecting glycerol interaction).

The loading profile of PC1 (Figure 2.3c) shows that the separation in the 3 different clusters is due mainly to the  $\text{-O-H}$  stretching vibration at  $3265\text{ cm}^{-1}$ , the  $\text{-O-H}$  bending at  $1665\text{ cm}^{-1}$ , the vibrations of  $\text{-C-H}$  group at  $1433\text{ cm}^{-1}$ , reflecting the increased glycerol and water content of the films, and to the C-O stretch vibrations with bands between  $1300$  to  $1000\text{ cm}^{-1}$  range, reflecting differences in the interaction between the different components (chitosan/glycerol/residual lactic acid) depending on film forming solution composition. Figure 2.3d also shows the separation of the films along the PC2 - in this case the contribution for this separation was attributed to the chitosan interaction, which increased with FFS chitosan concentration.

It is important to notice that the separation of samples within the same cluster decreased as the proportion chitosan/glycerol decreases (Table 2.1). This may be taken as an indication of chitosan conformational changes within the film with the increasing plasticiser agent, and shows the influence of polymer/plasticiser content on the film's final structure.



## 2.4. Conclusions

The properties of films produced with FFS at 3 different concentrations of chitosan and 3 different levels of glycerol were measured.

It was observed that the rheological behaviour of the FFS was chitosan concentration dependent.  $K$  (and indirectly the molecular entanglement in the solution) affected the MC and the properties of the films obtained after drying. This may be due to differences on the drying behaviour during film production and thus significantly affecting the mechanical and thermal properties of the obtained films.

Glycerol addition caused changes in the films structure, by increasing free volume. This was reflected on the mechanical and thermal behaviour of the films and also in the barrier and water related properties. Moreover, glycerol affected the crystalline lattice of the film, by changing the H-bonds in chitosan crystals. This conclusion is also supported by the FTIR results, where different interaction groups were observed according with the chitosan/glycerol ratios.

The effect of polysaccharide/plasticiser concentration on the microstructure and molecular dynamics of polymeric films systems will be a complementary study for understanding the behaviour of these structures.



## **CHAPTER 3**

**Molecular dynamics, composition and structure analysis**

---



**Abstract**

This chapter has the purpose to investigate the effect of polysaccharide/plasticiser concentration on the microstructure and molecular dynamics of polymeric film systems, using transmission electron microscope imaging (TEM) and nuclear magnetic resonance (NMR) techniques. Experiments were carried out in chitosan/glycerol films prepared with solutions of different composition. The films obtained after drying and equilibration were characterised in terms of composition, thickness and water activity.

Results show that glycerol quantities used in FFS were responsible for films composition; while polymer/total plasticiser ratio in the solution determined the thickness (and thus structure) of the films. These results were confirmed by TEM.

NMR allowed understanding the films molecular rearrangement. Two different behaviours for the two components analysed, water and glycerol, were observed: the first is predominantly moving free in the matrix, while glycerol is mainly bounded to the chitosan chain.

### 3.1. Introduction

In the last years nuclear magnetic resonance (NMR) has been presented as a powerful technique to understand and evaluate molecular mobility of semi crystalline systems. Specifically,  $^1\text{H}$  NMR has been used to investigate water dynamics and physical structures of foods through analysis of nuclear magnetisation relaxation times (Li et al., 2000). In these measurements the samples are submitted to a static magnetic field and the protons are excited by means of a radiofrequency pulse. The analysis of the signal emitted while the sample returns to equilibrium (FID) allows determining the spin-lattice ( $T_1$ ) and spin-spin or transverse ( $T_2$ ) relaxation. This later variable is related with the mobility of the protons in the samples matrix. The stability of food “matrix” (system) depends strongly on its molecular mobility (as discussed before) but also on its microstructure. Foods are highly structured and heterogeneous materials composed of architectural elements. The types of such structural units and their interactions are decisive in the food stability, since they influence water/solute interactions and hence the water availability to participate in degradation reactions. Microscopy techniques have been widely used in foods to study their architecture and microstructure (Aguilera et al., 2000). Transmission Electron Microscopy (TEM) specifically, visualises the internal structure of food samples (Kaláb et al., 1995), helping to clarify biological systems dynamics.

Edible films have been studied for a long time for their potential to improve shelf-life and safety of food products (Aider, 2010; Epure et al., 2011). These systems are partially crystalline/partially amorphous, easily reproducible materials and are thus very interesting food model systems to molecular mobility studies and microstructure studies. The addition of low molecular weight plasticisers to amorphous biopolymers increases the matrix free volume and the molecular mobility, in an effect similar to increasing temperature (Lazaridou and Biliaderis, 2002; Lefebvre and Escaig, 1993). These additives reduce the tension of deformation, hardness, density, viscosity

and electrostatic charge of a polymer, at the same time increasing chain flexibility, resistance and dielectric constant (Ferry, 1980). Plasticisers modify the matrix second-order interactions of materials (which are responsible for polymeric materials crystalline structures), without altering their fundamental chemical character. This modification is achieved by forming weak second-order or covalent bonds with the polymer. However, plasticisers can also migrate in the polymer leading to material recrystallization and a loss of elasticity (Domjan et al., 2009). In addition plasticisers can also affect water retention capacity (Lefebvre and Escaig, 1993).

Water, considered a plasticiser, is one of the most important solvent medium in biological systems (Matveeva et al., 2000). It greatly affects the mobility of biopolymers components and is considered as an abundant and very effective solvent/plasticiser for hydrophilic materials (Lazaridou and Biliaderis, 2002). On a molecular level, water plasticisation of a polymer leads to increased free volume, decreased local viscosity and increased back-bone chain mobility (Slade and Levine, 1991).

Chitosan, structurally considered as a semicrystalline biopolymer (Bangyekan et al., 2006; Pillai et al., 2009; Rinaudo, 2006), is a polysaccharide composed mainly of (1→4) linked residues of N-acetyl β-d-glucosamine and (1→4) β-d-glucosamine (Arzate-Vázquez et al., 2012; Ostrowska-Czubenko and ska, 2009; Prashanth and Tharanathan, 2007; Rinaudo, 2006; Yang et al., 2010). Chitosan crystal structure is stabilised by intramolecular and intermolecular H-bonds, with the acetamide groups playing the major role in the formation of second-order bonds between adjacent chains (Okuyama et al., 1997), making the chitosan structure on a film very dependent on the type and quantity of plasticisers used.

Through this chapter an effort is made to understand the relationship between the composition of FFS and the properties (composition and microstructure) of the obtained glycerol plasticised chitosan films, evaluating the role of water and glycerol

as plasticiser agents, and the effect of their concentrations in the systems performance. Also, we aimed at analysing the molecular mobility of such films, in order to recognise its properties and improve its suitability as models for more complex food systems. For that purpose, film forming solutions of different polymer/plasticiser concentrations were prepared and the obtained films characterised in terms of composition, molecular mobility and microstructure.

## **3.2. Materials and methods**

### ***3.2.1. Chitosan films preparation***

Chitosan films preparation was performed as described in section 2.2.1.

### ***3.2.2. Characterisation of the chitosan films***

#### *3.2.2.1. Chemical composition*

The final composition in chitosan, glycerol and water of the obtained films was determined. Chitosan concentration was estimated using a spectrophotometric method (Muzzarelli, 1998). Briefly, chitosan films were dissolved in 100 mL of lactic acid solution 4%. Cibacron brilliant red 3B-A from Sigma (Milano, Italy) was used as dye. A solution of dye was prepared by dissolving 150 mg of the powder in ultra-pure water, using a 100 mL volumetric flask. Aliquots of the dye solution (5 mL) were made up to 100 mL with 0.1 M glycine hydrochloride buffer. Spectrophotometric measurements were done at room temperature and at 575 nm, with a wavelength spectrophotometer (UV – 1601; Shimadzu Co., Kyoto; Japan).

Glycerol concentration in films was determined using a quantitative enzymatic determination (Free Glycerol Determination Kit, from Sigma, Milano, Italy).



Spectrophotometric measurements were performed at room temperature and 540 nm wavelength, using the same spectrophotometer.

Water content was determined by difference.

#### 3.2.2.2. Thickness

Thickness of films was determined as described in section 2.2.4.3

#### 3.2.2.3. Water activity

Films  $a_w$  was determined as described in section 2.2.2.2.

#### 3.2.2.4. Nuclear magnetic relaxation

A Bruker AVANCE III solid state spectrometer (300 MHz) was used to determine the samples nuclear transverse relaxation time, or spin-spin,  $T_2$ , of the protons.

These values were obtained from the exponential or bi-exponential echoes envelope of a series of Carr- Purcell-Meiboom-Gill (CPMG) multi-echo pulse sequence, which circumvents the field and sample heterogeneities and gives access to the intrinsic  $T_2$  of the protons, while the Free Induction Decay (FID) obtained from a single pulse just gives a  $T_2^*$  determined mainly by the field non-uniformity in the heterogeneous film sample contained in the NMR 5 mm tubes.

The analysis of the CPMG echoes envelope showed that the relaxation of the protons in chitosan/glycerol films follow a bi-exponential function. Both  $T_2$  values were obtained by a non-linear least-square fit of the envelope data  $T_2$  water and  $T_2$  glycerol, of the function:

$$A = A_1 e^{-\frac{t}{T_{2\text{water}}}} + A_2 e^{-\frac{t}{T_{2\text{glycerol}}}} \quad (3.1)$$

$A_1$ : water population;  $t$ : time;  $T_{2water}$ : water proton transverse relaxation time;  $A_2$ : glycerol population;  $T_{2glycerol}$ : glycerol proton transverse relaxation time

The first point of the multi-echo acquisition pattern was normalised to unity; therefore  $A_1$  and  $A_2$  relate to the corresponding populations' percentage.

#### 3.2.2.5. Microstructure

Transmission electron microscope analyses were performed according to a literature described methodology (Tapia-Blácido et al., 2011). Small pieces of films were prepared by fixation in 20 mL L<sup>-1</sup> glutaraldehyde and post-fixed in 20 g L<sup>-1</sup> OsO<sub>4</sub>. Samples were dehydrated for 15 min in an ethanol series (30, 50, 70, 90 mL/100 mL), three times for 15 min at 99.5 mL/ 100 mL, and twice for 20 min in propylene oxide. The samples were then embedded in increasing concentrations of propylene oxide: resin (2:1, 1:1, and 1:2) for 1 h, and for 48 h in Epon 812 resin. The polymerization of the resin subsequently proceeded at 60 °C for 24 h.

Ultrathin sections (40-60 nm thickness) were prepared on a Reichert SUPERNOVA LEICA Ultramicrotome (Germany) using diamond knives (DDK, Wilmington, DE, USA). The sections were mounted on 300 mesh nickel grids, and examined under a JEOL JEM 1400 TEM (Tokyo, Japan). Images were digitally recorded using a Gatan SC 1000 ORIUS CCD camera (Warrendale, PA, USA).

### 3.3. Results and discussion

#### 3.3.1. Composition of the films

Drying is one of the critical processes in film preparation, since during this process, the polymer and/or plasticiser concentrations may change (Wong et al.,

2004). In this study, the drying process was kept constant in all films, but film forming solutions with different compositions were tested.

The composition and thickness of the films obtained after drying are shown in Table 3.1. It can be observed that the chitosan concentration in the obtained films does not correlate with the chitosan content of the solutions used for preparing each film. For example, films prepared using 1% (w/w) chitosan FFS presented different final polymer content. However, it is possible to find a relationship between the glycerol added to the FFS and the composition of the obtained film: for solutions with constant polymer concentration, when the amount of plasticiser in the solution increases, the chitosan content in the film decreases. Moreover, it is possible to observe that polymer concentration in the solution is correlated with the thickness of the obtained films (Table 3.1), i.e. increasing the content of chitosan in the solution will originate thicker films (data in Appendix B, Table B.1.1).

**Table 3.1** Composition and thickness of the films obtained, using different polymer/plasticiser percentages in film forming solutions.

FFS				Films				
Samples	Chit (g)	Gly (g)	Ratio (Chit/Gly)	Chitosan content (mg g <sup>-1</sup> film)	Glycerol content (mg g <sup>-1</sup> film)	Ratio (Chit/ Gly)	Water content (mg g <sup>-1</sup> film)	Thickness (mm)
<b>1%10%</b>	5	0.63	7.94	388.13±16.885 <sup>a</sup>	11.47±0.019 <sup>a</sup>	33.84	600.40	0.0642
<b>1%50%</b>	5	3.15	1.59	196.13±34.261 <sup>a</sup>	31.68±0.143 <sup>a</sup>	6.19	810.17	0.0556
<b>1%90%</b>	5	5.67	0.88	158.15±21.535 <sup>a</sup>	47.90±0.058 <sup>a</sup>	3.30	755.97	0.0605
<b>2%10%</b>	10	1.26	7.94	356.88±23.494 <sup>a</sup>	13.47±0.027 <sup>a</sup>	26.49	629.65	0.1344
<b>2%50%</b>	10	6.31	1.58	171.85±39.978 <sup>a</sup>	30.04±0.119 <sup>a</sup>	5.72	798.11	0.1357
<b>2%90%</b>	10	11.40	0.88	164.43±9.240 <sup>a</sup>	36.72±0.068 <sup>a</sup>	4.20	798.85	0.1527
<b>3%10%</b>	15	1.89	7.94	388.14±20.396 <sup>a</sup>	14.72±0.050 <sup>a</sup>	26.37	597.14	0.2844
<b>3%50%</b>	15	9.46	1.59	181.63±30.075 <sup>a</sup>	46.18±0.039 <sup>a</sup>	3.93	772.19	0.2348
<b>3%90%</b>	15	17.10	0.88	195.71±37.529 <sup>a</sup>	53.36±0.083 <sup>a</sup>	3.67	750.93	0.2452

±95% Confidence error

These results suggest that films composition is governed by the amount of plasticiser in the FFS, while the amount of polymer added will influence the structural rearrangement of the film. i.e., with this work experiment design were obtained films with similar composition (chitosan, glycerol and water  $\text{mg g}^{-1}\text{film}$ ) with thickness varying ca 5 fold. This may indicate that chitosan and plasticiser molecules are arranged in different structures in the matrix, e.g. different crystal size and quantities and/or types. This hypothesis is supported by the fact that, these films (of same composition, but different thickness) presented different crystallinity (evaluated by the change in enthalpy (results included in Appendix A, Table A.2.5) and by TEM observation (see discussion below). The phenomenon responsible for this observation is not clear. However, it can be observed that the solutions used to prepare these films had all the same chitosan/glycerol ratio but different chitosan/total plasticiser (i.e. glycerol + water) ratio. This seems to indicate that this ratio is the one actually responsible for the type of bonds and interactions formed during the drying process.

### ***3.3.2. Molecular mobility***

Molecular mechanisms that control functionality in polymeric films are still poorly understood, particularly in chitosan films. Studies on the mobility of the different components at molecular level in the films matrix may help to explain structural phenomenon and simultaneously the effect of plasticiser addition. An example obtained from NMR measurements is shown in Figure 3.1.

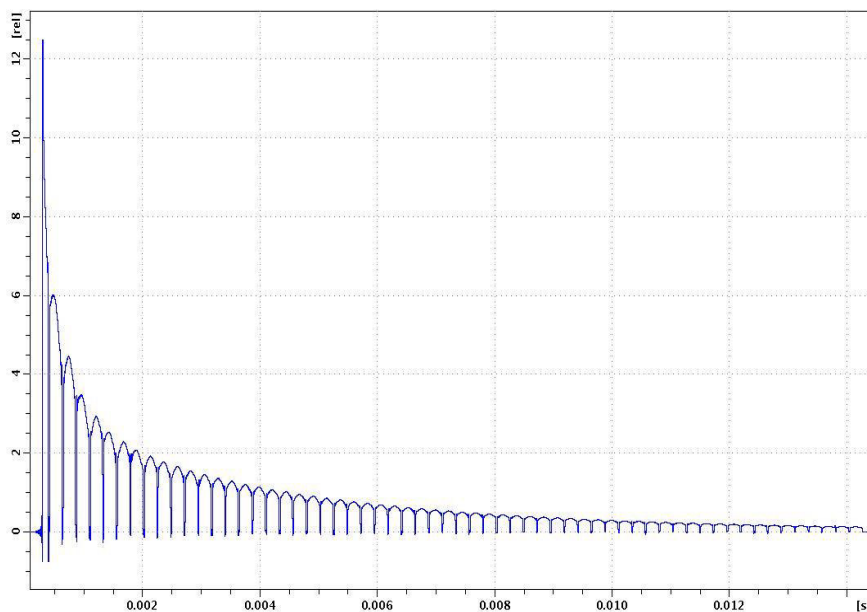


**Figure 3.1** Proton multi-echo acquisition of a chitosan/glycerol sample with a CPMG multi-pulse sequence. The echo envelope is bi-exponential, with a fast and a slow decay of the transverse nuclear magnetism.

Results show that the relaxation of protons in chitosan/glycerol films follow a two components bi-exponential function, indicating the existence of two different populations, with distinct relaxation behaviour (Hills et al., 1991) (data included in Appendix B, Table B.2.1). The two relaxation times determined in each film were assigned to water and glycerol, as they were the only components with a proton with the capacity to move. Considering the relative size of the water and glycerol molecules, the higher relaxation time, corresponding to a more mobile molecule, was assigned to the water proton and the lower relaxation times to the glycerol proton. No relaxation attributable to polymer mobility was observed in the obtained spectra, even if the plasticisers in the system are expected to soften the rigid structure of the chitosan polymeric chain (Domjan et al., 2009).

As discussed above, plasticisers are responsible for modifications in biopolymers physical properties (Hills et al., 1991). As referred in previous chapters,

water also acts as a plasticiser, since, water molecules can create hydrogen bonds with the polymeric chains present in the system, thus increasing the macromolecular system free volume and contributing to a more flexible polymeric chain. In this study, the molecular mobility in the films was evaluated using nuclear magnetic resonance techniques (NMR) to determine relaxation time of the molecules present in the system.

Figure 3.2a shows the  $T_2$  of the water molecules against the composition of the different films. It is possible to observe that water relaxation time ( $T_{2water}$ ), did not seem to be dependent on the chitosan content in the films, but increases with increasing glycerol content. This is due to the plasticiser effect, which reduces the intermolecular forces and increases the overall mobility in the matrix (Srinivasa et al., 2007). On Figure 3.2b, it is possible to observe that water mobility decreased with increasing chitosan/glycerol ratio in the film.

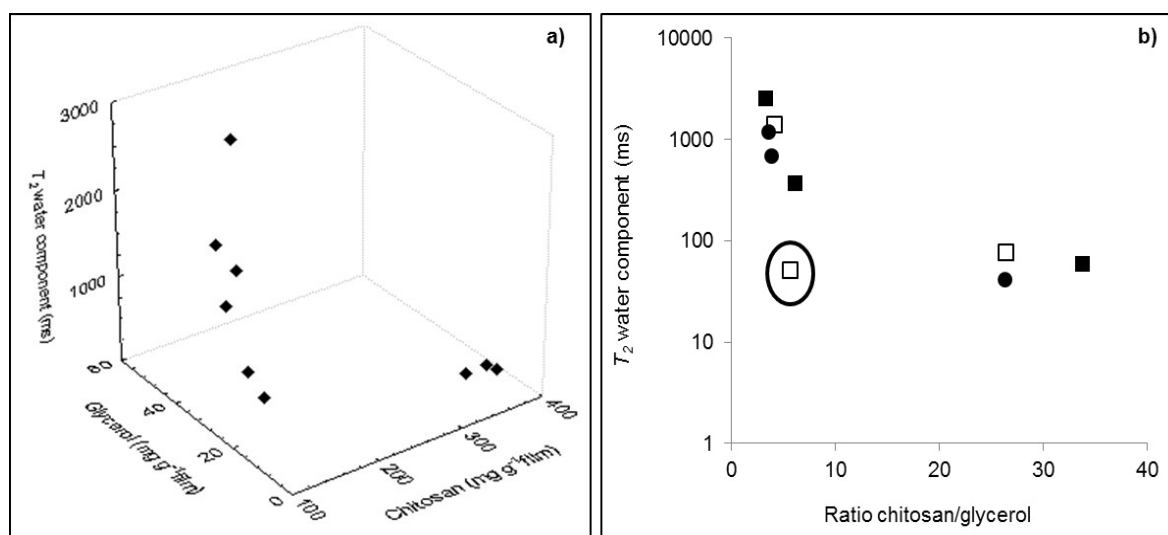


**Figure 3.2** Films relaxation time ( $T_2$ ) for water molecules as function of different chitosan and glycerol concentrations (a) and for the ratio chitosan/glycerol in the films (b). Results grouped films of the same final thickness: produced with ■ 1%, □ 2% and ● 3% chitosan in the film forming solutions.

A similar effect was observed in starch/glycerol films (Godbillot et al., 2006). In this study, the authors postulate that the number of available binding sites in the polymer chain will be “preferentially” occupied with glycerol, while water will only occupy polymer binding sites in the case no sufficient glycerol molecules are available. Our results for a chitosan/glycerol system follow the same observation: when the film glycerol content was not sufficient to occupy all the free sites on the polymer chain, the water molecules presented a decreased relaxation time, indicating water is bound to chitosan. When the amount of plasticiser molecules increase, the polymer binding sites get more and more occupied by the glycerol molecules, leaving the water free to move in the chitosan matrix. There was an exception to this behaviour: films produced with 2% chitosan and 50% glycerol (marked on Figure 3.2 with a circle) presented a much lower  $T_2$  than the one observed in films with similar composition, and a deviate behaviour regarding the expected  $T_2$  for the determined ratio chitosan/glycerol. This phenomenon has been reported in literature as the antiplasticisation phenomenon (Lourdin et al., 1997) attributable to a strong interaction occurring between the polymer and the plasticiser, producing a “cross-linker” effect, which decreases the free volume and the molecular mobility (Lourdin et al., 1997).

In order to better evaluate the role of polymer, plasticiser and/or water binding and interactions, were compared the results of water mobility with the films water content and  $a_w$  (Figure 3.3). Figure 3.3a shows the relationship between water  $T_2$  and water content of the films. The water molecular mobility increases with water content, which in turn is higher for samples with higher glycerol content. These results confirm the above discussed preferred affinity between chitosan and glycerol: i.e. the water molecules are free in the matrix to move, because the polymer binding sites are occupied with glycerol (Godbillot et al., 2006).



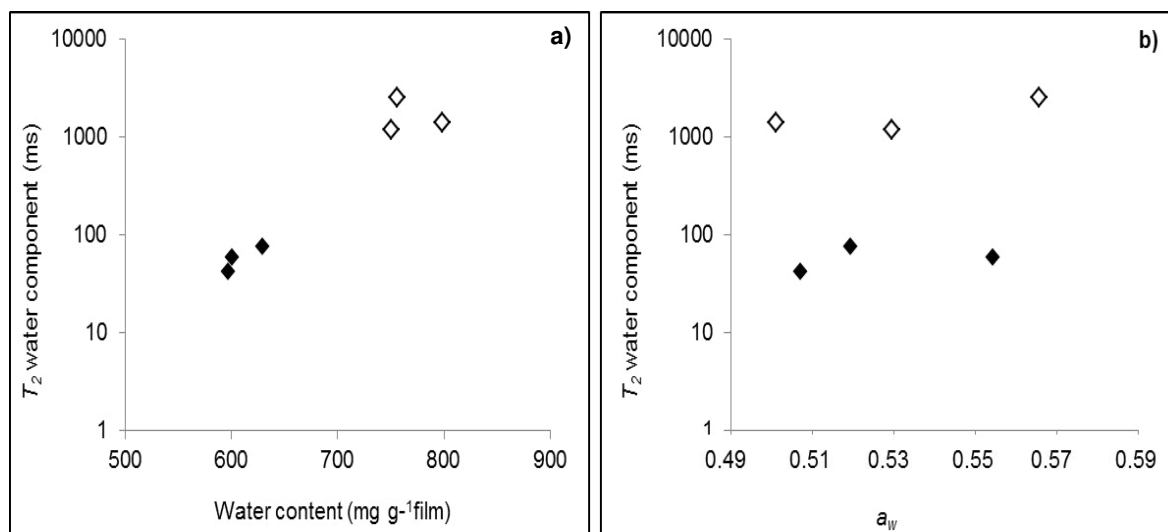


**Figure 3.3** Films relaxation time ( $T_2$ ) for water molecules as a function of water content (a) and *water activity* (b). Results grouped by films of same final composition: produced with 10% glycerol solution (white bullets) and 90% glycerol solution (black bullets). Samples prepared with 50% of glycerol are not shown because of the deviant behaviour (antiplasticisation), which impairs the data analysis.

Literature reports that water in biopolymer systems can be present in three different states: free in the bulk, at the surface and bound (Hills et al., 1996c). Other authors have indicated that water activity is the result of the bulk and surface water (Mathlouthi, 2001). Since water bounded to the polymeric chain has no mobility, from our results, it is clear that the measured relaxation time refers to the water in the bulk: in films of the same composition (same total water content) the increase in water activity (water at the surface and in the bulk) does not reflect on water mobility (Figure 3.3b). This observation may be of great value for studies on degradation reactions in food systems and contribute for understanding differences in the stability of foods with same  $a_w$ .

In respect to the mobility of glycerol, different tendencies were observed (Figure 3.4). Glycerol  $T_2$  decreased with increasing of chitosan concentrations, especially for the higher concentrations, again suggesting that glycerol may be closely

bond to the chitosan chain network (Figure 3.4a). This is in accordance with the results above described. Again, it is possible to observe the antiplasticisation phenomenon in the films produced with 2% of chitosan and 50% of glycerol (also marked with a circle).

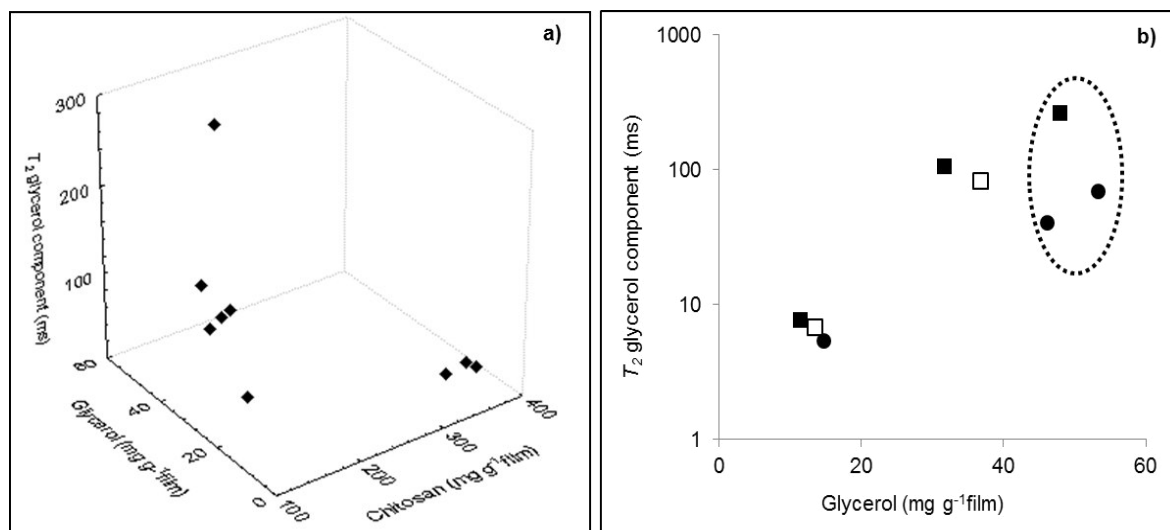


**Figure 3.4** Films relaxation time ( $T_2$ ) for glycerol molecules of: a) different chitosan and glycerol concentration, and b) glycerol content ( $\text{mg g}^{-1}\text{film}$ ). Films produced with ■ 1%, □ 2% and ● 3% chitosan in the film forming solutions, each group corresponding to thickness of the obtained film. Again, antiplasticised samples are not shown.

In Figure 3.4b it is possible to observe the relationship between glycerol mobility and glycerol content of films, grouped by films of similar thickness. It shows that for films with the same thickness, glycerol mobility increases with increasing glycerol content. However, comparing films with approximately the same amount of glycerol,  $T_2$  decreases with increasing thickness of the film (see for example the data points highlighted with a dashed circle). At a first glance these results are unexpected: the films present approximately the same amount of chitosan, which would imply that an increase in thickness means an increase of the free volume in the matrix. However, the thicker films are produced with less water molecules per chitosan

molecules in the FFS and thus it is possible that during the drying process more glycerol molecules bind to the polymeric chain – hence glycerol is not free to move in the matrix of the obtained film. This result supports our previous hypothesis that the ratio polymer/total plasticiser in the FFS is critical for the type of bonds formed during the films drying.

### **3.3.3. Microstructure**

As discussed above, in this study were obtained films with similar composition and significantly different thickness (Table 3.1), which may indicate differences in the films structure. To investigate such possibility, the films were observed using TEM. This microscopy technique allows characterising the interior of the films since the electron beam is transmitted through the sample, allowing specific observation of structures in the sample (Andreuccetti et al., 2009; Denavi et al., 2009; Tapia-Blácido et al., 2011).

Chitosan films transmission electron images are presented in Figure 3.5, which shows the films semicrystalline structure. The black aggregates represent the crystalline component, whereas the homogeneous crowd corresponds to the amorphous constituent of the sample. As above, samples images are grouped by films with similar composition and films with similar thickness.

Images show that the films with similar thickness present similar structures, with visible crystals decreasing with decreasing chitosan content: i.e. films produced with 1% chitosan FFS have clearly evident crystals, scattered in matrix, showing a heterogeneous feature. As the chitosan content decreases, crystals are not anymore observed in the obtained images. However, this may not correspond to an absence of crystals in the samples: the crystals may be smaller than the resolution of the equipment.

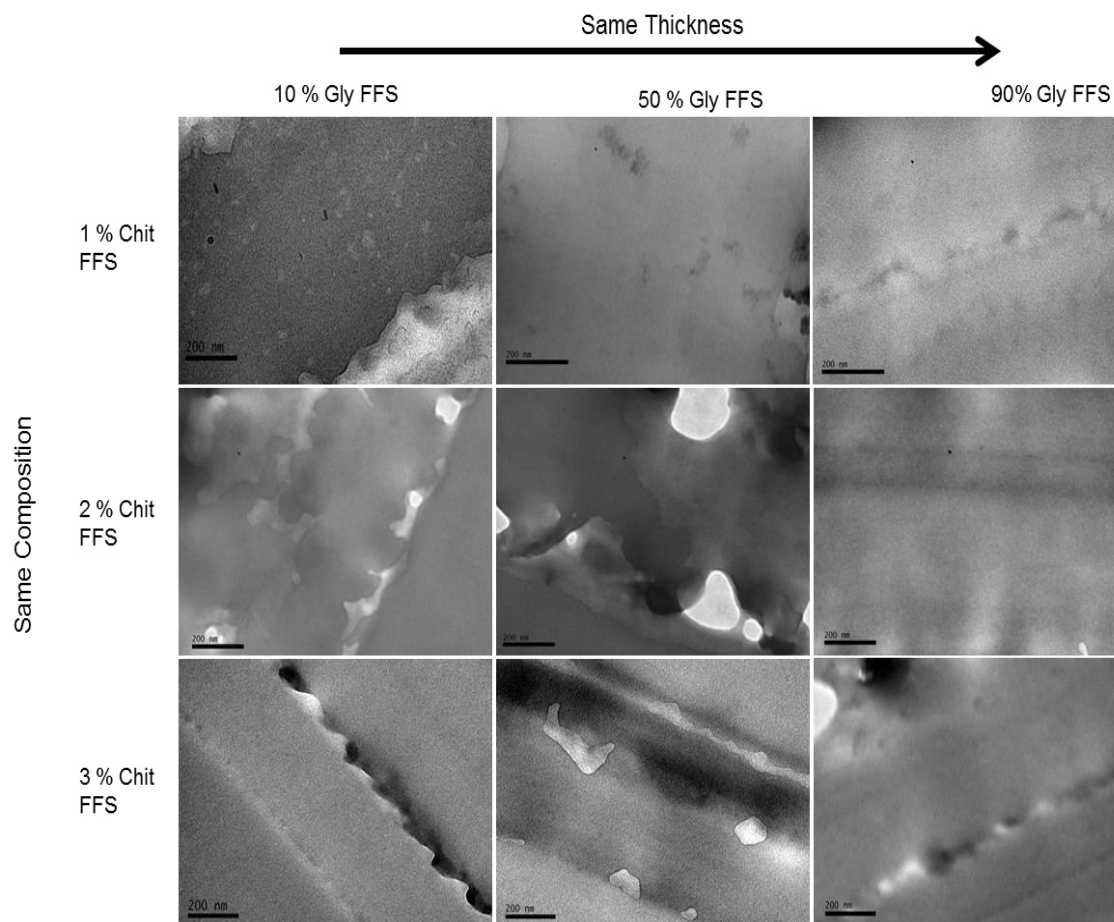


**Figure 3.5** TEM micrographs of the films produced with different polymer/plasticiser concentrations.

Furthermore, films with the same thickness were prepared by FFS with the same chitosan content (see Table 3.1). This confirms the above hypothesis that it is the chitosan-water ratio in the FFS that define the quantity/type of structures formed in the film. These structures are important, because they may interfere with transport phenomena in the film and how they are formed can be important information for functional films development. For films with similar composition, there is no apparent relationship with the structures visible in the image, which may be an indication that film composition may not be related with the functionality at macroscopic level (Vargas et al., 2011).

The results of the microstructure observations also confirm the discussions above on the polymer-plasticiser-water interactions and their effect on the molecular mobility: the films with more visible crystals correspond to the films with higher water relaxation times (higher free volume) – i.e. in the films where chitosan binding sites are “occupied” by polymer-polymer interactions in the crystalline lattice, the water and glycerol molecules are free to move in the matrix.

### 3.4. Conclusions

Results from this chapter demonstrated that glycerol quantities used in film forming solutions were responsible for chitosan concentration obtained in films and, consequently for films composition; while film forming solutions polymer/total plasticiser ratio determined the thickness (and thus structure) of the films and these conclusions were confirmed by TEM. These results can be useful for the development of edible films of improved functionality.

Results on molecular mobility contributed to the understanding of the films molecular rearrangement. NMR measurements showed two different behaviours for the two components analysed, water and glycerol: while glycerol is mainly bounded to the chitosan chain network, the water present in the system is predominantly free from the polymeric chain. However, it was possible to infer that for lower glycerol concentrations, free chitosan binding sites can also be occupied by water molecules.

Water content and  $a_w$  measurements also allowed concluding that not only the water content affects the water mobility, but also structural differences in the film may influence the water relaxation time. Also it was possible to observe that water mobility relates to the water in the bulk and thus complements information on water activity of a system.

## **CHAPTER 4**

### **Molecular dynamics and functional properties**

---





**Abstract**

Foods, from a fundamental perspective, are partially crystalline partially amorphous systems. Edible films are considered good models for food systems, because of their interesting physical properties, quite straightforward matrices, and easy reproduction. Chitosan has been thoroughly used in edible films studies.

The purpose of this chapter is to investigate the relationship between the molecular relaxation time in chitosan films, their microstructure (crystallinity) and functional properties. Analyses were carried out using data on chitosan/ glycerol films prepared with different polymer/plasticiser concentration.

In general, results demonstrate that there is a relationship between macroscopic properties and water and glycerol relaxation times. Moreover, results also show that while water is free in matrix, glycerol is linked to the chitosan polymeric chains, decreasing intermolecular attractions and increasing free volume, thus facilitating molecular migration. Also the data analysis reveals the usefulness of NMR and molecular mobility studies in the matrix for characterisation and development of polymeric structures.

#### 4.1. Introduction

Foods are essentially semicrystalline matrices, basically composite materials with crystalline and noncrystalline regions (Jeck et al., 2012; Spathis and Kontou, 1998), whose configuration exhibit remarkably complex arrangements at the molecular scale (Corté and Leibler, 2007).

The glass transition temperature concept has been applied in food science and technology research (Slade and Levine, 1991) and recognises the noncrystalline (amorphous) or partially crystalline state of solid foods, and solids plasticisation by water. This concept, that links food stability and glass transition, has been extensively studied by the food science and technology community, in order to better understand the molecular mobility point of view. Molecular mobility is considered a fundamental parameter in knowledge and understanding the dynamic properties of food components (Roudaut et al., 2004) Nowadays, in order to better understand this parameter, NMR is being used as a powerful technique to understand and evaluate molecular mobility of semicrystalline systems, including food systems, since it is able to provide information on molecular dynamics of different components in complex systems (Domjan et al., 2009)

As it was mentioned before, the stability of a food system depends strongly on its molecular mobility. Thus, studies on relaxation times of food matrices components (mainly water) and its correlation with macroscopic properties seems to be of great value for studies on degradation reactions and can, as an example, contribute to understand differences in the stability of foods with the same water activity. Consequently, it is useful to determine how molecular mobility modulates such properties of foods (Ludescher et al., 2001). These studies are also of great interest in edible films, since they are models for more complex food systems, and also very useful products in food technology. Chitosan is a polymer that has been widely used due to its characteristics, namely its excellent filmogenic properties (Aider, 2010;

Martínez-Camacho et al., 2010; Rinaudo, 2006) It is of great interest to fully characterise the solid state physical and physicochemical properties of chitosan films, including the molecular mobility that occurs within the polymeric structure, in both wide temperature and time scale ranges (Viciosa et al., 2004). Moreover, the molecular mechanisms that control functionality in polymeric films, like chitosan, are poorly understood and it is important to clarify the solid-state structure and molecular mobility for better understanding of the physical properties of semicrystalline matrices (Kuwabara et al., 2004).

The objective of this chapter was to systematically evaluate the link between molecular mobility and the thermo-mechanical properties in water glycerol plasticised chitosan films, as semicrystalline matrices.

## **4.2. Materials and methods**

The data used for the analysis presented in this chapter was reported previously in chapters 2 and 3. Briefly, chitosan/glycerol films were prepared with solutions of different polymer and plasticiser concentrations. The thermal, mechanical and water permeability properties of the obtained films after drying and equilibration were determined. The transverse relaxation time of the protons was also determined using NMR, showing two main proton populations corresponding to water and glycerol.

## **4.3. Results and discussion**

The composition and thickness of the films, resulting from the different chitosan/glycerol combinations used in FFS preparation, are presented in Table 4.1. It can be observed that films with the same composition can present different thickness (this was dependent on the ratio polymer/plasticiser of the FFS), i.e. the same amount

of molecules can be more or less dispersed in the matrix. It indicates that in these films the polymer may be re-arranged in different structures.

**Table 4.1**

Polymer/plasticiser/water composition and thickness of films produced with different formulations.

FFS					Films						
Samples		Chit (g)	Gly (g)	Ratio (Chit/ Gly)	Chit content		Gly content		Ratio (Chit/ Gly)	Water content ( mg g <sup>-1</sup> film )	Thickness (mm)
Chit (%)	Gly (%)				mg g <sup>-1</sup> film	average	mg g <sup>-1</sup> film	average			
1	10	5	0.63	7.94	388.13	388.13	11.47	13.10	33.84	600.40	0.0642
3	10	15	1.89	7.94	388.14		14.72		26.37	597.14	0.2844
1	50	5	3.15	1.59	196.13	188.88	31.68	38.93	6.19	810.17	0.0556
3	50	15	9.46	1.59	181.63		46.18		3.93	772.19	0.2348
1	90	5	5.67	0.88	158.15	176.96	47.90	50.60	3.30	755.97	0.0605
3	90	15	17.10	0.88	195.71		53.36		3.67	750.93	0.2452

#### **4.3.1. Molecular mobility versus thermal properties**

Figure 4.1a and b present, respectively, chitosan films water  $T_2$  and glycerol  $T_2$  as a function of  $T_g$ . Glass transition temperature can be correlated with the molecules mobility in matrices, since it is considered the macroscopic manifestation of cooperative changes in the molecular mobility (Ludescher et al., 2001).

Both plasticisers (water and glycerol) had similar behaviour. However, water presented transverse relaxation times 10 times higher than the glycerol relaxation times, for the same glass transition temperature (i.e. for the same film). This is related with the available binding sites in the polymer chain that are preferentially occupied

with glycerol, leaving the water molecules free to move in the system (Godbillot et al., 2006).

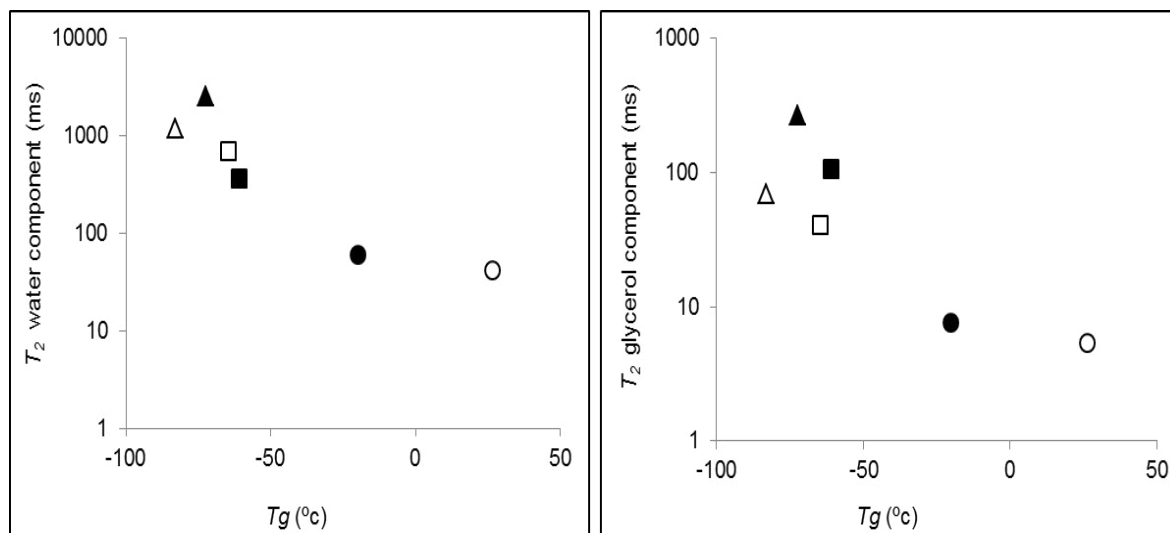


**Figure 4.1** Films water (a) and glycerol (b) relaxation time ( $T_2$ ), at room temperature, as a function of glass transition temperature ( $T_g$ ). Empty symbols correspond to thinnest films (range between 0.0556 and 0.0642 mm); fill symbols correspond to thickest films (range between 0.2348 and 0.2844 mm). Different data points symbols indicate the different compositions (see Table 4.1):

O/● - 388.13 Chit and 13.10Gly; □/■ - 188.88 Chit and 38.93Gly; Δ/▲ - 176.96 Chit and 50.60Gly

At room temperature,  $T_2$  decreases with increasing  $T_g$  (Figure 4.1), and this is in accordance with the classic polymer theory described before. These results show also that for similar thickness, films with different composition (see Table 4.1) present different  $T_g$ , i.e. free volume, stressing the importance of these two variables on the thermal behaviour of the system.

This is also evidenced on the films melting endotherm and the relationship with water and glycerol relaxation times (Figure 4.2). The melting endotherm is the energy required to melt the crystals present in the matrix and thus, an indirect measurement of the crystallinity.

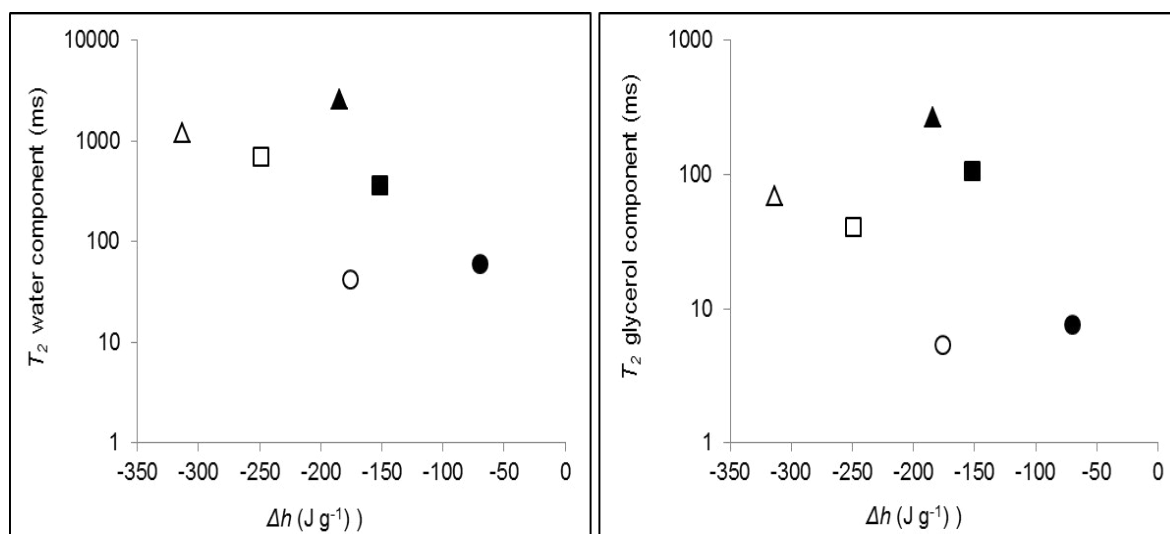


**Figure 4.2** Films water (a) and glycerol (b) relaxation time ( $T_2$ ), as a function of films melting enthalpy ( $\Delta h$ ). Empty symbols correspond to thinnest films (range between 0.0556 and 0.0642 mm); fill symbols correspond to thickest films (range between 0.2348 and 0.2844 mm). Different data points symbols indicate the different compositions (see Table 4.1):

$\circ/\bullet$  - 388.13 Chit and 13.10Gly;  $\square/\blacksquare$  - 188.88 Chit and 38.93Gly;  $\Delta/\blacktriangle$ -176.96 Chit and 50.60Gly

A relationship between crystallinity and relaxation times for both molecules can be observed:  $T_2$  increases with crystallinity (larger absolute value of  $\Delta h$ ). Literature reports that the presence of crystals can change the properties of the amorphous regions. This is because the polymeric chain is organised in the crystalline lattice and the polymer binding sites are “occupied” with polymer-polymer bonds. As such, two factors contribute to the increase of the transverse relaxation time with crystallinity: i) the free volume of the system increases, and ii) the water and glycerol molecules are free to move in the matrix.

### **4.3.2. Molecular mobility versus mechanical properties**

The relationship between molecular mobility and films structure is also observed on the mechanical properties. Figure 4.3 presents the water (a) and (c) and glycerol (b) and (d) relaxation times as a function of EB and TS.

These properties are critical for films development, since they reflect their ability to perform in different applications (Chen and Hwa, 1996; Leceta et al., 2013). It can be observed that when  $T_2$  increases, EB increases in an exponential relationship, while TS decreases also exponentially – showing clearly an effect of molecular mobility on mechanical properties. Above, it was concluded that films with higher molecular relaxation times are more crystalline and have more free volume. Figure 4.3 allows also to conclude that these films are more deformable (high EB) and easier to break (low TS). Again, the molecular bonds and molecular rearrangement are the key point. In such systems there are two main types of bonds: i) strong polymer/polymer interactions, and ii) weak polymer/plasticisers and plasticiser/plasticiser bonds. A similar co-relation between increased crystallinity on the mechanical properties has been reported in the literature (Bourbon et al., 2011; Ziani et al., 2008).

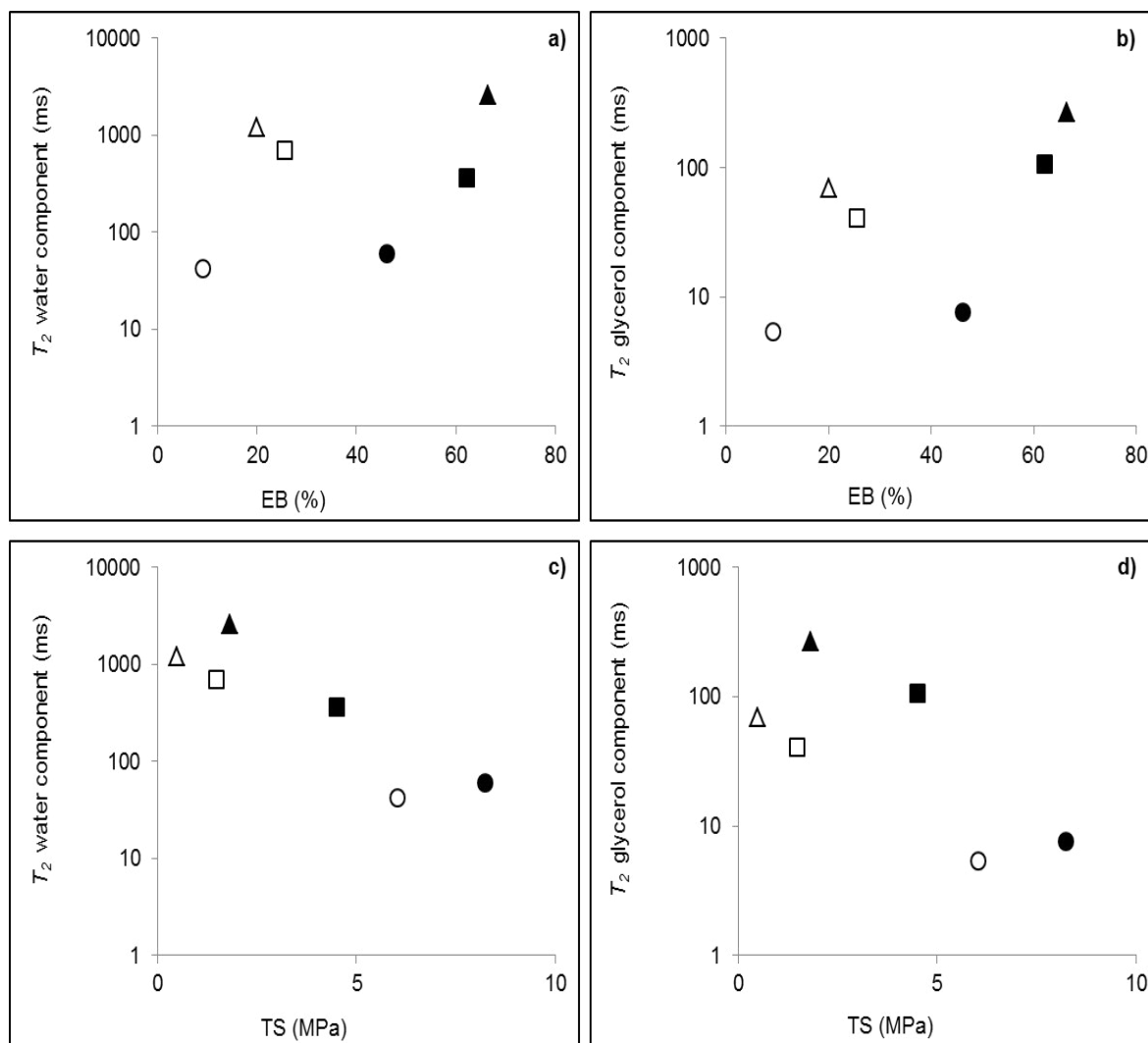


**Figure 4.3** Films water and glycerol relaxation time ( $T_2$ ) as a function of EB (respectively, Figures 4.3a and b) and TS (respectively, Figures 4.3c and d). Empty symbols correspond to thinnest films (range between 0.0556 and 0.0642 mm); fill symbols correspond to thickest films (range between 0.2348 and 0.2844 mm). Different data points symbols indicate the different compositions (see Table 4.1):

○/● - 388.13 Chit and 13.10Gly; □/■ - 188.88 Chit and 38.93Gly; △/▲ - 176.96 Chit and 50.60Gly



### 4.3.3. Molecular mobility versus water vapour permeability

Figure 4.4 displays water (a) and glycerol (b)  $T_2$  against WVP. It is possible to observe two different behaviours depending on the studied film thickness.

For thicker chitosan films (range between 0.2348 and 0.2844 mm), WVP increases with  $T_2$ , and this may be related with the increase of Brownian motion in the matrix with higher mobility, thus increasing the Fickian mass transport phenomena (Pineiro et al., 2013), i.e. higher molecular mobility makes the diffusion of water through the film easier. For the thinner films (range between 0.0556 and 0.0642mm), WVP is almost constant, with no apparent correlation with molecular mobility. This may be due to a lower resistance to mass transport – making the structural differences in the matrix not sufficient to influence the mass transfer rate (Crank, 1975).

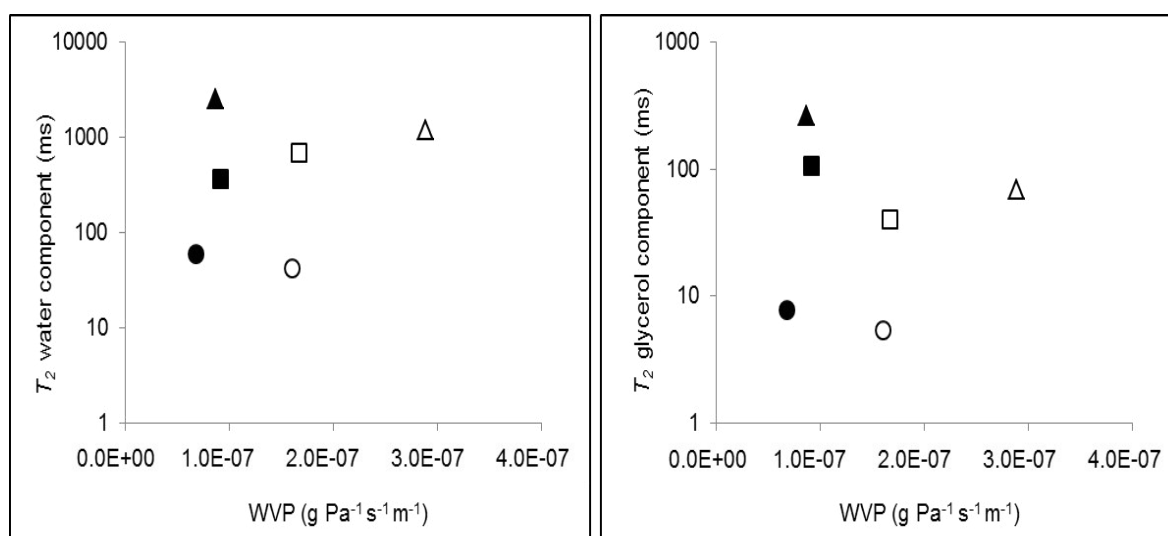


**Figure 4.4** Films water (a) and glycerol (b) relaxation time ( $T_2$ ) as a function of water vapour permeability (WVP). Empty symbols correspond to thinnest films (range between 0.0556 and 0.0642 mm); fill symbols correspond to thickest films (range between 0.2348 and 0.2844 mm). Different data points symbols indicate the different compositions (see Table 4.1):

○/● - 388.13 Chit and 13.10Gly; □/■ - 188.88 Chit and 38.93Gly; △/▲ - 176.96 Chit and 50.60Gly

Moreover, thicker films have higher WVP (Figure 4.4). This effect has been reported in the literature (McHugh et al., 1993; Zivanovic et al., 2007) and was attributed to an increase of the relative humidity in vicinity of the films, altering the water vapour kinetics.

WVP increases with crystallinity (larger absolute values of  $\Delta h$ ) (Figure 4.5), again supporting that for samples with higher crystallinity there is a higher free volume in the matrix.

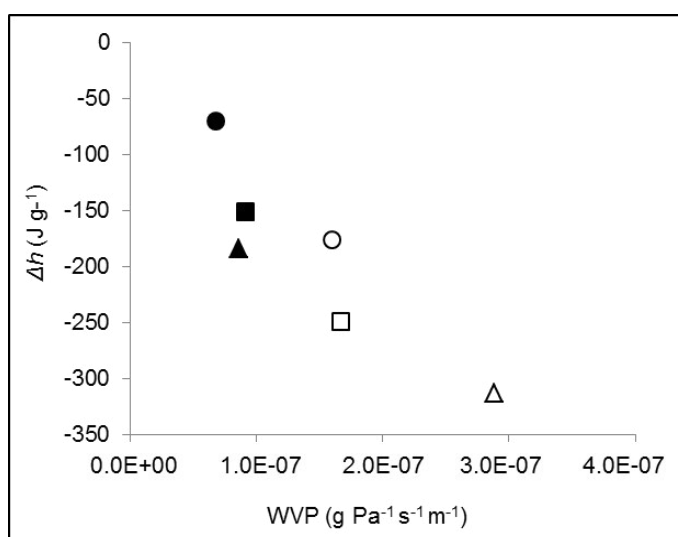


**Figure 4.5** Samples crystallinity ( $\Delta h$ ) as function as water vapour permeability (WVP). Empty symbols correspond to thinnest films (range between 0.0556 and 0.0642 mm); fill symbols correspond to thickest films (range between 0.2348 and 0.2844 mm). Different data points correspond to the different compositions (see table 4.1.):

O/● - 388.13 Chit and 13.10Gly; □/■ - 188.88 Chit and 38.93Gly; △/▲ - 176.96 Chit and 50.60Gly

#### 4.4. Conclusions

The relationship between the  $T_2$ , the microstructure and the macroscopic properties of water/glycerol plasticised chitosan films was systematically analysed and discussed.

At room temperature,  $T_2$  decreases with the increase of  $T_g$ , according to classic polymer theory. The crystallinity increased with increasing water and glycerol mobility, showing that once the polymeric chains are organised in the crystalline lattice, the interaction polymer/plasticiser is minimised, the free volume of the system increases and the water and glycerol molecules are thus free to move in the matrix.

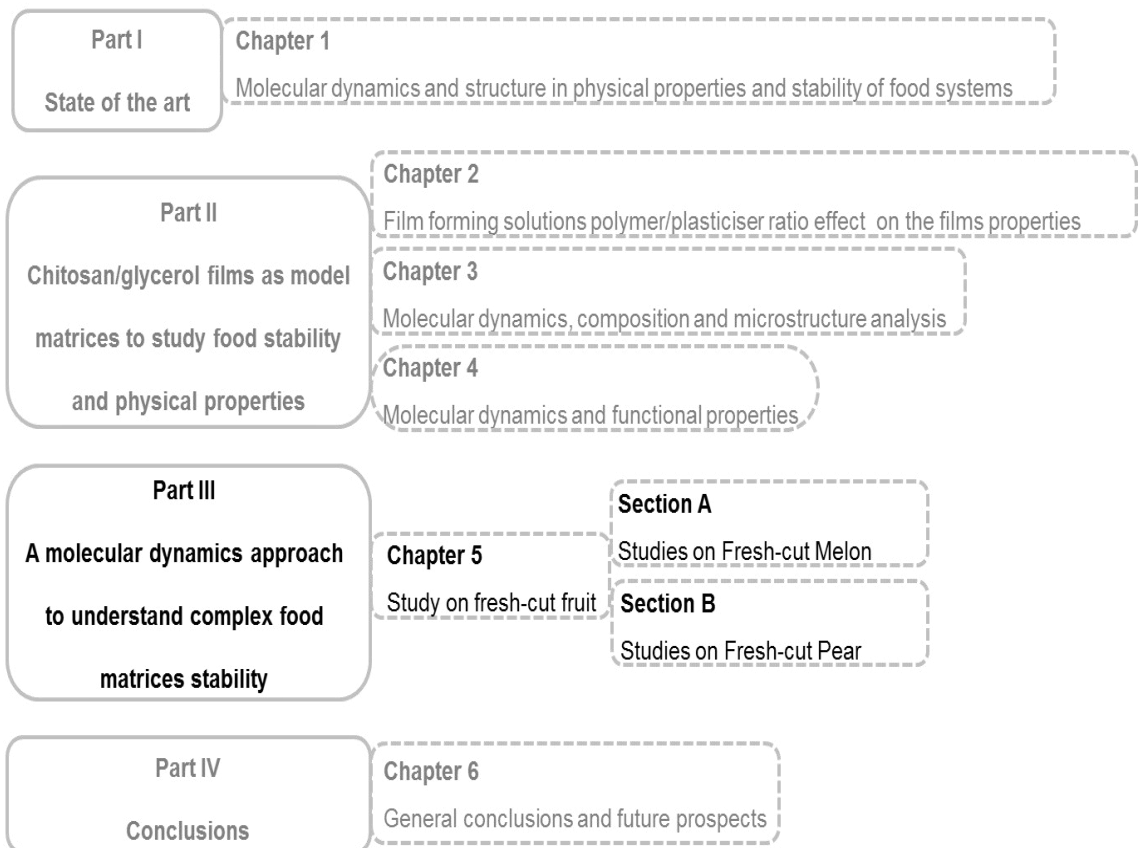
The deformability (EB) increased with water and glycerol relaxation times, while TS decreased, showing again the impact of the polymer/polymer and polymer/plasticiser bonds effect on the properties of the system. WVP was also correlated with molecular mobility. This was dependent on films thickness; in thicker films WVP increases with relaxation time – indicating that the molecular mobility is related with the Brownian motion in the matrix, hence making the diffusion of water through the film easier; for the thinner films no apparent correlation with molecular mobility was found.

All these results show the usefulness of NMR and molecular mobility studies for characterising and developing polymeric structures with improved functionality. Moreover, such concept can be associated to food science and be of great value for studies on degradation reactions and stability of more complex food systems.



# PART III

---





## **CHAPTER 5**

### **Studies on fresh-cut fruit**

---





**Abstract**

Molecular mobility is a fundamental parameter which reflects the dynamic properties of food components and contributes to food degradation reactions comprehension. Fresh-cut fruits have become an important food market segment. However, processing of fruits promotes faster physiological deterioration, biochemical changes and microbial degradation. The purpose of this chapter was to use NMR methodology as a tool to evaluate fresh-cut fruit quality, during storage at refrigerated conditions. The fresh-cut melon and pear transverse relaxation times ( $T_2$ ) were measured for a period of 7 days of storage, at 5 °C. The relationship between the obtained values, microstructure and quality parameters was investigated. In general, results show the existence of one class of water fluidity in the system, the one present in cells after processing.  $T_2$ , a measure of this fluidity, is affected by processing and storage time. Also, a close relationship between  $T_2$  and quality parameters of total colour difference (TCD), firmness and  $a_w$  was found.

## 5.1. Introduction

Stability of biological systems, including foods, depends strongly on molecular mobility (Roudaut et al., 2004) and water “availability”. This availability is a manifestation of how freely water molecules can participate in reactions, namely degradation reactions (Ruan and Chen, 1998). Water activity has been considered, for a long time, as a primary guideline for safety and quality control of foods (Labuza, 1977). However, the limitation of this measurement has been expressed (Hills et al., 1996a; Mathlouthi, 2001; Slade and Levine, 1991), and nuclear magnetic resonance spectroscopy has evolved to become a powerful tool to probe the structure and dynamics of food constituents in solid state. Specifically,  $^1\text{H}$  NMR has been used to investigate water dynamics and physical structure of foods through analysis of nuclear magnetisation relaxation times (Li et al., 2000). Foods and biological materials consist largely of water and macromolecules rich in protons and, since water protons are major contributors to the proton relaxation, the interactions between water and macromolecules represent the most important factors affecting the proton relaxation process (Ludescher et al., 2001). In this way, this could be an interesting technique to evaluate food quality during storage period, since degradation reactions, water interactions, structure and chemical compounds changes result in altered NMR properties (Ludescher et al., 2001).

Minimally processed fruit has become an important market segment due to the increasing demand for fresh, healthy and convenient foods (Rico et al., 2007). However, it is well known that processing fruits enhances physiological and biochemical changes, and microbial degradation, which result in degradation of fruit colour and texture. Fresh-cut melon and pear degradation during storage may be characterised by many physical and chemical parameters, such as changes in colour, firmness, aroma (Oms-Oliu et al., 2008) and  $a_w$ . Due to processing operations, a great

number of cells are disrupted, which induces the release of enzymes and their substrates resulting in accelerated quality losses.

The purpose of this chapter was to utilize NMR parameters to evaluate water behaviour in fresh-cut melon and pear along refrigerated storage and find and understand a relationship between water molecular dynamics and some of the most important physiological quality parameters, i.e. colour and softening rate.

Material and methods will be presented as a common section while results and discussion will be separate in section A for melon and section B for pear. Due to the biochemical and structural differences between samples, separate sections will be helpful for the interpretation and explanation of the results.

## **5.2. Materials and methods**

### **5.2.1 Fruit material, processing, packaging and storage conditions**

'Piel de Sapo' melons and 'Rocha' pear were obtained at a local supermarket, at commercial maturity. In order to characterise the fruit initial maturity state, soluble solids content was determined using a refractometer method (Amaro, 2012; Simandjuntak et al., 1996). Fruits were carefully inspected for bruising and compression damage and only those without visual defects and uniform in shape and size were selected for processing and analysis.

Melon and pear fruits were washed in running cold water, dipped in  $100 \mu\text{g L}^{-1}$  hypochlorite solution for 2 min, rinsed with deioniser water and allowed to drain. All cutting tools and containers were sanitised with 70% ethanol and allowed to dry before usage.

The melon rind was removed with a sharp stainless steel knife, the blossom and stem ends were discarded, placental tissue and seeds were removed, and the

mesocarp was prepared in cubes of 2.5 cm<sup>3</sup>. Pears were cut into longitudinal slices (ca. 10–20 mm thick) also with a sharp stainless steel knife.

Melon cubes or pear slices were randomly placed in vented polypropylene clamshells (~175 g) and stored at 5 °C for 7 days. To avoid the accumulation of ethylene and carbon dioxide inside the packages (Vilas-Boas and Kader, 2007), clamshells were perforated with single 6 mm vents. Samples were analysed at different days after cutting preparation.

### **5.2.2. Transverse relaxation times measurements**

A Bruker AVANCE III solid state NMR spectrometer (300MHz for proton) was used to determine the samples transverse or spin-spin relaxation times,  $T_2$ . The transverse relaxation time was obtained with a Carr-Prucell-Meiboom-Gill (CPMG) pulse sequence with a 90°-180° pulse spacing of 500 ms and a repetition time of 15 s. The magnetisation was recorded after 18 echoes arrays, with the precaution that the number of echoes always permits to define an exponential decay for the magnetisation. The samples were cut in small cylinders, 1.5 cm high, and placed in a 5 mm standard NMR tube, for the  $T_2$  measurement.

For each sampling day after cutting, three samples were studied for their transverse relaxation time evaluation.

### **5.2.3. Microscope techniques**

Optical and scanning electron microscopes were used to observe any microstructural changes that occurred in fruit samples during storage. Hence, at each storage time (0, 2, 4 and 6 days), a thin surface layer of the fruits tissue was removed, at 3 different sections and in duplicate, for both type of microscopy techniques.

For the optical microscopy, the fruit sample was emerged to staining, in a solution of toluidine blue O at 0.5% (w/v), for 2 hours. The stain solution was

disposed, and the fruits stained portions were washed in ethanol at 97%, during 10 seconds, and then washed with water during 30 seconds. Then the stained tissues were dried in microscope slides in a desiccator, during 24 hours. After this time, visualisation was made using a final magnification of 400 times.

Typical fixation of the material for SEM investigations involves dehydration, which can remove or alter lipids that form the wax coating on the fruit surface, and critical point drying can shrink and destroy tissues. Therefore, a modified and simplified methodology was used in order to prevent destruction of the epicuticular wax. The cut samples were wiped with a paper towel, carefully mounted onto stubs and examined under a JEOL-5600 Lv microscope (Tokyo, Japan), operated under low vacuum mode, using a spot size of 30 and a potential of 10-15 kV. All analyses were performed at room temperature (20 °C), using a 200 times magnification. For both techniques, photographs were obtained of three sections cut from each fruit

#### 5.2.4. Measuring quality parameters

The fruit quality parameters evaluated were total colour difference (TCD), softening rate and water activity.

Colour of the fresh-cut fruit surface was measured in the CIE L\*a\*b\* colour space with a Konica-Minolta CR-400 chromameter (Osaka, Japan) equipped with a D65 illuminant and the 2° observer for colour interpretation. In this scale, L\* ranges from 0 (black) to 100 (white), a\* indicates the degree of greenness (for negative values) and the degree of redness (for positive values). Axis b\* also ranges from negative to positive values indicating, respectively, degree of blueness to yellowness. L\*<sub>0</sub>, a\*<sub>0</sub> and b\*<sub>0</sub> were evaluated from freshly cut fruit (time 0). Colour changes were assessed using TCD, calculated through the formula

$$\text{TCD} = \sqrt{(L^* - L_0^*)^2 + (a^* - a_0^*)^2 + (b^* - b_0^*)^2} \quad (5.1)$$

One measurement was made in each five melon cubes and pear slices from three duplicated clamshells per replicate.

Firmness was measured using a TA-XT2 Plus texture analyser (Stable Micro Systems, Surrey, UK) equipped with a 5 kg load cell. The force to drive a cylindrical probe, with 5 mm diameter to perforate 5 mm into the tissue, at a speed of 1.5 mm s<sup>-1</sup> was recorded (Amaro et al., 2013). One measurement was taken on the lateral surfaces of each five cubes/slices from three clamshells, respecting to one replicate, from a total of two replicates, for each sampling day.

Water activity was measured using a dew point hygrometer (Aqualab Series 3, Decagon Devices Inc., Pullman, WA, USA). Three measurements were performed for each replicate and for each sampling day.

The quality data was subjected to statistical analysis performed using the software packages STASTICS© 6.0 (StatSoft, Tulsa, OK). An individual package constituted an experimental unit which was used as one replicate on each sampling day. Three replicated packages were analysed. The experiment trial was carried out twice.

## **Section A**

### **Studies on fresh-cut melon**

.....





### **5A.3. Results and discussion**

Maturity stage is an important factor that may affect the intensity of wound response in fresh-cut tissues (Beaulieu and Lea, 2007; Watada and Qi, 1999). These variances in samples maturity stage contribute, along with the natural variability between complex biological systems, for the differences obtained between the replicates. To characterise the melon maturity stage, the soluble solids content (SSC) was measured. The initial SSC ranged between 8.6 and 10.6, with no significant differences observed throughout storage. Melon SSC undergoes minor changes during postharvest storage of whole or fresh-cut fruit (Portela and Cantwell, 1998).

#### ***5A.3.1. Transverse relaxation times***

$T_2$  of the samples was obtained with the purpose of evaluating water molecules dynamics and environment during the fruit storage degradation process. The CPMG data was analysed as a continuous distribution of exponential relaxation times with CONTIN program (Provencher, 1982), and the results are presented in Figure 5A.1 (data in Appendix C, Table C.1.1).

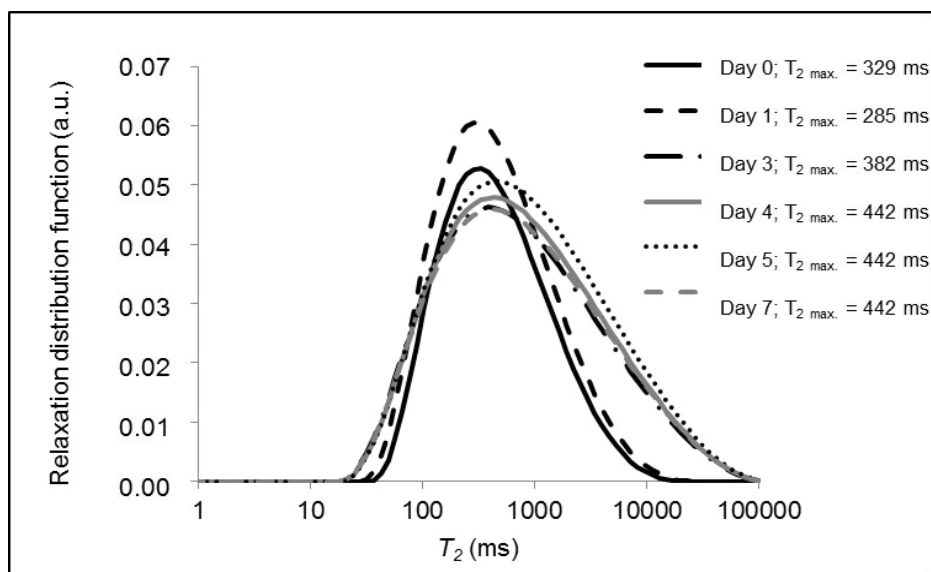


**Figure 5A.1** Distribution of water relaxation time ( $T_2$ ) in fresh-cut melon measured at 300 MHz and room temperature.

It is clear from Figure 5A.1 that all values of  $T_2$  range from about 50 ms to very high values (<10 s) presented in the samples, with only one pronounced maximum. In the first 24 hours after processing, the maximum amplitude  $T_2$  value evolves from 329 to 285 ms. At the third day of storage, the maximum amplitude  $T_2$  value is 382 ms and after that remains unchanged at 442 ms until day 7.

Comparing Figure 5A.1 with the results on whole apples, kiwifruits and pears, reported elsewhere (Hernández-Sánchez et al., 2007; Hills and Remigereau, 1997; Tylewicz et al., 2011), where pools of water are attributed to vacuole, cytoplasm and cellular wall, in our experiment, only one peak for water relaxation times was detected, probably due to loss of cellular compartmentation, as a consequence of wounding.

Regarding the maximum amplitude,  $T_2$  value shifts to shorter values in the first 24 hours after processing. Literature reports that after wounding there is major tissue disruption, whereby enzymes and substrates sequestered in different organelles come into contact (Beaulieu and Gorny, 2001) and signalling-induced wound responses are initiated with microbiological, enzymatic, and physicochemical reactions

simultaneously taking place, decreasing water availability (Artés et al., 2007) possibility due to an increase in 'water binding' (Chen et al., 1997), as the subcellular structures are disrupted and the release of solutes that were retained in the organelles occurs, and the consequent association of these solutes with water through hydrogen bonds. After this 24 hour period, where metabolic rate is elevated, water is continuously released from the physical barriers in the system and the observed  $T_2$  is more often at values closer to the free water  $T_2$ . By day 4 of storage,  $T_2$  maximum amplitude occurs for the highest  $T_2$  value and remained constant until the end of storage. This may indicate that by day 4 of storage, cells reach a threshold where metabolic rate is decreased, wounding reactions are diminished along with increased membrane degradation and turgor loss. These alterations lead to a higher water transverse relaxation time expression in cells. This interpretation is according with quality changes data obtained and discussed in point 5A.3.3.

The maximum amplitude  $T_2$  value evolving to higher  $T_2$  values with storage time can be interpreted as the enhanced range of water relaxation time detected and attributed to cell structure disorder due to the occurrence of membrane rupture and plasmolise (Toivonen and Brummel, 2008). Once this water proton behaviour indicates an alteration in cellular structure and also in water solute bonds, which can be associated with fresh-cut fruits quality loss during the storage period. This relation will be explored in the following sections.

### **5A.3.2. Microstructure analysis**

The use of two different techniques allows obtaining complementary results: with light microscope (LM) it is possible to get a qualitative description of the samples structure, while scanning electron microscope (SEM) is used to examine surfaces, with an improved resolution (Kaláb et al., 1995).

Figure 5A.2 presents the LM photos of the transversal cuts of fresh-cut melon (complementary microscope images in Appendix C, Section C.2.1). Toluidine Blue, used as dye, is especially useful for examination of fruit tissues, more specifically the fruit parenchyma cells, which constitute the fruit mesocarp (Kaláb et al., 1995). At day 0 of storage, intercellular spaces and vesicles are visible in fresh-cut melon mesocarp. All spaces presented are round and turgid with a visible cellular wall structure. This visual definition is mainly attributed to the water inside the cells. By day 4 of storage, it is already possible to observe a decrease in cell wall strength, which could be related with its pectin solubilising (Fernandes et al., 2008). The observed changes correlate with the  $T_2$  distribution function, discussed in the previous section, and are also supported by the changes in the quality parameters measurements discussed below (see section 5A.3.3).

As for the images obtained with SEM, Figure 5A.2 shows, for day 0, closely bonded cells and defined cellular walls, reinforcing the results obtained with LM. In fact, it is actually possible to observe chloroplasts. Chloroplasts are an important cellular organelle, as they contain chlorophylls and carotenoids that are pigments responsible for melon colour, as discussed in section 5A.3.3. After 4 days of storage, image shows a great number of cell walls broken down and the few remaining cells with severely distorted walls. This phenomenon stimulates the cellular disorganisation and cell size and shape variations. The cell plasmolise is also seen superficially by SEM, and confirms the observations of optical microscopy. Also after day 4, the observation of chloroplasts becomes more difficult.

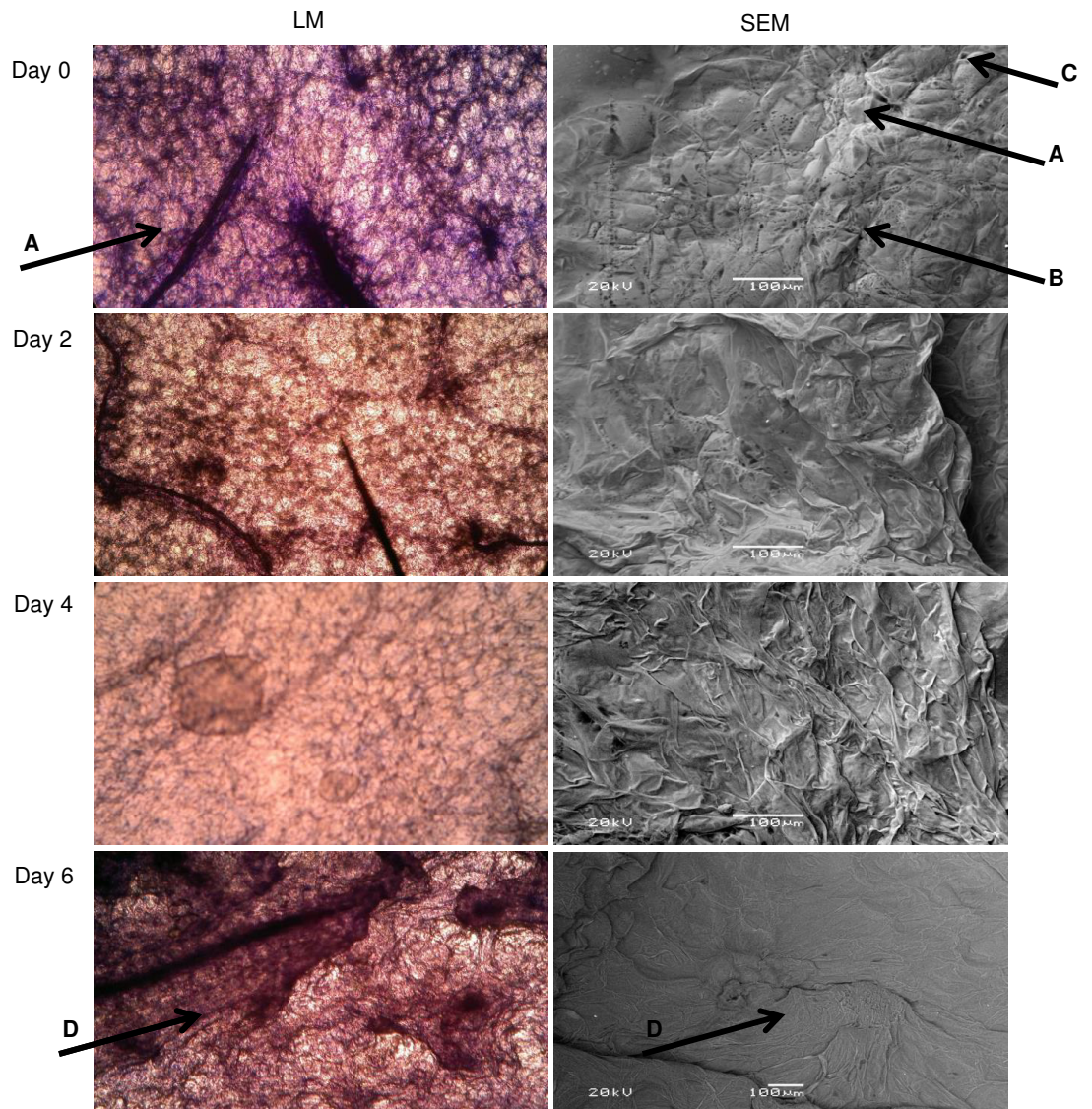


**Figure 5A.2** Light and scanning electron microscope images of fresh-cut melon, at different days of storage. (A-cellular wall; B-cellular organelles; C-chloroplasts; D-plasmalemma).

### 5A.3.3. Quality parameters

As discussed in the introduction section, colour, firmness and water activity are considered important parameters in fresh-cut fruit quality assessment (Figure 5A.3) (results in Appendix C, Table C.3.1). Differences found between measurements are explained by the fruits initial maturity and the natural variability of the complex biological systems, as explained before.

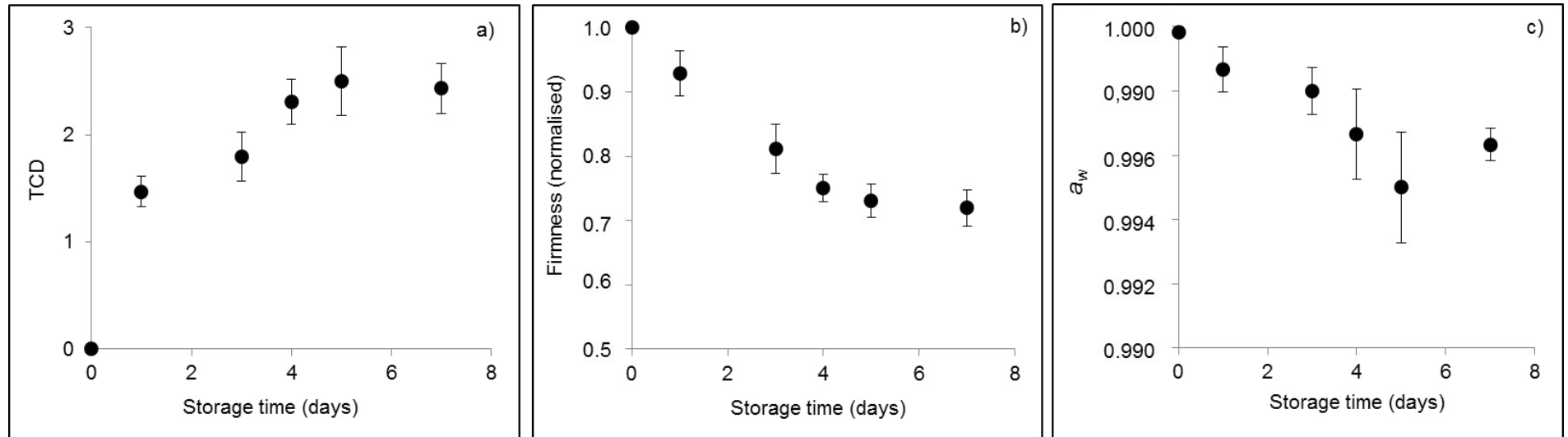


**Figure 5A.3** Fresh-melon quality parameters: a) total colour difference (TCD), b) firmness, and c) water activity ( $a_w$ ), during 7 days of storage. Vertical bars present the mean standard error.

Figure 5A.3a presents melon samples TCD tendency, along storage. As expected, and in accordance with literature (Toivonen and Brummel, 2008), TCD increases with storage time. In the specific case of fresh-cut melon, changes in colour are attributed to different biochemical processes, mainly chlorophyll and carotenoids degradation, since melon is not very susceptible to surface browning (Munira et al., 2013; Toivonen and Brummel, 2008). The increase in colour changes observed during fresh-cut melon storage is generally attributed to translucency or water-soaking symptoms (Munira et al., 2013; Portela and Cantwell, 1998). Particularly, literature reported (Portela and Cantwell, 1998), also for a non-climacteric melon, that colour is attributed to the combination of low concentration of carotenoids and chlorophylls in plastids, that are inside the chloroplasts. As the storage time increases and the plastids degradation occurs, the pigment concentrations in melon changes and consequently so does colour.

Fresh-cut melon firmness during the storage period is shown in Figure 5A.3b. Results demonstrate a rapid increase in firmness loss with storage time, particularly until day 4 of storage. At the end of storage, samples showed a degree of firmness around 30% (expressed as percentage of loss compared with the firmness measured at day 0). These changes in melon cubes firmness during storage were already reported for other melon cultivars and also for 'Piel de Sapo' (Aguayo et al., 2004). Fresh-cut melon is very susceptible to softening during storage, even under low temperatures, due to enzymatic degradation of the cell wall, specifically the middle lamella, and to loss of cell adhesion (Toivonen and Brummel, 2008). The enhanced activity of melon cell wall hydrolases in the first hours after processing, along with the transformation of protopectin to water-soluble pectin, lead to later alterations in structural features, namely thickness of the cell wall size and shape of cells, and volume of intercellular spaces (Rojas et al., 2001; Toivonen and Brummel, 2008)

These modifications are according to the observed light and scanning microscope images, presented in Figure 5A.2.

Figure 5A.3c shows fresh-cut melon samples water activity decreasing along storage. Literature reports water activity as a parameter for food stability control, namely chemical reactions in foods (Labuza, 1977). As discussed in section 5A.3.1 the decrease in this parameter may be due to the fact that water is being used for the physic and biochemical degradation reactions and/or microbial growth, occurring during the storage period.

#### **5A.3.4. Relaxation time versus quality parameters**

In Figure 5A.4 it is possible to observe the behaviour tendency between maximum distribution  $T_2$  value and fresh-cut melon quality parameters, TCD, softening rate and water activity. Figure 5A.4a) shows the maximum distribution  $T_2$  value against the total colour difference. Although a weak tendency was noticed, it is possible to observe  $T_2$  increasing with TCD. This tendency may result from translucency or water-soaking symptoms derived from disruption of cellular structures. As discussed above, alterations in fresh-cut melon colour are mainly attributed to altered combination of low carotenoids and chlorophylls in plastids (Portela and Cantwell, 1998), and not so related with water system dynamics.

Figure 5.4b demonstrates the relationship between maximum distribution  $T_2$  value and firmness loss/softening. As expected,  $T_2$  maximum value increases with the melon softening (lower firmness). At day 4, maximum distribution  $T_2$  value reaches the highest value, while softening of fresh-cut melon tissue stabilises from this day on.



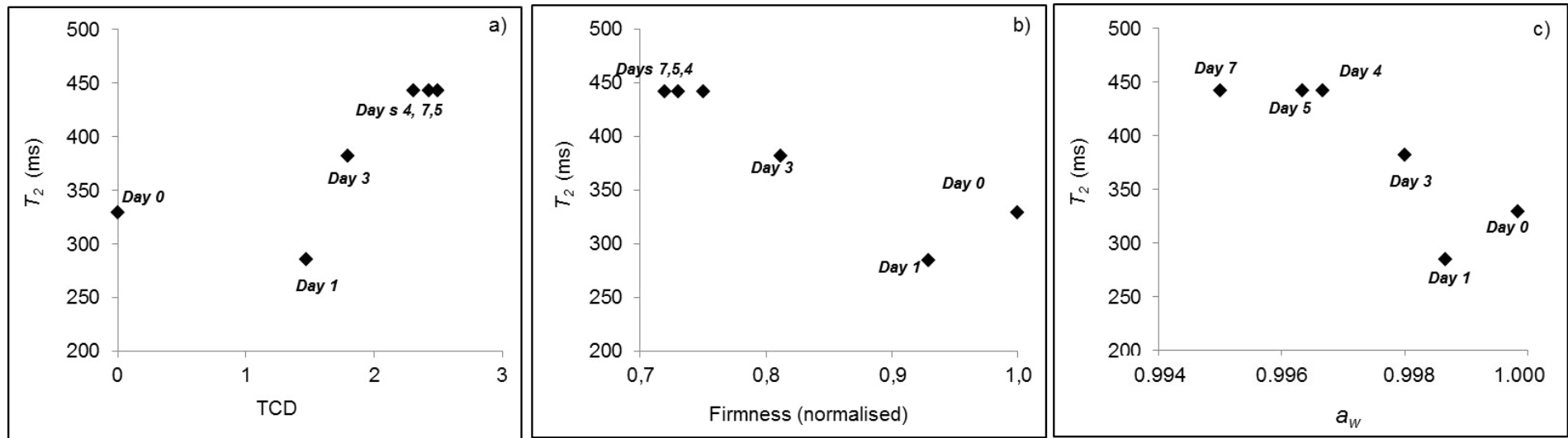


**Figure 5A.4** Fresh-cut melon relaxation time ( $T_2$ ) as function of a) total colour difference (TCD), b) firmness, and c) water activity ( $a_w$ ).

The softening together with cell wall degradation and loss of physical barriers, possible to observe by microscope images in Figure 5A.2, allows the leakage of cellular osmotic solutes into the apoplastic space, which then results in altered water mobility/availability (Toivonen and Brummel, 2008).

Water activity relationship with water relaxation time is presented in figure 5A.4c). It is possible to observe a tendency between these two parameters, i.e., cell water maximum distribution  $T_2$  value decreases with increasing  $a_w$ . Despite of  $a_w$  being considered as a critical parameter of food systems stability (Labuza, 1977), the usual measuring methods do not consider microstructure nor the possibility that there may be local regions differing in water content, and presumably, water availability (Hills et al., 1996a; Mathlouthi, 2001). These results demonstrate that, considering the lowest water activity values, the increase in this parameter does not reflect on water mobility. Although it is possible to observe a relationship between these two parameters, water activity measurements may not provide, for example, the relationship of the evolution of the structural changes of the food material with the changes of the water-macromolecules and water-water interactions that occur during food shelf-life (Wang and Liapis, 2012), and studies have stressed that under many common circumstances the thermodynamics activity of water is far less relevant to processing and storage than structure-related properties, which can restrict the mobility and diffusion of the reactants (Anese et al., 1996; Slade and Levine, 1991).

**Section B**

**Studies on fresh-cut pear**

.....



### 5B.3. Results and discussion

As was discussed in point 5A.3, maturity stage is an important factor that may affect the intensity of wound response in fresh-cut tissues (Beaulieu and Lea, 2007; Watada and Qi, 1999). Furthermore, the natural variability between complex biological systems, in this case pear fruits, contribute for the differences obtained between the three true replicates. To characterise pears maturity stage soluble solids content (SSC) was measured. The initial SSC ranged between 12.9 and 14.2 with no differences observed during storage time.

#### 5B.3.1. Transverse relaxation times

As happened for melon samples, fresh-cut pear transverse relaxation time ( $T_2$ ) was determined with the purpose of evaluating water molecules dynamics and environment during fruit storage time. Figure 5B.1 shows the distribution of water proton relaxation times of fresh-cut pears during storage (data in Appendix C, Table C.1.1). It can be observed that all values of  $T_2$  from about 50 ms to very high values are presented in the fruit samples, with only one pronounced maximum of  $T_2$  value. This fact means that water, normally stored in different sub-cellular organelles in intact cells and often characterised by different proton relaxation times, attributed to vacuole, cytoplasm and cellular wall relaxation times was in our experiment free from organelles, as a consequence of pear processing (Hernández-Sánchez et al., 2007; Hills and Remigereau, 1997; Tylewicz et al., 2011). Thus, the one maximum peak of relaxation time detected can be attributed to the total water after the loss of cellular compartmentation as a consequence of wounding.

Similarly with fresh-cut melon samples, after 24 hours of processing, the maximum amplitude values of  $T_2$  shifted to lower values. Wounding, causes cell disruption whereby enzymes and substrates sequestered in different organelles come in contact (Beaulieu and Gorny, 2001). As a consequence, a signalling-induced

wound response takes place and enzymatic, microbiological, physicochemical reactions initiate. According to the literature, as the subcellular structures are disrupted and the release of solutes that were retained in the organelles occurs, with the association of this solutes with water through hydrogen bonds a decrease in water availability or an increase in 'water binding' can be detected (Artés et al., 2007; Chen et al., 1997). After this first day, where metabolic rate is elevated, water is continuously released from physical barriers in the system and the relaxation values occurred more often at values closer to free water. By day 3 of storage,  $T_2$  maximum amplitude occurs for the highest  $T_2$  value and, after this day, decreases until the end of the storage period. The maximum amplitude  $T_2$  value evolving to higher  $T_2$  values with storage time can be interpreted as the enhanced range of water relaxation time detected and attributed to cell structure disorder due to the occurrence of membrane rupture and even plasmolise (Toivonen and Brummel, 2008). The decrease of the signal values from water protons suggests that cells can undergo shrinkage, which can indicate a dehydration phenomenon (Tylewicz et al., 2011). This interpretation is in agreement with the quality parameters results discussed in point 5B.3.3.

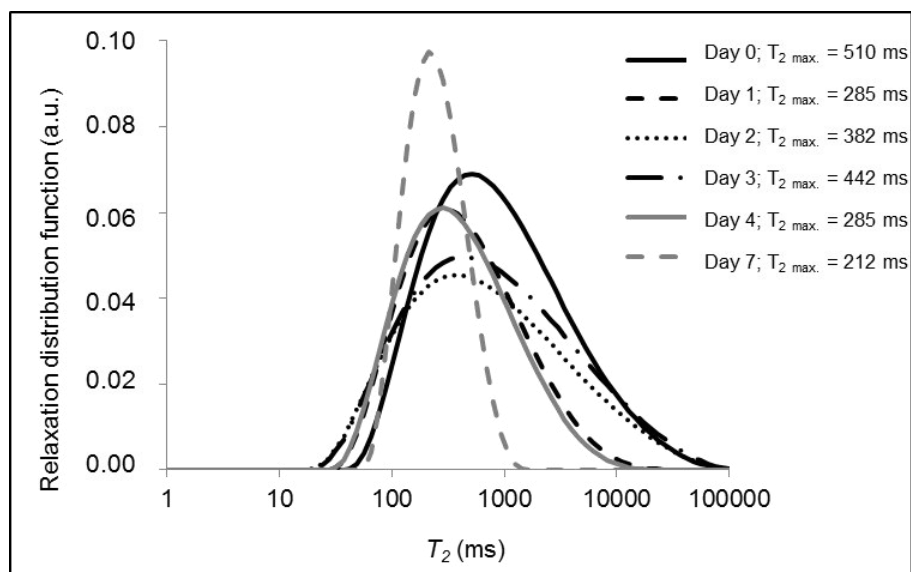


**Figure 5B.1** Distribution of transverse water proton relaxation times ( $T_2$ ) in fresh-cut pear measured at 300 MHz and room temperature.

### 5B.3.2. Microstructure analysis

Similarly to what was performed to fresh-cut melon, LM and SEM techniques were used (complementary microscope images in Appendix C, Section C.2.2).

LM images showed the transversal cuts of fresh-cut pear. At day 0 intercellular spaces are visible in all samples mesocarp. Spaces are round and turgid with visible cellular wall structure. As for the images obtained with SEM, figure 5B.2 shows, for day 0, closely bonded cells and defined cellular walls, reinforcing the results obtained with light microscope (LM) and corresponding to what happen with fresh-cut melon samples. Also, LM allows the observation of the sclereids or stone cells, with a shape of star and responsible for the gritty appearance and grainy mouthfeel of pears (Reeve, 1970). Image shows a loss of definition of these structures with storage. Images from day 4 show the sclereids spreading along the matrix. This fact may be related with the loss of cells natural angular morphology and integrity, together with the loss of compactness and coherence for whole tissue, stimulated by the great number of cell wall disruption and could contribute to explain the  $T_2$  decrease

obtained after day 3. By this day the loss of sclereids definition may decrease the free volume in the matrix and hence the mobility of the water proton. The phenomenon is also seen superficially by SEM, and confirms the observations of optical microscopy.

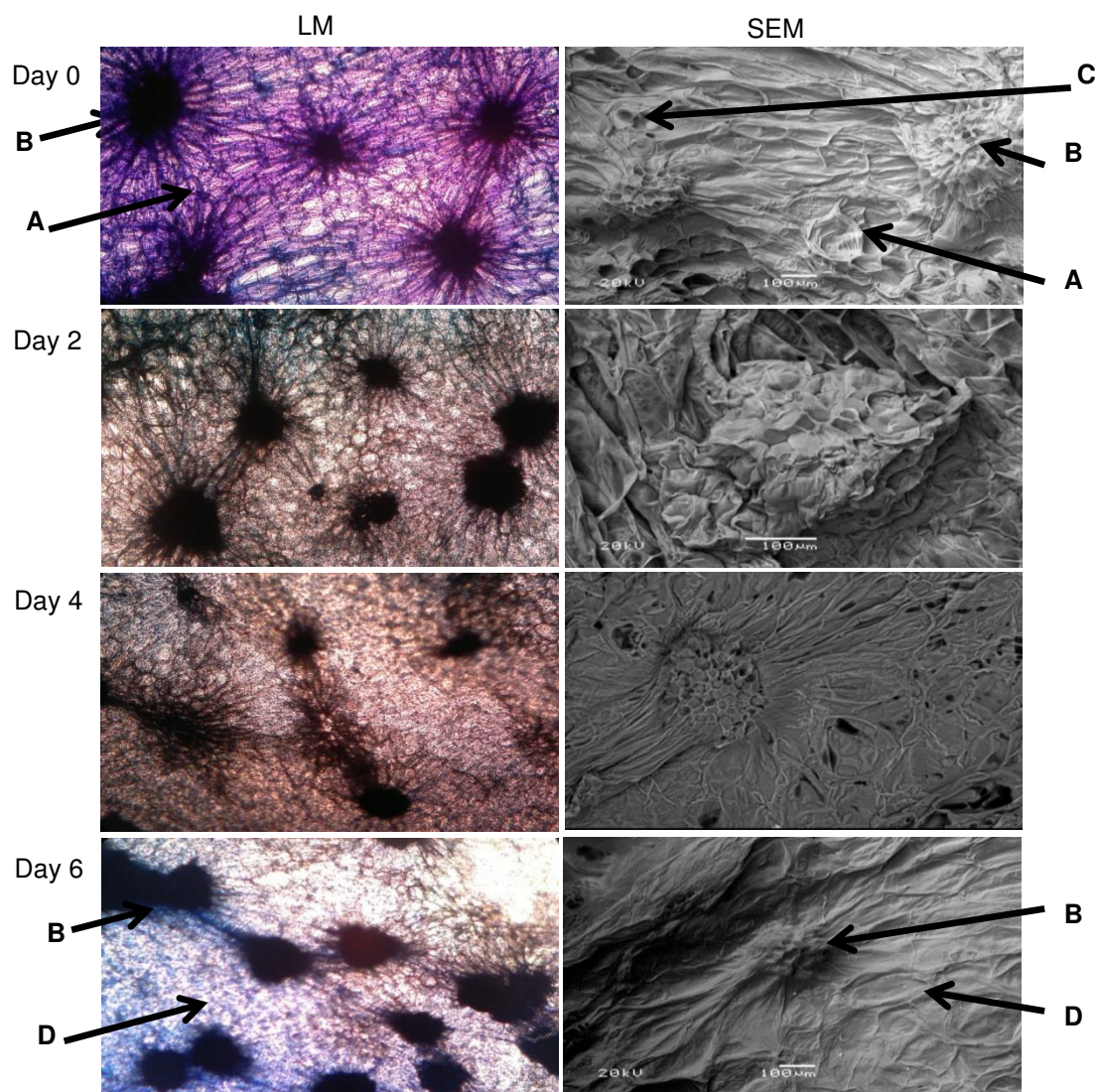


**Figure 5B.2** Light and scanning electron microscope images of fresh-cut pear, at different days of storage. (A-cellular wall; B-sclereids; C-cellular organelles; D-plasmalemma).



### 5B.3.3. Quality parameters

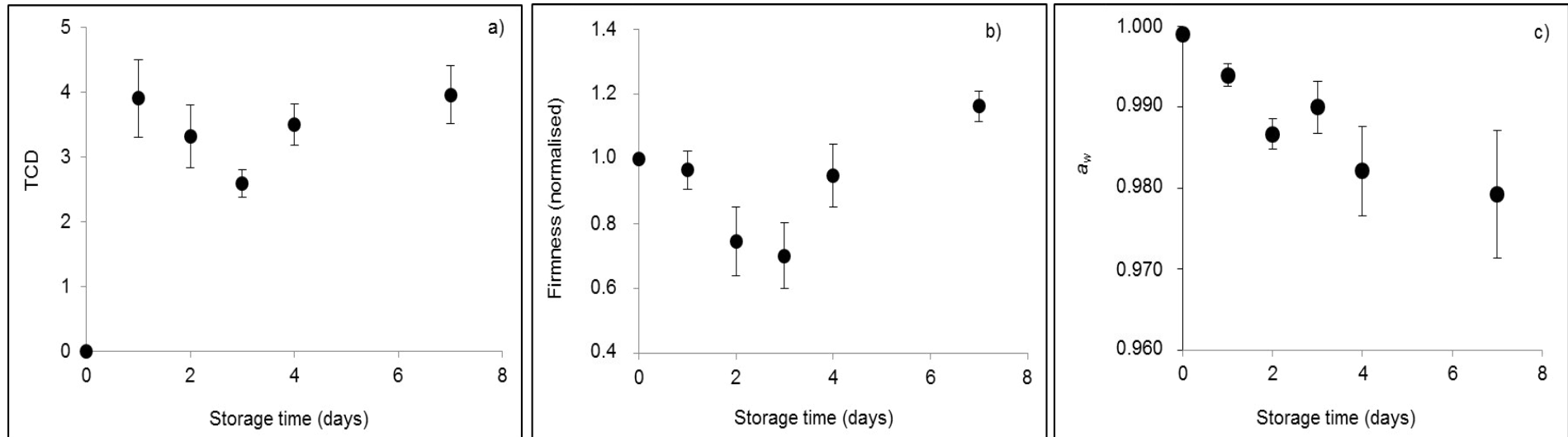
Figure 5B.3 shows the quality parameters: total colour difference (a), firmness (b) and water activity (c) of fresh-cut pears, along 7 days storage (results are included in Appendix C, Table C.3.2).

Figure 5B.3a shows that TCD increases drastically in the first 24 hours and after this period remained almost constant. This colour differences increases was already described in the literature (Gomes et al., 2010; Toivonen and Brummel, 2008). Colour alterations in pears are attributed to the browning reactions in which the mechanism involves the biochemistry of the polyphenol oxidase (PPO) enzyme and its interaction with polyphenols and oxygen (Martinez and Whitaker, 1995; Toivonen and Brummel, 2008). In this specific case, the browning detected on the surfaces of pear slices cannot be strictly considered a metabolic change, as it is also a biochemical reaction of a cell-free extracts as consequence of membrane damage. PPO previously located in plastids and phenolic compounds previously sequestered in the vacuole come in contact (Marangoni et al., 1996) then, PPO catalyses the oxidation of *o*-diphenols into *o*-quinones which polymerise forming dark melanins (Franck et al., 2007; Toivonen and Brummel, 2008).

Results from firmness are shown in Figure 5B.3b. From day 1 until day 3 it is observed a decrease in this parameter, around 10%. This is probably due to the loss of membrane integrity, cellular leakage, and the flooding of intercellular spaces (Soliva-Fortuny et al., 2002; Toivonen and Brummel, 2008). After day 3 of storage, an increase in the firmness of fresh-cut pears was observed. Fresh-cut pears become harder in relation to day 0 (around 10 and 15% expressed as percentage of the initial value of firmness). Increases in firmness of fresh-cut pear have been observed when puncture methods are used (Dong et al., 2008; Gomes et al., 2010; Soliva-Fortuny et al., 2004). This increase in firmness can be caused by the partial dehydration of the cut surface and the development of abrasive surface texture, by the heterogeneous

distribution of scleride cells in the pear tissue, or by maturation differences among individual pieces (Lesage and Destain, 1996). The increase in firmness at day 3 of storage coincides with the maximum water relaxation time as described in section 5B.3.1.

Figure 5B.3c shows that  $a_w$  decrease in all pear samples during storage. Literature reports  $a_w$  as a parameter for food stability control, namely chemical reactions in foods (Labuza, 1977). As discussed in section 5B.3.1 the decrease in this parameter suggests that water is being used for the physic and biochemical degradation reactions and/or microbial growth, occurring during the storage period.



**Figure 5B.3** Fresh-pear quality parameters: a) total colour difference (TCD), b) firmness, and c) water activity ( $a_w$ ), during 7 days of storage. Vertical bars present the mean standard error.

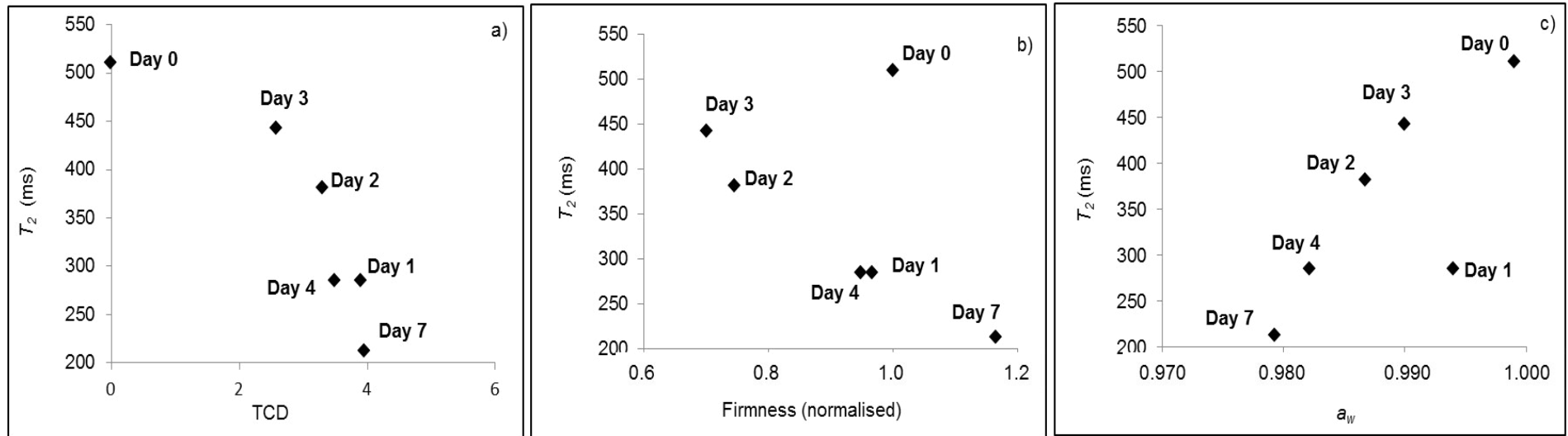
#### **5B.3.4. Relaxation time versus quality parameters**

Figure 5B.4 shows the behaviour tendency between maximum distribution  $T_2$  value and pear quality parameters. The maximum distribution  $T_2$  value against TCD is shown in Figure 6.4a where it is observed a decrease in TCD with  $T_2$ . As discussed in section 5B.3.3, alterations in colour are largely a result of biochemical reactions occurring in the cell-free environment of the cell structure with water playing a vital role for the evolution of these biochemical degradative reactions.

Figure 5B.4b demonstrates the relationship between maximum distribution  $T_2$  value and firmness.  $T_2$  maximum value increases with pear firmness loss/softening, as expected. The cell wall degradation together with cell structure alteration/ loss (e.g. sclereids spreading along the matrix), both observed along the storage period, by microscope images in Figure 5B.2, allows firmness modifications with impact in free volume and in the leakage of cellular osmotic solutes into the apoplastic space, which then result in altered water mobility/ availability.

Figure 5B.4c demonstrates the relationship between water activity and maximum distribution  $T_2$  value. It can be seen that  $a_w$  increased with water relaxation. Despite of  $a_w$  be considered as a critical parameter of food systems stability (Labuza, 1977) the usual measuring methods do not consider microstructure or the possibility that there may be local regions differing in water content, and presumably, of water availability (Hills et al., 1996a; Mathlouthi, 2001).

Although, it was recognised a relationship between  $a_w$  and water relaxation times, water activity may not provide the relationship of the evolution of the structural changes of the food material with the changes of the water-macromolecules and water-water interactions that occurring during food shelf-life (Wang and Liapis, 2012).



**Figure 5B.4** Fresh-cut pear relaxation time ( $T_2$ ) as function of a) total colour difference (TCD), b) firmness, and c) water activity ( $a_w$ ).

## 5.4. Conclusions

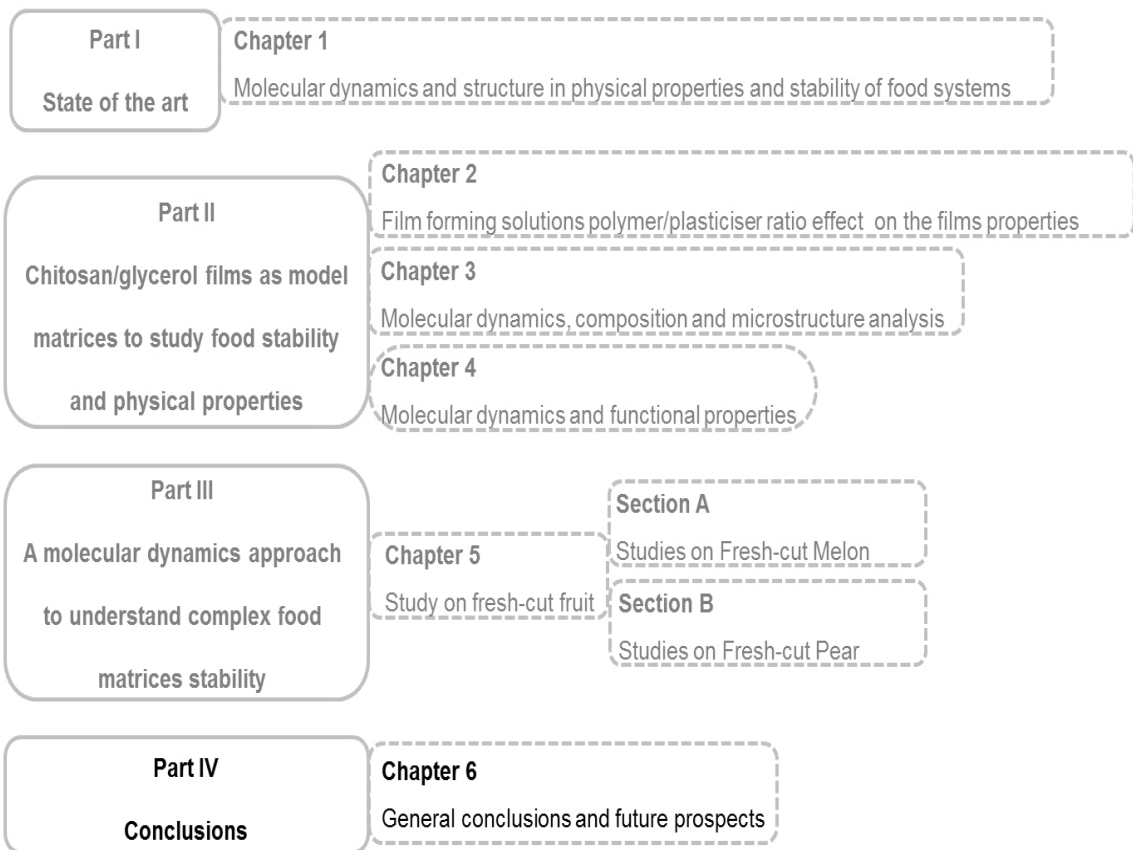
Water proton relaxation time from fresh-cut melon and pear samples was analysed during 7 days of storage. The distribution function for  $T_2$  presents one peak corresponding to cells total water. The peak position ( $T_2$ ) decreased in the first day of storage, indicating an increase in biochemical reactions and water-solutes bonds in the first 24 hours after processing.

Respecting to fresh-cut melon this peak position increased from day 1 to day 4, remained constant until the end of storage. This indicates cellular structure degradation, where water became free from physical barriers. For fresh-cut pear the peak position behaviour was slightly different, i.e. increased from day 1 to day 3 (showing a cellular structure degradation where water became free from physical barriers), and decreased again until the end of storage. This decrease of the water protons signal values, observed after day 3, suggests that cells can undergo shrinkage indicating a dehydration phenomenon, or could be associated to the cellular disassembly of the stone cells. Both melon and pear results are supported by light and scanning electron microscope.

Samples quality parameters analysed demonstrated a close relationship with the value of  $T_2$  where the distribution function is maxima. These relationships are explained by several phenomena such as loss of membrane integrity, cellular structures disruption and leakage of cellular osmotic solutes into the apoplastic space; all alterations enhanced by processing-cutting. However, the relationships were different for melon and pear, stressing the relevance of structure on water dynamics and food stability.

# PART IV

---







## **CHAPTER 6**

### **General conclusions and future prospects**

---



## 6.1. General conclusions

As discussed in the general introduction, the primary driving force for the research presented in this dissertation was to contribute for a deeper understanding of the molecular dynamics concept on degradation reactions and stability of complex food systems.

From the literature review, it was possible to identify critical issues and research needs on food molecular dynamics, particularly water molecular dynamics. Water is one of the most important components at a structural and development level on both studied matrices: chitosan/glycerol films and fresh-cut-fruit.

Chitosan/glycerol films, used as food model matrices, allowed evaluating and systematising the plasticiser's performance. Results demonstrated the relevance of the film forming solutions (FFS) composition. Rheological behaviour of the forming solutions was dependent on polymer concentration. Consistency coefficient affected the properties of the films obtained after drying, namely moisture content.. Glycerol used in FFS was responsible for films composition, by establishing the films chitosan concentration, while the ratio polymer/plasticiser determined the films thickness and indirectly structure, i.e. plasticiser addition promoted a free volume increase. These results were confirmed by TEM photographs. FFS glycerol addition affected the crystalline lattice of the film, by changing the H-bonds in chitosan crystals. This fact was reflected on the macroscopic properties of films, such as water and barrier properties or thermomechanical.

Films molecular mobility results demonstrate two different behaviours for the two plasticisers analysed: water and glycerol. While glycerol was mainly bounded to the chitosan chain network, the water present in the system was predominantly free from the polymeric chain. Furthermore, it was possible to infer that for lower glycerol concentrations, free chitosan binding sites can be occupied by water molecules. This thesis also allowed to conclude that not only the water content affects the water

mobility, but also structural differences in the films influence the  $T_2$ . Water mobility relates to the water in the bulk and thus complements information on  $a_w$  of a system.

Likewise, a relationship between plasticisers, i.e. water and glycerol, and films macroscopic properties and microstructure were determined. For both water and glycerol,  $T_2$  decreased with the increase of glass transition temperature. The crystallinity increased with increasing water and glycerol mobilities, showing that once the polymeric chains are organised in the crystalline lattice, the interaction polymer/plasticiser was minimised, the free volume of the system increased and the water and glycerol molecules were thus free to move in the matrix. The EB increased with the water and glycerol relaxation times, while TS decreased, showing again the impact of the polymer/polymer and polymer/plasticiser bonds effects on the system properties.. Water vapour permeability was also correlated with the molecular mobility. This was dependent on films thickness: in thicker films WVP increased with relaxation time – indicating that the molecular mobility is related with the Brownian motion in the matrix, hence the diffusion of water through the film was easier; for the thinner films no apparent correlation was found.

All these results, obtained in straightforward matrices, are useful for characterising and developing polymeric structures with improved functionality. Furthermore, such results can be also of great value if used as a starting point for studies on degradation reactions and stability of more complex food systems, such as fresh-cut fruit.

Fresh-cut fruit experimental work was focused on two different and well-recognised fruits: pear and melon. Melon is one of the most important fruits in the world fresh-cut fruit market, while pear ('Rocha' pear) represents an important fruit market segment in Portugal. For both melon and pear, the effect of wounding was observed through the NMR measurements, where the distribution function for  $T_2$

presented one peak corresponding to cells total water, after the loss of cellular compartmentation, as a consequence of fruit processing. The increase in biochemical reactions and water solute bonds, that occur in the first 24 hours after processing as consequence of wounding, is demonstrated by the decrease of peak position ( $T_2$ ), observed in this period. This biochemical response is characteristic to most of minimally processed fruits and, as was expected, is observed for both melon and pear. After this period, different water dynamics tendencies were found. These results are related with differences in fruits physiological processes and highlight the role of structure on food stability.

Quality parameters analysed demonstrated a close relationship with the value of  $T_2$  where the distribution function is maxima. These relationships are explained by several phenomena such as loss of membrane integrity, cellular structures disruption, or leakage of cellular osmotic solutes into the apoplastic space, which are alterations enhanced by processing-related wounding.

All these studies show the usefulness of gathering the NMR concept and methodologies with food science, and demonstrate the great value of these studies on degradation reactions and stability in more complex food systems.

## 6.2. Future prospects

The reported research results raised new opportunities for further research:

- Mathematically describe the relationship between the molecular and macroscopic parameters in different complexity levels of food matrices.
- Clarify the role of structure on systems dynamics, since it was identified as a key factor on food matrices performance.
- Understand how food preservation processes can change the dynamics of water in the systems. For example, during freezing water suffers interesting phase changes, like crystallisation and vitrification, facts that make this process especially interesting for mobility studies.
- Identify the “baseline” mobility for stability in high water content food products.
- Apply this knowledge to food industries aiming at minimising water loss along distribution chain and maximising incomes.

## REFERENCES

---





## REFERENCES

Aguayo, E., Escalona, V.H., Artés, F., (2004). Metabolic Behavior and Quality Changes of Whole and Fresh Processed Melon *Journal of Food Science* 69(4), SNQ148-SNQ155.

Aguilera, J.M., (2000). Food Microstructure., *Food Engineering - Encyclopedia of Life Support Systems*.

Aguilera, J.M., Stanley, D.W., Bakerc, K.W., (2000). New dimensions in microstructure of food products. *Trends in Food Science & Technology* 11(3-9).

Aider, M., (2010). Chitosan application for active bio-based films production and potential in the food industry: Review. *LWT - Food Science and Technology* 43, 837–842.

Amaro, A.L., (2012). Modulation of aroma volatiles and phytochemical quality of fresh-cut melon (*Cucumis melo L.*) by oxygen levels, 1-Methylcyclopropene and Lysophosphatideylethanolamine. Universidade Católica Portuguesa, Porto.

Amaro, A.L., Fundo, J.F., Oliveira, A., Beaulieu, J.C., Fernández-Trujillo, J.P., Almeida, D.P.F., (2013). 1-Methylcyclopropene effects on temporal changes of aroma volatiles and phytochemicals of fresh-cut cantaloupe. *Journal of Science of Food and Agriculture* 93, 828-837.

Andreuccetti, C., Carvalho, R.A., Grosso, C.R.F., (2009). Effect of hydrophobic plasticizers on functional properties of gelatin-based films. *Food Research International* 42(8), 1113-1121.

Anese, M., Shtylla, I., Torreggiani, D., Maltini, E., (1996). Water activity and viscosity - relations with glass transition temperatures in model fod systems. *Thermochimica Acta* 275, 131-137.

Angel, C.A., (1996). The glass transition. *Current Opinion in Solid State & Materials Science* 1, 578-585.

Artés, F., Gómez, P., Artés-Hernández, F., (2007). Physical, physiological and microbial deterioration of minimally fresh processed fruits and vegetables. *Food Science and Technology International* 13, 177-188.

Arvanitoyannisa, I.S., Nakayamab, A., Aibab, S.-i., (1998). Chitosan and gelatin based edible films: state diagrams, mechanical and permeation properties. *Carbohydrate Polymers* 37, 371-382.

Arzate-Vázquez, I., Chanona-Pérez, J.J., Georgina Calderón-Domínguez, Terres-Rojasc, E., Garibay-Feblesc, V., Martínez-Rivasb, A., Gutiérrez-López, G.F., (2012). Microstructural characterization of chitosan and alginate films by microscopy techniques and texture image analysis. *Carbohydrate Polymers* 87(1), 289-299.

Bangyekan, C., Aht-Ong, D., Srikulkit, K., (2006). Preparation and properties evaluation of chitosan-coated cassava starch films. *Carbohydrate Polymers* 63, 61-67.

Barros, A., (1999). Contribution à la sélection et la comparaison de variables caractéristiques, Institut National Agronomique Paris-Grignon Paris, France.

Beaulieu, J.C., Gorny, J.R., (2001). *Fresh-cut fruits*. USDA Handbook 66, USDA, Washington, D.C, USA.

Beaulieu, J.C., Lea, J.M., (2007). Quality Changes in Cantaloupe During Growth, Maturation, and in Stored Fresh-cut Cubes Prepared from Fruit Harvested at Various Maturities. *Journal of the American Society for Horticultural Science* 132(5), 720-728.

Berk, Z., (2013). *Physical Properties of Food Materials* (2<sup>nd</sup> Edition ed). Elsevier Inc.

Bourbon, A.I., Pinheiro, A.C., Cerqueira, M.A., Rocha, C.M.R., Avides, M.C., Quintas, M.A.C., Vicente, A.A., (2011). Physico-chemical characterization of chitosan-based edible films incorporating bioactive compounds of different molecular weight. *Journal of Food Engineering* 106, 111-118.

Bourtoom, T., (2008). Factors Affecting the Properties of Edible Film Prepared from Mung Bean Proteins. *International Food Research Journal* 15(2), 167-180.

Butler, B.L., Vergano, P.J., Testin, R.F., Bunn, J.M., Wiles, J.L., (1996). Mechanical and Barrier Properties of Edible Chitosan Films as affected by Composition and Storage. *Journal of Food Science* 61(5), 953-956.

Champion, D., Meste, M.L., Simatos, D., (2000). Towards an improved understanding of glass transition and relaxations in foods: molecular mobility in the glass transition range. *Trends in Food Science & Technology* 11, 41-55.

- Chen, P.L., Long, Z., Ruan, R., Labuza, T.P., (1997). Nuclear Magnetic Resonance Studies of Water Mobility in Bread during Storage. *LWT - Food Science and Technology* 30(2), 178-183.
- Chen, R.H., Hwa, H.-D., (1996). Effect of molecular weight of chitosan with the same degree of deacetylation on the thermal, mechanical, and permeability properties of the prepared membrane. *Carbohydrate Polymers* 29, 353-358.
- Chillo, S., Flores, S., Mastromatteo, M., Conte, A., Gerschenson, L., Nobile, M.A.D., (2008). Influence of glycerol and chitosan on tapioca starch-based edible film properties. *Journal of Food Engineering* 88, 159-168.
- Chirife, J., Buera, M.D.P., (1994). Water Activity, Glass Transition and Microbial Stability in Concentrated/Semimoist Food Systems. *Journal of Food Science* 59(5), 921-927.
- Chirife, J., Buera, M.P., (1995). A Critical Review of Some Non-equilibrium Situations and Glass Transitions on Water Activity Values of Foods in the Microbiological Growth Range. *Journal of Food Engineering* 25, 531-552.
- Claridge, T.D.W., (2009). High-Resolution NMR Techniques in Organic Chemistry, in: J.-E. Backvall, Baldwin, J.E., Williams, R.M. (Eds.), *Tetrahedron Organic Chemistry Series*, 2<sup>nd</sup> ed. Elsevier, p. 383.
- Corté, L., Leibler, L., (2007). A Model for Toughening of Semicrystalline Polymers. *Macromolecules* 40, 5606-5611.
- Crank, J., (1975). *The Mathematics of Diffusion* (2<sup>nd</sup> ed). Clarendon Press, Oxford.
- Cuq, B., Gontard, N., Cuq, J.-L., Guilbert, S., (1997). Selected Functional Properties of Fish Myofibrillar Protein-Based Films As Affected by Hydrophilic Plasticizers. *Journal of Agriculture and Food Chemistry* 45, 622-626.
- Dai, C.-A., Chen, Y.-F., Liu, M.-W., (2006). Thermal Properties Measurements of Renatured Gelatin Using Conventional and Temperature Modulated Differential Scanning Calorimetry. *Journal of Applied Polymer Science* 99, 1795-1801.
- Denavi, G., Tapia-Blácido, D.R., Añón, M.C., Sobral, P.J.A., Mauri, A.N., Menegalli, F.C., (2009). Effects of drying conditions on some physical properties of soy protein films. *Journal of Food Engineering* 90(3), 341-349.

- Dlubek, G., Gupta, A.S., Pionteckc, J., R. Haßler, Krause-Rehberg, R., Kaspere, H., Lochhaase, K.H., (2005). Glass transition and free volume in the mobile (MAF) and rigid (RAF) amorphous fractions of semicrystalline PTFE: a positron lifetime and PVT study. *Polymer* 46 6075-6089.
- Domjan, A., Bajdik, J., Pintye-Hódi, K., (2009). Understanding of the Plasticizing Effects of Glycerol and PEG 400 on Chitosan Films Using Solid-State NMR Spectroscopy. *Macromolecules* 42, 4667-4673.
- Dong, X., Wrolstad, R.E., Sugar, D., (2008). Extending Shelf Life of Fresh-cut Pears. *Journal of Food Science* 65(1), 1-6.
- Epure, V., Griffon, M., Pollet, E., Avérous, L., (2011). Structure and properties of glycerol-plasticized chitosan obtained by mechanical kneading. *Carbohydrate Polymers* 83, 947-952.
- Fennema, O.R., (1996). *Water and ice*. Marcel Dekker, Inc, New York.
- Fernandes, F.A.N., Gallão, M.I., Rodrigues, S., (2008). Effect of osmotic dehydration and ultrasound pre-treatment on cell structure: Melon dehydration. *LWT - Food Science and Technology* 41(4), 604-610.
- Ferry, J.D., (1980). *Viscoelastic Properties of Polymers* (3<sup>rd</sup> ed). John Wiley & Sons , Inc, New York.
- Franck, C., Lammertyna, J., Ho, Q.T., Verboven, P., Verlinden, B., Nicolai, B.M., (2007). Browning disorders in pear fruit. *Postharvest Biology and Technology* 43, 1-13.
- Gao, C., Stading, M., Wellner, N., Parker, M.L., Noel, T.R., Mills, E.N.C., Belton, P.S., (2006). Plasticization of a Protein-Based Film by Glycerol: A Spectroscopic, Mechanical, and Thermal Study. *Journal Agricultural Food Chemistry* 54, 4611-4616.
- Garcia, M.A., Pinotti, A., Martino, M.N., Zaritzky, N.E., (2004). Characterization of composite hydrocolloid films. *Carbohydrate Polymers* 56, 339-345.
- Godbillot, L., Dole, P., Joly, C., Rogé, B., Mathlouthi, M., (2006). Analysis of water binding in starch plasticized films. *Food Chemistry* 96, 380–386.

- Gomes, M.H., Fundo, J.F., Santos, S., Amaro, A.L., Almeida, D.P.F., (2010). Hydrogen ion concentration affects quality retention and modifies the effect of calcium additives on fresh-cut 'Rocha' pear. *Postharvest Biology and Technology* 58, 239-246.
- Hasegawa, M., Isogai, A., Onabe, F., Usuda, M., Atalla, R.H., (1992). Characterization of cellulose–chitosan blend films. *Journal of Applied Polymer Science* 45(11), 1873-1879.
- Hernández-Sánchez, N., Hills, B.P., Barreiro, P., Marigheto, N., (2007). An NMR study on internal browning in pears. *Postharvest Biology and Technology* 44, 260-270.
- Hills, B.P., Cano, C., Belton, P.S., (1991). Proton NMR Relaxation Studies of Aqueous Polysaccharide Systems. *Macromolecules* 24, 2944-2950.
- Hills, B.P., Manning, C.E., Ridge, Y., (1996a). New theory of water activity in heterogeneous systems. *Journal Chemical Society* 92(6), 979-983.
- Hills, B.P., Manning, C.E., Ridge, Y., Brocklehurst, T., (1996b). NMR Water Relaxation, Water Activity and - Bacterial Survival in Porous Media. *Journal of the Science of Food and Agriculture* 71, 185-194.
- Hills, B.P., Manning, C.E., Ridge, Y., Brocklehurst, T., (1996c). NMR Water Relaxation, Water Activity and Bacterial Survival in Porous Media. *Journal of the Science of Food and Agriculture* 71(2), 185–194.
- Hills, B.P., Manning, C.E., Ridge, Y., Brocklehurst, T., (1997). Water availability and the survival of *Salmonella typhimurium* in porous systems. *International Journal of Food Microbiology* 36, 187- 198.
- Hills, B.P., Remigereau, B., (1997). NMR studies of changes in subcellular water compartmentation in parenchyma apple tissue during drying and freezing. *International Journal of Food Science and Technology* 32(1), 51-61.
- Jeck, S., Scharfer, P., Schabel, W., Kind, M., (2012). Water sorption in semicrystalline poly(vinyl alcohol) membranes: In situ characterisation of solvent-induced structural rearrangements. *Journal of Membrane Science* 389, 162- 172.
- Kaláb, M., Allan-Wojm, P., Miller, S.S., (1995). Microscopy ,and other imaging techniques in food structure analysis. *Trends in Food Science & Technology* 6, 177-186.

- Keeler, J., (2002). Understanding NMR Spectroscopy, in: University of Cambridge, D.o.C. (Ed.). John Wiley & Sons , Inc, New York.
- Kou, Y., Molitor, P.F., Schmidt, S.J., (1999). Mobility and stability characterization of model food systems using NMR, DSC, and *Conidia* germination techniques. *Journal of Food Science* 64(6), 950-957.
- Kuwabara, K., Gana, Z., Nakamura, T., Abea, H., Doia, Y., (2004). Molecular mobility and crystalline phase structure of biodegradable poly[(R)-3-hydroxybutyric acid-co-(R)-3-hydroxyhexanoic acid]. *Polymer Degradation and Stability* 84, 135-141.
- Labuza, T.P., (1977). The properties of water in relationship to water binding in foods: A review. *Journal of Food Processing and Preservation* 1(2), 167-190.
- Labuza, T.P., Cassil, S., Sinskey, A.J., (1972). Stability of intermediate moisture foods . 2. Microbiology. *Journal of Food Science* 37, 160-162.
- Lavorgna, M., Piscitelli, F., Mangiacapra, P., Buonocore, G.G., (2010). Study of the combined effect of both clay and glycerol plasticizer on the properties of chitosan films. *Carbohydrate Polymers* 82, 291-298.
- Lawrie, G., Keen, I., Drew, B., Chandler-Temple, A., Rintoul, L., Fredericks, P., Grøndahl, L., (2007). Interactions between Alginate and Chitosan Biopolymers Characterized Using FTIR and XPS. *Biomacromolecules* 8, 2533-2541.
- Lazaridou, A., Biliaderis, C.G., (2002). Thermophysical properties of chitosan, chitosan-starch and chitosan-pullulan films near the glass transition. *Carbohydrate Polymers* 48, 179-190.
- Leceta, I., Guerrero, P., Caba, K.d.I., (2013). Functional properties of chitosan-based films. *Carbohydrate Polymers* 93, 339-346.
- Lefebvre, J.M., Escaig, B., (1993). The role of molecular mobility in the yielding of solid polymers. *Polymer* 34(3), 518-527.
- León, P.G., Lamanna, M.E., Gerschenson, L.N., Rojas, A.M., (2008). Influence of composition of edible films based on gellan polymers on l-(+)-ascorbic acid stability. *Food Research International* 41(6), 667-675.

- Lesage, P., Destain, M.-F., (1996). Measurement of tomato firmness by using a non-destructive mechanical sensor. *Postharvest Biology and Technology* 8, 45-55.
- Lesmes, U., McClements, D.J., (2009). Structure-function relationships to guide rational design and fabrication of particulate food delivery systems. *Trends in Food Science & Technology* 20, 448-457.
- Lewicki, P.P., (2004). Water as the determinant of food engineering properties. A review. *Journal of Food Engineering* 61, 483-495.
- Li, R., Kerr, W.L., Toledo, R.T., Carpenter, J.A., (2000). <sup>1</sup>H NMR Studies of Water in Chicken Breast Marinated with Different Phosphates. *Journal of Food Science* 65(4), 575-580.
- Lin, X., Ruan, R.R., Chen, P.L., Chung, M., Ye, X., Yang, T., Doona, C., Wagner, T., (2006). NMR state diagram concept *Journal of Food Science* 71(9), 136-143.
- Liu, H., Adhikari, R., Guo, Q., Adhikari, B., (2013). Preparation and characterization of glycerol plasticized (high-amylose) starch–chitosan films *Journal of Food Engineering* 116(2), 588-597.
- Lourdin, D., H. Bizot, Colonna, P., (1997). “Antiplasticization” in Starch-Glycerol Films? *Journal of Applied Polymer Science* 63, 1047-1053.
- Ludescher, R.D., Shah, N.K., McCaul, C.P., Simon, K.V., (2001). Beyond Tg: optical luminescence measurements of molecular mobility in amorphous solid foods. *Food Hydrocolloids* 15, 331-339.
- Maltini, E., Torreggiani, D., Venir, E., Bertolo, G., (2003). Water activity and the preservation of plant foods. *Food Chemistry* 82, 79-86.
- Marangoni, A.G., Palma, T., Stanley, D.W., (1996). Membrane effects in postharvest physiology. *Postharvest Biology and Technology*(7), 193-217.
- Marcone, M.F., Wang, S., Albabish, W., Nie, S., Somnarain, D., Hill, A., (2013). Diverse food-based applications of nuclear magnetic resonance (NMR) technology. *Food Research International* 51, 729-747.
- Marigheto, N., Venturi, L., Hills, B., (2008). Two-dimensional NMR relaxation studies of apple quality. *Postharvest Biology and Technology* 48, 331-340.

Martínez-Camacho, A.P., Cortez-Rocha, M.O., Ezquerro-Brauer, J.M., Graciano-Verdugo, A.Z., Rodríguez-Félix, F., Castillo-Ortega, M.M., Yépez-Gómez, M.S., Plascencia-Jatomea, M., (2010). Chitosan composite films: Thermal, structural, mechanical and antifungal properties. *Carbohydrate Polymers* 82, 305–315.

Martinez, M.V., Whitaker, J.R., (1995). The biochemistry and control of enzymatic browning. *Trends in Food Science and Technology* 6, 195-200.

Martins, J.T., Cerqueira, M.A., Bartolomeu W. S. Souza, Avides, M.D.C., Vicente, A.A., (2010). Shelf Life Extension of Ricotta Cheese Using Coatings of Galactomannans from Nonconventional Sources Incorporating Nisin against *Listeria monocytogenes*. *Journal of Agricultural and Food Chemistry* 58, 1884-1891.

Mathlouthi, M., (2001). Water content, water activity, water structure and the stability of foodstuffs. *Food Control* 12(7), 409-417.

Matveeva, Y.I., Grinberga, V.Y., Tolstoguzov, V.B., (2000). The plasticizing effect of water on proteins, polysaccharides and their mixtures. Glassy state of biopolymers, food and seeds. *Food Hydrocolloids* 14 425-437.

McHugh, T.H., Avena-Bustillos, R., Krochta, J.M., (1993). Hydrophilic Edible Films: Modified Procedure for Water Vapor Permeability and Explanation of Thickness Effects. *Journal of Food Science* 58(4), 899-903.

Melissa Gurgel Adeodato Vieira, M.A.d.S., Lucielen Oliveira dos Santos, Marisa Masumi Beppu, (2011). Natural-based plasticizers and biopolymer films: A review. *European Polymer Journal* In Press.

Munira, Z.A., Rosnah, S., Zaulia, O., Russly, A.R., (2013). Effect of postharvest storage of whole fruit on physico-chemical and microbial changes of fresh-cut cantaloupe (*Cucumis melo L. reticulatus* cv. Glamour). *International Food Research Journal* 20(1), 501-508.

Muzzarelli, R.A.A., (1998). Colorimetric Determination of Chitosan Analytical Biochemistry 260, 255-257.



- Neto, C.G.T., Giacometti, J.A., Job, A.E., Ferreira, F.C., Fonseca, J.L.C., Pereira, M.R., (2005). Thermal Analysis of Chitosan Based Networks. *Carbohydrate Polymers* 62, 97-103.
- Okuyama, K., Noguchi, K., Miyazawa, T., (1997). Molecular and Crystal Structure of Hydrated Chitosan. *Macromolecules* 30, 5849-5855.
- Olsen, N.V., Sijtsema, S.J., Hall, G., (2010). Predicting consumers' intention to consume ready-to-eat meals. The role of moral attitude. *Appetite* 55, 534-539.
- Oms-Oliu, G., Raybaudi-Massilia Martánez, R.M., Soliva-Fortuny, R., Martán-Belloso, O., (2008). Effect of superatmospheric and low oxygen modified atmospheres on shelf-life extension of fresh-cut melon. *Food Control* 19(2), 191-199.
- Ostrowska-Czubenko, J., ska, M.G.-D.-z., (2009). Effect of ionic crosslinking on the water state in hydrogel chitosan membranes. *Carbohydrate Polymers* 77, 590-598.
- Palzer, S., (2010). The relation between material properties and supra-molecular structure of watersoluble food solids. *Trends in Food Science & Technology* 21, 12-15.
- Panarese, V., Laghi, L., Pisi, A., Tylewicz, U., Rosa, M.D., Rocculi, P., (2012). Effect of osmotic dehydration on *Actinidia deliciosa* Kiwifruit: A combined NMR and ultrastructural study. *Food Chemistry* 132, 1076 - 1712.
- Peppas, N.A., Brannon-Peppas, L., (1994). Water diffusion and sorption in amorphous macromolecular systems and foods *Journal of Food Engineering* 22(1-4), 189-210.
- Pillai, C.K.S., Paul, W., Sharma, C.P., (2009). Chitin and chitosan polymers: Chemistry, solubility and fiber formation. *Progress in Polymer Science* 34, 641–678.
- Pinheiro, A.C., Bourbon, A.I., Vicente, A.A., Quintas, M.A.C., (2013). Transport mechanism of macromolecules on hydrophilic bio-polymeric matrices – Diffusion of protein-based compounds from chitosan films. *Journal of Food Engineering* 116(3), 633-638.
- Pittia, P., Sacchetti, G., (2008). Antiplasticization effect of water in amorphous foods. A review. *Food Chemistry* 106 1417-1427.
- Portela, S.I., Cantwell, M.I., (1998). Quality changes of minimally processed honeydew melons stored in air or controlled atmosphere. *Postharvest Biology and Technology* 14(3), 351-357.

Prashanth, K.V.H., Tharanathan, R.N., (2007). Chitin/chitosan: modifications and their unlimited application potential - an overview. *Trends in Food Science & Technology* 18, 117-131.

Provencher, S.W., (1982). A constrained regularization method for inverting data represented by linear algebraic or integral equations. *Computer Physics Communications* 27, 213-227.

Quijada-Garrido, I., Iglesias-González, V., Mazo'n-Arechederra, J.M., Barrales-Rienda, J.M., (2007). The role played by the interactions of small molecules with chitosan and their transition temperatures. *Glass-forming liquids: 1,2,3-Propantriol (glycerol)*. *Carbohydrate Polymers* 68, 173-186.

Quintas, M.A.C., Fundo, J.F., Silva, C.L.M., (2010). Sucrose in the Concentrated Solution or the Supercooled "State": A Review of Caramelisation Reactions and Physical Behaviour. *Food Engineering Reviews* 2, 204-215.

Raffo, A., Gianferri, R., Barbieri, R., Brosio, E., (2005). Ripening of banana fruit monitored by water relaxation and diffusion  $^1\text{H-NMR}$  measurements. *Food Chemistry* 89, 149-158.

Rahman, M.S., (2006). State diagram of foods: Its potential use in food processing and product stability. *Trends in Food Science & Technology* 17, 129-141.

Rahman, M.S., (2010). Food stability determination by macro–micro region concept in the state diagram and by defining a critical temperature. *Journal of Food Engineering* 99, 402-416.

Rico, D., Martín-Diana, A.B., Barat, J.M., Barry-Ryan, C., (2007). Extending and measuring the quality of fresh-cut fruit and vegetables: a review. *Trends in Food Science & Technology* 18(7), 373-386.

Rinaudo, M., (2006). Chitin and chitosan: Properties and applications. *Progress Polymer Science* 31, 603-632.

Rivero, S., García, M.A., Pinotti, A., (2010). Correlations between structural, barrier, thermal and mechanical properties of plasticized gelatin films. *Innovative Food Science and Emerging Technologies* 11, 369-375.

- Rojas, A.M., Castro, M.A., Alzamora, S.M., Gerschenson, L.N., (2001). Turgor Pressure Effects on Textural Behavior of Honeydew Melon. *Journal of Food Science* 66(1), 111-117.
- Roos, Y., (1995). Characterization of Food Polymers Using State Diagrams. *Journal of Food Engineering* 24, 339-360.
- Roos, Y.H., (1998). Phase transitions and structure of solid food matrices. *Current Opinion in Colloid & Interface Science* 3, 651-656.
- Roudaut, G., Simatos, D., Champion, D., Contreras-Lopez, E., Meste, M.L., (2004). Molecular mobility around the glass transition temperature: a mini review. *Innovative Food Science and Emerging Technologies* 5, 127-134.
- Ruan, R.R., Chen, P.L., (1998). *Water in foods and biological materials - A nuclear magnetic resonance approach*. Technomic Publishing Company, Inc., Lancaster, Pennsylvania.
- Sablani, S.S., Kasapis, S., Rahman, M.S., (2007). Evaluating water activity and glass transition concepts for food stability. *Journal of Food Engineering* 78, 266-271.
- Scholten, E., Moschakis, T., Biliaderis, C.G., (2014). Biopolymer composites for engineering food structures to control product functionality. *Food Structure* 1, 39-54.
- Simandjuntak, V., Barrett, D.M., Wrolstad, R.E., (1996). Cultivar and Frozen Storage Effects on Muskmelon (*Cucumis melo*) Colour, Texture and Cell Wall Polysaccharide Composition. *Journal of Science of Food and Agricultural* 71(3), 291-206.
- Slade, L., Levine, H., (1991). Beyond water activity: Recent advances based on an alternative approach to the assessment of food quality and safety. *Critical Reviews in Food Science and Nutrition* 30(2-3), 115-360.
- Slade, L., Levine, H., (1995). Water and the glass transition - Dependence of the glass transition on composition and chemical structures: Special implications for flour functionality in cookie baking. *Journal of Food Engineering* 24, 431-509.
- Snaar, J.E.M., Van As, H., (1992). Probing water compartments and membrane permeability in plant cells by <sup>1</sup>H NMR relaxation measurements. *Journal Biophysics* 63, 1654-1658.

Sobral, P.J.A., Menegalli, F.C., Hubinger, M.D., Roques, M.A., (2001). Mechanical, water vapour barrier and thermal properties of gelatin based edible films. *Food Hydrocolloids* 15, 423-432.

Soliva-Fortuny, R.C., Alós-Saiz, N., Espachs-Barroso, A., Martín-Belloso, O., (2004). Influence of Maturity at Processing on Quality Attributes of Fresh-cut Conference Pears. *Journal of Food Science* 69(7), 290-294.

Soliva-Fortuny, R.C., Grigelmo-Miguel, N., Hernando, I., Lluch, M.Á., Martín-Belloso, O., (2002). Effect of minimal processing on the textural and structural properties of fresh-cut pears. *Journal of the Science of Food and Agriculture* 82, 1682-1688.

Spathis, G., Kontou, E., (1998). Experimental and theoretical description of the plastic behaviour of semicrystalline polymers. *Polymer* 39(1), 135-142.

Srinivasa, P.C., Ramesh, M.N., Tharanathan, R.N., (2007). Effect of plasticizers and fatty acids on mechanical and permeability characteristics of chitosan films. *Food Hydrocolloids* 21, 1113-1122.

Steffe, J.F., (1996). *Rheological Methods in Food Process Engineering* (2<sup>nd</sup> ed). Freeman Press, East Lansing, MI.

Suyatma, N.E., Tighzert, L., Copinet, A., (2005). Effects of Hydrophilic Plasticizers on Mechanical, Thermal, and Surface Properties of Chitosan Films. *Journal of Agricultural and Food Chemistry* 53, 3950-3957.

Tapia-Blácido, D.R., Sobral, P.J.d.A., Menegalli, F.C., (2011). Optimization of amaranth flour films plasticized with glycerol and sorbitol by multi-response analysis. *LWT - Food Science and Technology* 44, 1731-1738.

Toivonen, P.M.A., Brummel, D.A., (2008). Biochemical bases of appearance and texture changes in fresh-cut fruit and vegetables. *Postharvest Biology and Technology* 48, 1-14.

Tu, S.S., Choi, Y.J., McCarthy, M.J., McCarthy, K.L., (2007). Tomato quality evaluation by peak force and NMR spin-spin relaxation time. *Postharvest Biology and Technology* 44(2), 157-164.

Tylewicz, U., Panarese, V., Laghi, L., Rocculi, P., Nowacka, M., Placucci, G., Rosa, M.D., (2011). NMR and DSC Water Study During Osmotic Dehydration of *Actinidia deliciosa* and *Actinidia chinensis* Kiwifruit. *Food Biophysics* 6, 327-333.

Ubbink, J., Kruger, J., (2006). Physical approaches for the delivery of active ingredients in foods. *Trends in Food Science & Technology* 17(5), 244-254.

V. Guillard, B.B., C. Bonazzi, S. Guilbert, N. Gontard, (2003). Preventing Moisture Transfer in a Composite Food Using Edible Films: Experimental and Mathematical Study. *Journal of Food Science* 68(7), 2267–2277.

Vargas, M., Perdones, Á., Chiralt, A., Cháfer, M., González-Martínez, C., (2011). Effect of homogenization conditions on physicochemical properties of chitosan-based film-forming dispersions and films. *Food Hydrocolloids* 25(5), 1158-1164.

Viciosa, M.T., Dionísio, M., Silva, R.M., Reis, R.L., Mano, J.F., (2004). Molecular Motions in Chitosan Studied by Dielectric Relaxation Spectroscopy. *Biomacromolecules* 5, 2073-2078.

Vilas-Boas, E.V.d.B., Kader, A.A., (2007). Effect of 1-methylcyclopropene (1-MCP) on softening of fresh-cut kiwifruit, mango and persimmon slices. *Postharvest Biology and Technology* 43(2), 238-244.

Vittadini, E., Chinachoti, P., (2003). Effect of physico-chemical and molecular mobility parameters on *Staphylococcus aureus* growth. *International Journal of Food Science and Technology* 38, 841-847.

Vittadini, E., Chinachoti, P., Lavoie, J.P., Pham, X., (2005). Correlation of microbial response in model food systems with physico-chemical and mobility descriptors of the media. *Innovative Food Science and Emerging Technologies* 6, 21-28.

Vittadini, E., Dickinson, L.C., Lavoie, J.P., Pham, X., Chinachoti, P., (2003). Water Mobility in Multicomponent Model Media As Studied by  $^2\text{H}$  and  $^{17}\text{O}$  NMR. *Journal of Agricultural and Food Chemistry* 51, 1647-1652.

Wang, J.-C., Liapis, A.I., (2012). Water-water and water-macromolecules interactions in food dehydration and the effects of the pore structure of food on the energetics of the interactions. *Journal of Food Engineering* 110, 514-524.

Watada, A.E., Qi, L., (1999). Quality of fresh-cut produce. *Postharvest Biology and Technology* 15(3), 201-205.

Wong, S.-S., Altinkaya, S.A., Mallapragada, S.K., (2004). Drying of semicrystalline polymers: mathematical modeling and experimental characterization of poly(vinyl alcohol) films. *Polymer* 45, 5151–5161.

Xiong, X., Narsimhan, G., Okos, M.R., (1992). Effect of composition and pore structure on binding energy and effective diffusivity of moisture in porous food *Journal of Food Engineering* 15(3), 187-208.

Yan, Z.-Y., McCarthy, M.J., Klemann, L., Otterburn, M.S., Finley, J., (1996). NMR Applications in Complex Food Systems. *Magnetic Resonance Image* 14(7/8), 979-981.

Yang, Y., Liu, C., Wu, H., Li, R., (2010). Preparation and characterization of films based on zirconium sulfophenyl phosphonate and chitosan. *Carbohydrate Research* 345, 148-153.

Zhang, L., McCarthy, M.J., (2013). Effect of controlled atmosphere storage on pomegranate quality investigated by two dimensional NMR correlation spectroscopy. *LWT - Food Science and Technology* 54, 302-306.

Zhang, X., Iko Burgar, M.D.D., Lourbakos, E., (2005). Intermolecular Interactions and Phase Structures of Plasticized Wheat Proteins Materials. *Biomacromolecules* 6, 1661-1671.

Ziani, K., Osés, J., Coma, V., Maté, J.I., (2008). Effect of the presence of glycerol and Tween 20 on the chemical and physical properties of films based on chitosan with different degree of deacetylation. *LWT - Food Science and Technology* 41(10), 2159-2165.

Zivanovic, S., Jiajie Li, Davidson, P.M., Kit, K., (2007). Physical, Mechanical, and Antibacterial Properties of Chitosan/ PEO Blend Films *Biomacromolecules* 8, 1505-1510.

## **APPENDICES**

---





## **Appendix A**

---

*Appendix to Chapter 2*



## A.1 Experimental results of film forming solution (FFS) macroscopic properties

**Table A.1.1** Experimental data of FFS rheological measurements

Gly (%)	Chit (%)	Sample	Experiment 1		Experiment 2	
			Shear stress (Pa)	Shear rate (s <sup>-1</sup> )	Shear stress (Pa)	Shear rate (s <sup>-1</sup> )
1	90	1	2.1	20.0	1.9	20.0
1	90	1	3.2	30.9	2.9	30.9
1	90	1	4.9	47.7	4.4	47.7
1	90	1	7.4	73.7	6.7	73.7
1	90	1	11.1	113.8	10.1	113.8
1	90	1	16.2	175.7	14.9	175.7
1	90	1	22.7	271.3	21.4	271.3
1	90	1	33.5	419.1	31.1	419.1
1	90	1	43.7	647.2	42.8	647.2
1	90	1	63.9	999.6	61.1	999.6
1	90	2	1.9	20.0	1.7	20.0
1	90	2	2.9	30.9	2.7	30.9
1	90	2	4.4	47.7	4.1	47.7
1	90	2	6.7	73.7	6.2	73.7
1	90	2	9.9	113.8	9.3	113.8
1	90	2	14.5	175.7	13.8	175.7
1	90	2	20.3	271.3	23.2	271.3
1	90	2	30.1	419.1	28.6	419.1
1	90	2	37.4	647.2	40.3	647.2
1	90	2	56.9	999.6	56.9	999.6
1	90	3	2.2	20.0	1.5	20.0
1	90	3	3.4	30.9	2.2	30.9
1	90	3	5.2	47.7	3.4	47.7
1	90	3	7.8	73.7	5.2	73.7
1	90	3	11.6	113.8	7.8	113.8
1	90	3	17.0	175.7	11.6	175.7
1	90	3	22.3	271.3	15.9	271.3
1	90	3	34.4	419.1	24.1	419.1
1	90	3	44.8	647.2	30.4	647.2
1	90	3	67.5	999.6	47.8	999.6
1	50	1	2.0	20.0	2.2	20.0
1	50	1	3.1	30.9	3.4	30.9
1	50	1	4.7	47.7	5.2	47.7
1	50	1	7.1	73.7	7.7	73.7
1	50	1	10.9	113.8	10.7	113.8
1	50	1	15.6	175.7	16.8	175.7
1	50	1	21.3	271.3	24.2	271.3

**Table A.1.1 (continued)** Experimental data of FFS rheological measurements

Gly (%)	Chit (%)	Sample	Experiment 1		Experiment 2	
			Shear stress (Pa)	Shear rate (s <sup>-1</sup> )	Shear stress (Pa)	Shear rate (s <sup>-1</sup> )
1	50	1	30.9	419.1	33.9	419.1
1	50	1	40.6	647.2	54.2	647.2
1	50	1	62.4	999.6	64.9	999.6
1	50	2	1.9	20.0	1.9	20.0
1	50	2	2.9	30.9	2.9	30.9
1	50	2	4.5	47.7	4.4	47.7
1	50	2	6.8	73.7	6.6	73.7
1	50	2	10.1	113.8	9.8	113.8
1	50	2	14.8	175.7	14.2	175.7
1	50	2	22.9	271.3	19.4	271.3
1	50	2	30.5	419.1	28.8	419.1
1	50	2	44.2	647.2	41.9	647.2
1	50	2	59.0	999.6	54.7	999.6
1	50	3	2.1	20.0	2.6	20.0
1	50	3	3.2	30.9	3.9	30.9
1	50	3	4.8	47.7	5.9	47.7
1	50	3	7.3	73.7	8.9	73.7
1	50	3	10.9	113.8	13.2	113.8
1	50	3	16.0	175.7	19.2	175.7
1	50	3	21.8	271.3	26.3	271.3
1	50	3	32.2	419.1	39.1	419.1
1	50	3	48.5	647.2	59.7	647.2
1	50	3	63.4	999.6	75.4	999.6
1	10	1	2.3	20.0	1.9	20.0
1	10	1	3.6	30.9	2.9	30.9
1	10	1	5.5	47.7	4.5	47.7
1	10	1	8.3	73.7	6.8	73.7
1	10	1	12.3	113.8	10.2	113.8
1	10	1	18.1	175.7	15.2	175.7
1	10	1	26.3	271.3	24.6	271.3
1	10	1	37.3	419.1	32.5	419.1
1	10	1	53.7	647.3	46.9	647.2
1	10	1	72.7	999.6	63.3	999.6
1	10	2	1.6	20.0	1.6	20.0
1	10	2	2.3	30.9	2.5	30.9
1	10	2	3.6	47.7	3.7	47.7
1	10	2	5.4	73.7	5.9	73.7

**Table A.1.1 (continued)** Experimental data of FFS rheological measurements

Gly (%)	Chit (%)	Sample	Experiment 1		Experiment 2	
			Shear stress (Pa)	Shear rate (s <sup>-1</sup> )	Shear stress (Pa)	Shear rate (s <sup>-1</sup> )
1	10	2	8.1	113.8	8.9	113.8
1	10	2	11.8	175.7	13.1	175.7
1	10	2	18.0	271.3	19.3	271.3
1	10	2	25.0	419.1	28.1	419.1
1	10	2	27.8	647.2	37.6	647.2
1	10	2	47.3	999.6	54.2	999.6
1	10	3	1.4	20.0	1.5	20.0
1	10	3	2.1	30.9	2.3	30.9
1	10	3	3.2	47.7	3.5	47.7
1	10	3	4.8	73.7	5.3	73.7
1	10	3	7.2	113.8	8.1	113.8
1	10	3	10.6	175.7	11.9	175.7
1	10	3	14.1	271.3	16.6	271.3
1	10	3	22.6	419.1	25.7	419.1
1	10	3	36.4	647.2	36.3	647.3
1	10	3	41.8	999.6	50.3	999.6
2	90	1	10.5	20.0	8.1	20.0
2	90	1	15.5	30.9	12.0	30.9
2	90	1	22.5	47.7	17.7	47.7
2	90	1	32.3	73.7	25.6	73.7
2	90	1	45.5	113.8	37.3	113.8
2	90	1	63.0	175.7	50.9	175.7
2	90	1	85.8	271.3	68.7	271.3
2	90	1	114.5	419.1	94.6	419.1
2	90	1	145.7	647.1	117.3	647.2
2	90	1	195.0	999.6	164.0	999.6
2	90	2	8.4	20.0	7.8	20.0
2	90	2	12.5	30.9	11.7	30.9
2	90	2	18.2	47.7	17.3	47.7
2	90	2	26.2	73.7	25.1	73.7
2	90	2	36.9	113.8	35.7	113.8
2	90	2	51.1	175.7	50.0	175.7
2	90	2	68.6	271.3	70.6	271.3
2	90	2	92.6	419.1	92.5	419.1
2	90	2	120.2	647.2	123.5	647.2
2	90	2	159.3	999.6	160.0	999.6
2	90	3	10.4	20.0	7.1	20.0

**Table A.1.1 (continued)** Experimental data of FFS rheological measurements

Gly (%)	Chit (%)	Sample	Experiment 1		Experiment 2	
			Shear stress (Pa)	Shear rate (s <sup>-1</sup> )	Shear stress (Pa)	Shear rate (s <sup>-1</sup> )
2	90	3	15.5	30.9	10.6	30.9
2	90	3	22.1	47.7	15.6	47.7
2	90	3	31.4	73.7	23.0	73.6
2	90	3	44.0	113.8	32.3	113.8
2	90	3	60.3	175.7	45.2	175.7
2	90	3	81.7	271.3	62.3	271.3
2	90	3	105.2	419.1	83.6	419.1
2	90	3	138.5	647.2	111.3	647.2
2	90	3	179.6	999.6	146.6	999.6
2	50	1	8.1	20.0	6.8	20.0
2	50	1	12.1	30.9	10.0	30.9
2	50	1	17.6	47.7	14.6	47.7
2	50	1	25.4	73.7	21.0	73.7
2	50	1	35.8	113.8	29.7	113.8
2	50	1	49.8	175.7	41.2	175.7
2	50	1	66.0	271.3	56.3	271.3
2	50	1	90.9	419.1	74.8	419.1
2	50	1	118.5	647.2	97.7	647.2
2	50	1	155.5	999.6	128.9	999.6
2	50	2	8.2	20.0	7.8	20.0
2	50	2	12.2	30.9	11.5	30.9
2	50	2	17.9	47.7	16.9	47.7
2	50	2	25.7	73.7	24.3	73.7
2	50	2	36.4	113.8	34.3	113.8
2	50	2	50.6	175.7	47.5	175.7
2	50	2	68.4	271.3	63.2	271.3
2	50	2	92.0	419.1	86.7	419.1
2	50	2	118.1	647.2	118.3	647.2
2	50	2	158.9	999.6	150.0	999.6
2	50	3	9.9	20.0	8.5	20.0
2	50	3	14.7	30.9	12.6	30.9
2	50	3	21.5	47.7	18.5	47.7
2	50	3	30.9	73.7	26.6	73.7
2	50	3	43.7	113.8	37.6	113.8
2	50	3	60.8	175.7	52.1	175.7
2	50	3	83.4	271.3	69.4	271.3
2	50	3	111.1	419.1	94.3	419.1

**Table A.1.1 (continued)** Experimental data of FFS rheological measurements

Gly (%)	Chit (%)	Sample	Experiment 1		Experiment 2	
			Shear stress (Pa)	Shear rate (s <sup>-1</sup> )	Shear stress (Pa)	Shear rate (s <sup>-1</sup> )
2	50	3	145.4	647.2	131.5	647.2
2	50	3	191.3	999.6	163.2	999.6
2	10	1	9.2	20.0	14.9	20.0
2	10	1	13.6	30.9	21.8	30.9
2	10	1	19.7	47.7	31.4	47.7
2	10	1	28.1	73.7	44.4	73.7
2	10	1	39.3	113.8	61.5	113.8
2	10	1	53.8	175.7	83.9	175.7
2	10	1	70.1	271.3	113.6	271.3
2	10	1	95.8	419.1	148.1	419.1
2	10	1	123.5	647.2	191.4	647.2
2	10	1	151.2	999.6	245.7	999.6
2	10	2	11.6	20.0	14.4	20.0
2	10	2	17.1	30.9	21.1	30.9
2	10	2	24.7	47.7	30.3	47.7
2	10	2	35.1	73.7	42.8	73.7
2	10	2	48.9	113.8	59.4	113.8
2	10	2	66.9	175.7	80.9	175.7
2	10	2	90.9	271.3	107.8	271.3
2	10	2	118.3	419.1	142.8	419.1
2	10	2	147.6	647.2	180.2	647.2
2	10	2	197.8	999.6	235.1	999.6
2	10	3	9.5	20.0	14.0	20.0
2	10	3	13.9	30.9	20.5	30.9
2	10	3	20.0	47.7	29.5	47.7
2	10	3	28.4	73.7	41.7	73.7
2	10	3	39.5	113.8	57.9	113.8
2	10	3	53.9	175.7	79.0	175.7
2	10	3	71.2	271.3	104.2	271.3
2	10	3	96.0	419.1	138.9	419.1
2	10	3	124.6	647.2	180.1	647.2
2	10	3	150.9	999.6	229.4	999.6
3	90	1	15.3	20.0	15.8	20.0
3	90	1	22.3	30.9	23.0	30.9
3	90	1	31.8	47.7	33.1	47.7
3	90	1	44.6	73.7	46.7	73.7
2	50	3	145.4	647.2	131.5	647.2

**Table A.1.1 (continued)** Experimental data of FFS rheological measurements

Gly (%)	Chit (%)	Sample	Experiment 1		Experiment 2	
			Shear stress (Pa)	Shear rate (s <sup>-1</sup> )	Shear stress (Pa)	Shear rate (s <sup>-1</sup> )
3	90	1	61.5	113.8	64.8	113.8
3	90	1	83.1	175.7	88.2	175.7
3	90	1	111.6	271.3	115.8	271.3
3	90	1	143.5	419.1	154.1	419.1
3	90	1	180.1	647.2	204.6	647.3
3	90	1	238.8	999.6	253.7	999.6
3	90	2	14.7	20.0	16.0	20.0
3	90	2	21.3	30.9	23.4	30.9
3	90	2	30.4	47.7	34.4	47.7
3	90	2	42.7	73.7	47.5	73.7
3	90	2	58.9	113.8	65.8	113.8
3	90	2	79.6	175.7	89.2	175.7
3	90	2	105.7	271.3	119.7	271.3
3	90	2	138.4	419.1	154.6	419.1
3	90	2	174.7	647.2	199.3	647.2
3	90	2	228.8	999.6	256.2	999.6
3	90	3	13.6	20.0	15.2	20.0
3	90	3	19.7	30.9	22.2	30.9
3	90	3	28.2	47.7	31.7	47.7
3	90	3	39.0	73.6	44.7	73.7
3	90	3	54.8	113.8	61.9	113.8
3	90	3	74.3	175.7	84.1	175.7
3	90	3	97.8	271.3	112.9	271.3
3	90	3	129.2	419.1	146.4	419.1
3	90	3	164.7	647.2	196.2	647.2
3	90	3	215.0	999.6	243.3	999.6
3	50	1	15.4	20.0	16.1	20.0
3	50	1	22.4	30.9	23.2	30.9
3	50	1	32.0	47.7	32.9	47.7
3	50	1	44.9	73.7	45.9	73.6
3	50	1	61.7	113.8	62.7	113.8
3	50	1	83.2	175.7	83.8	175.7
3	50	1	109.6	271.3	111.7	271.3
3	50	1	144.0	419.1	143.1	419.1
3	50	1	187.2	647.2	186.3	647.2
3	50	1	235.4	999.6	235.0	999.6
3	50	2	14.5	20.0	16.7	20.0



**Table A.1.1 (continued)** Experimental data of FFS rheological measurements

Gly (%)	Chit (%)	Sample	Experiment 1		Experiment 2	
			Shear stress (Pa)	Shear rate (s <sup>-1</sup> )	Shear stress (Pa)	Shear rate (s <sup>-1</sup> )
3	50	2	21.0	30.9	24.1	30.9
3	50	2	29.8	47.7	34.2	47.7
3	50	2	41.6	73.7	47.6	73.7
3	50	2	57.1	113.8	65.2	113.8
3	50	2	76.7	175.7	87.2	175.7
3	50	2	102.9	271.3	113.5	271.3
3	50	2	132.5	419.1	150.3	419.1
3	50	2	171.3	647.2	188.1	647.2
3	50	2	219.2	999.6	243.1	999.6
3	50	3	15.8	20.0	15.3	20.0
3	50	3	23.0	30.9	22.1	30.9
3	50	3	32.8	47.7	31.5	47.7
3	50	3	46.0	73.7	44.0	73.7
3	50	3	63.3	113.8	60.4	113.8
3	50	3	85.5	175.7	81.1	175.7
3	50	3	113.9	271.3	106.9	271.3
3	50	3	148.2	419.1	139.1	419.1
3	50	3	189.8	647.2	179.8	647.2
3	50	3	242.8	999.6	230.2	999.6
3	10	1	18.6	20.0	16.5	20.0
3	10	1	26.8	30.9	23.9	30.9
3	10	1	38.0	47.7	34.2	47.7
3	10	1	52.9	73.6	47.9	73.7
3	10	1	72.4	113.8	66.0	113.8
3	10	1	97.0	175.7	89.1	175.7
3	10	1	128.9	271.3	120.0	271.3
3	10	1	166.4	419.1	152.2	419.1
3	10	1	211.2	647.2	196.5	647.2
3	10	1	268.5	999.6	249.8	999.6
3	10	2	14.9	20.0	12.8	20.0
3	10	2	21.5	30.9	18.8	30.9
3	10	2	30.3	47.7	26.6	47.7
3	10	2	42.2	73.7	37.3	73.7
3	10	2	57.4	113.8	51.4	113.8
3	10	2	76.8	175.7	69.5	175.7
3	10	2	101.7	271.3	93.0	271.3
3	10	2	131.6	419.1	120.8	419.1

**Table A.1.1 (continued)** Experimental data of FFS rheological measurements

Gly (%)	Chit (%)	Sample	Experiment 1		Experiment 2	
			Shear stress (Pa)	Shear rate (s <sup>-1</sup> )	Shear stress (Pa)	Shear rate (s <sup>-1</sup> )
3	10	2	176.2	647.2	154.9	647.2
3	10	2	214.2	999.6	198.6	999.6
3	10	3	17.8	20.0	15.3	20.0
3	10	3	25.7	30.9	22.2	30.9
3	10	3	36.9	47.7	31.7	47.7
3	10	3	50.7	73.6	44.5	73.7
3	10	3	69.3	113.8	61.3	113.8
3	10	3	92.9	175.7	82.8	175.7
3	10	3	123.5	271.3	110.8	271.3
3	10	3	158.8	419.1	143.7	419.1
3	10	3	205.5	647.2	186.1	647.2

**Table A.1.2** Results of  $a_w$  measurements from different FFS compositions

Gly (%)	Sample	Measure	FFS $a_w$					
			Experiment 1			Experiment 2		
			<i>Chit 1</i>	<i>Chit 2</i>	<i>Chit 3</i>	<i>Chit 1</i>	<i>Chit 2</i>	<i>Chit 3</i>
90	1	1	0.999	0.996	0.994	1.003	0.998	0.993
90	1	2	0.998	0.996	0.994	0.999	0.996	0.994
90	1	3	0.997	0.997	0.994	0.998	0.995	0.995
90	2	1	0.996	0.996	0.995	1.002	1.000	0.999
90	2	2	0.997	0.998	0.994	1.000	0.998	0.996
90	2	3	0.997	0.998	0.993	1.000	0.997	0.997
90	3	1	0.998	0.998	0.995	1.001	1.000	0.997
90	3	2	0.998	0.998	0.993	1.000	0.998	0.997
90	3	3	0.998	0.997	0.994	0.999	0.998	0.997
50	1	1	1.002	1.001	1.001	1.000	1.002	1.000
50	1	2	1.000	1.001	1.000	0.999	1.001	1.000
50	1	3	1.000	1.001	1.000	0.998	1.000	0.999
50	2	1	1.002	1.000	1.000	1.001	1.000	0.998
50	2	2	1.000	1.001	1.000	0.999	0.999	0.999
50	2	3	1.000	1.001	0.999	1.000	0.999	1.000
50	3	1	1.002	1.000	0.998	1.001	1.001	0.997
50	3	2	1.001	1.001	0.998	1.000	1.001	0.999
50	3	3	1.001	1.001	0.998	1.000	0.999	1.000
10	1	1	1.001	1.000	1.002	1.002	1.003	1.003
10	1	2	1.000	1.002	1.002	1.000	1.001	1.001
10	1	3	1.000	1.002	1.002	1.000	1.001	1.001
10	2	1	1.003	0.998	1.003	1.002	1.003	1.000
10	2	2	1.002	1.002	1.003	1.000	1.001	1.003
10	2	3	1.002	1.002	1.004	1.000	1.001	1.002
10	3	1	1.003	1.001	1.005	1.004	1.003	1.001
10	3	2	1.003	1.001	1.003	1.002	1.001	1.001
10	3	3	1.002	1.001	1.003	1.002	1.001	1.002

## A.2 Experimental results of film macroscopic properties

**Table A.2.1** Experimental results of films  $a_w$  measurements

Gly (%)	Sample	Measure	Films $a_w$					
			Experiment 1			Experiment 2		
			<i>Chit 1</i>	<i>Chit 2</i>	<i>Chit 3</i>	<i>Chit 1</i>	<i>Chit 2</i>	<i>Chit 3</i>
90	1	1	0.553	0.499	0.526	0.576	0.514	0.540
90	1	2	0.552	0.498	0.526	0.576	0.513	0.544
90	1	3	0.553	0.498	0.526	0.561	0.513	0.535
90	2	1	0.556	0.498	0.520	0.558	0.504	0.536
90	2	2	0.560	0.499	0.521	0.558	0.504	0.535
90	2	3	0.558	0.501	0.521	0.558	0.504	0.538
90	3	1	0.556	0.499		0.609	0.493	0.537
90	3	2	0.557	0.500	0.516	0.587	0.492	0.537
90	3	3	0.560	0.500	0.516	0.591	0.491	0.510
50	1	1	0.523	0.525	0.523		0.507	0.505
50	1	2	0.559	0.524			0.508	0.505
50	1	3	0.561	0.524	0.524		0.508	0.507
50	2	1	0.575	0.495	0.518	0.600	0.509	0.506
50	2	2	0.571	0.494	0.517	0.597	0.509	0.505
50	2	3	0.577	0.495	0.517	0.600	0.503	0.509
50	3	1	0.511	0.505	0.510	0.552	0.481	0.508
50	3	2	0.514	0.505	0.510	0.568	0.479	0.507
50	3	3	0.516	0.505	0.510	0.531	0.480	0.509
10	1	1	0.546	0.521	0.508	0.575	0.513	0.507
10	1	2	0.550	0.516	0.509	0.540	0.510	0.507
10	1	3	0.551	0.515	0.508	0.570	0.507	0.504
10	2	1	0.543	0.541	0.508	0.544	0.510	0.504
10	2	2	0.545	0.534	0.508	0.587	0.508	0.503
10	2	3	0.549	0.533	0.508	0.599	0.508	0.510
10	3	1	0.550	0.540	0.513	0.548	0.511	0.509
10	3	2	0.550	0.533	0.508	0.547	0.510	0.500
10	3	3	0.552	0.532	0.507	0.550	0.509	0.501

**Table A.2.2** Experimental results of films water activity ( $a_w$ ) moisture content (MC) water solubility (SOL) and oxygen permeability ( $O_2P$ )

Chit (%)	Gly (%)	Sample	Measure	Experiment 1			Experiment 2		
				MC (%)	SOL (%)	$O_2P$ ( $m^{-1}s^{-1}Pa^{-1}$ )	MC (%)	SOL (%)	$O_2P$ ( $m^{-1}s^{-1}Pa^{-1}$ )
1	90	1	1	46.40	59.01	2.46E-09	48.71	67.38	2.93E-09
1	90	1	2			2.08E-09			2.13E-09
1	90	1	3			2.44E-09			1.61E-09
1	90	2	1	51.47	62.75	1.26E-09	53.85	79.49	6.34E-09
1	90	2	2			1.29E-09			4.40E-09
1	90	2	3			1.36E-09			7.03E-09
1	90	3	1	52.82	64.52		53.83	71.98	
1	50	1	1	42.21	56.28	1.27E-09	28.73	48.68	2.48E-09
1	50	1	2			5.09E-10			1.61E-09
1	50	1	3			6.28E-10			1.41E-09
1	50	2	1	44.67	57.37	8.89E-09	27.80	47.84	3.02E-09
1	50	2	2			1.49E-08			1.71E-09
1	50	2	3			1.53E-08			1.39E-09
1	50	3	1	46.14	57.93		30.27	56.44	
1	10	1	1	22.93	46.72	1.19E-09	28.54	51.33	4.47E-09
1	10	1	2			5.86E-10			2.87E-09
1	10	1	3			4.80E-10			2.37E-09
1	10	2	1	24.34	47.67	2.04E-09	28.94	48.50	3.85E-09
1	10	2	2			2.57E-09			2.03E-09
1	10	2	3			2.34E-09			1.79E-09
1	10	3	1	39.77	47.50		28.68	51.74	
2	90	1	1	56.40	65.60	2.04E-09	46.07	55.79	7.60E-09
2	90	1	2			1.15E-09			4.62E-09
2	90	1	3			2.40E-09			3.56E-09
2	90	2	1	55.83	64.58	3.13E-09	48.33	58.15	4.82E-09
2	90	2	2			1.49E-09			3.89E-09
2	90	2	3			1.50E-09			4.40E-09
2	90	3	1	55.56	65.14		49.35	59.13	
2	50	1	1	37.90	51.60	7.32E-09	41.70	52.18	3.34E-09
2	50	1	2			8.45E-09			3.71E-09
2	50	1	3			4.94E-09			3.12E-09
2	50	2	1	39.62	52.83	7.99E-09	29.47	43.39	6.98E-09
2	50	2	2			4.93E-09			4.82E-09
2	50	2	3			5.38E-09			3.92E-09
2	50	3	1	38.82	52.94		42.43	53.19	
2	10	1	1	16.53	37.70	5.86E-09	19.07	35.80	2.61E-08
2	10	1	2			2.42E-09			2.48E-08

**Table A.2.2 (continued)** Experimental results of films water activity ( $a_w$ ), moisture content (MC), water solubility (SOL) and oxygen permeability ( $O_2P$ )

Chit (%)	Gly (%)	Sample	Measure	Experiment 1			Experiment 2		
				MC (%)	SOL (%)	$O_2P$ ( $m^{-1}s^{-1}Pa^{-1}$ )	MC (%)	SOL (%)	$O_2P$ ( $m^{-1}s^{-1}Pa^{-1}$ )
2	10	1	3			2.60E-09			1.82E-08
2	10	2	1	16.77	35.82	4.79E-09	19.00	35.60	1.01E-08
2	10	2	2			2.59E-09			4.39E-09
2	10	2	3			2.37E-09			3.32E-09
2	10	3	1	16.70	34.92		18.93	36.49	
3	90	1	1	54.29	63.07	9.60E-12	55.79	64.09	6.36E-09
3	90	1	2			5.48E-09			8.77E-09
3	90	1	3			7.90E-09			7.76E-09
3	90	2	1	53.79	62.45	1.25E-08	55.47	64.17	8.64E-09
3	90	2	2			7.56E-09			7.60E-09
3	90	2	3			6.63E-09			5.53E-09
3	90	3	1	55.24	63.31		55.76	63.62	
3	50	1	1	37.31	48.76	6.10E-09	40.16	50.40	1.16E-08
3	50	1	2			5.16E-09			8.39E-09
3	50	1	3			6.17E-09			5.43E-09
3	50	2	1	37.50	48.54	6.65E-09	39.70	50.47	1.07E-08
3	50	2	2			6.91E-09			5.77E-09
3	50	2	3			1.97E-08			5.13E-09
3	50	3	1	38.24	50.00		40.34	50.47	
3	10	1	1	15.42	28.60	1.36E-08	17.08	30.13	2.33E-08
3	10	1	2			8.90E-09			1.18E-08
3	10	1	3			9.68E-09			9.87E-09
3	10	2	1	15.93	29.27	8.15E-09	17.70	31.56	1.85E-08
3	10	2	2			7.60E-09			1.08E-08
3	10	2	3			6.13E-09			9.77E-09
3	10	3	1	15.67	29.85		16.34	28.94	

**Table A.2.3** Experimental results of films water vapour permeability (WVP)

Gly (%)	Chit (%)	Sample	Experimental time (min)	Weight loss (g)	
				Experiment 1	Experiment 2
90	1	1	0	0.00	0.00
90	1	1	120	0.05	0.06
90	1	1	240	0.12	0.13
90	1	1	360	0.18	0.20
90	1	1	480	0.25	0.26
90	1	1	600	0.32	0.30
90	1	2	0	0.00	
90	1	2	120	0.06	
90	1	2	240	0.14	
90	1	2	360	0.21	
90	1	2	480	0.29	
90	1	2	600	0.37	
90	2	1	0	0.00	0.00
90	2	1	120	0.06	0.06
90	2	1	240	0.13	0.11
90	2	1	360	0.19	0.16
90	2	1	480	0.25	0.22
90	2	1	600	0.31	0.26
90	2	2	0	0.00	0.00
90	2	2	120	0.05	0.06
90	2	2	240	0.10	0.11
90	2	2	360	0.16	0.16
90	2	2	480	0.22	0.24
90	2	2	600	0.28	0.31
90	3	1	0	0.00	
90	3	1	120	0.03	
90	3	1	240	0.05	
90	3	1	360	0.08	
90	3	1	480	0.11	
90	3	1	600	0.15	
90	3	2	0	0.00	
90	3	2	120	0.05	
90	3	2	240	0.08	
90	3	2	360	0.11	
90	3	2	480	0.16	
90	3	2	600	0.20	

**Table A.2.3 (continued)** Experimental results of films water vapour permeability (WVP)

Gly (%)	Chit (%)	Sample	Experimental time (min)	Weight loss (g)	
				Experiment 1	Experiment 2
50	1	1	0		0.00
50	1	1	120		0.07
50	1	1	240		0.14
50	1	1	360		0.21
50	1	1	480		0.29
50	1	1	600		0.33
50	1	2	0		0.00
50	1	2	120		0.08
50	1	2	240		0.15
50	1	2	360		0.23
50	1	2	480		0.32
50	1	2	600		0.37
50	2	1	0	0.00	0.00
50	2	1	120	0.09	0.05
50	2	1	240	0.15	0.12
50	2	1	360	0.20	0.20
50	2	1	480	0.26	0.28
50	2	1	600	0.32	0.44
50	2	2	0	0.00	0.00
50	2	2	120	0.08	0.08
50	2	2	240	0.14	0.16
50	2	2	360	0.19	0.24
50	2	2	480	0.23	0.31
50	2	2	600	0.28	0.45
50	3	1	0	0.00	0.00
50	3	1	120	0.05	0.04
50	3	1	240	0.09	0.11
50	3	1	360	0.13	0.18
50	3	1	480	0.17	0.22
50	3	1	600	0.21	0.36
50	3	2	0	0.00	0.00
50	3	2	120	0.05	0.03
50	3	2	240	0.10	0.07
50	3	2	360	0.14	0.16
50	3	2	480	0.19	0.22
50	3	2	600	0.23	0.29



**Table A.2.3 (continued)** Experimental results of films water vapour permeability (WVP)

Gly (%)	Chit (%)	Sample	Experimental time (min)	Weight loss (g)	
				Experiment 1	Experiment 2
10	1	1	0	0.00	0.00
10	1	1	120	0.06	0.07
10	1	1	240	0.12	0.14
10	1	1	360	0.18	0.24
10	1	1	480	0.22	0.30
10	1	1	600	0.26	0.35
10	1	2	0	0.00	0.00
10	1	2	120	0.14	0.08
10	1	2	240	0.14	0.15
10	1	2	360	0.18	0.23
10	1	2	480	0.23	0.30
10	1	2	600	0.27	0.64
10	2	1	0	0.00	0.00
10	2	1	120	0.04	0.07
10	2	1	240	0.08	0.13
10	2	1	360	0.14	0.21
10	2	1	480	0.17	0.28
10	2	1	600	0.22	0.40
10	2	2	0	0.00	0.00
10	2	2	120	0.06	0.05
10	2	2	240	0.12	0.11
10	2	2	360	0.16	0.18
10	2	2	480	0.21	0.25
10	2	2	600	0.25	0.39
10	3	1	0	0.00	0.00
10	3	1	120	0.03	0.00
10	3	1	240	0.07	0.05
10	3	1	360	0.11	0.11
10	3	1	480	0.16	0.16
10	3	1	600	0.19	0.19
10	3	2	0	0.00	0.00
10	3	2	120	0.04	0.00
10	3	2	240	0.08	0.06
10	3	2	360	0.12	0.12
10	3	2	480	0.17	0.19
10	3	2	600	0.21	0.25

**Table A.2.4** Experimental results of films thickness

Gly (%)	Sample	Measure	Thickness (mm)					
			Experiment 1			Experiment 2		
			<i>Chit 1</i>	<i>Chit 2</i>	<i>Chit 3</i>	<i>Chit 1</i>	<i>Chit 2</i>	<i>Chit 3</i>
90	1	1	0.061	0.143	0.203	0.051	0.154	0.278
90	1	2	0.067	0.145	0.204	0.037	0.147	0.280
90	1	3	0.075	0.129	0.203	0.034	0.145	0.274
90	2	1	0.071	0.148	0.205	0.050	0.161	0.276
90	2	2	0.066	0.138	0.211	0.041	0.145	0.269
90	2	3	0.059	0.138	0.216	0.058	0.140	0.263
90	3	1	0.075	0.152	0.196	0.066	0.123	0.266
90	3	2	0.066	0.138	0.215	0.052	0.147	0.276
90	3	3	0.067	0.139	0.212	0.062	0.156	0.264
90	4	1	0.059	0.152	0.220	0.046	0.154	0.266
90	4	2	0.076	0.163	0.222	0.041	0.155	0.266
90	4	3	0.090	0.166	0.231	0.080	0.144	0.255
90	5	1	0.072	0.166	0.242		0.159	0.255
90	5	2	0.065	0.163	0.241		0.143	0.258
90	5	3	0.062	0.173	0.249		0.137	0.248
90	6	1	0.067	0.165	0.254		0.138	0.254
90	6	2	0.050	0.168	0.246		0.136	0.258
90	6	3	0.047	0.184	0.238		0.161	0.248
90	7	1	0.050	0.182	0.253		0.130	0.252
90	7	2	0.059	0.171	0.253		0.154	0.247
90	7	3	0.076	0.173	0.244		0.169	0.250
90	8	1		0.171	0.240		0.122	0.245
90	8	2		0.163	0.235		0.131	0.240
90	8	3		0.151	0.228		0.140	0.252
90	9	1		0.163	0.246		0.115	0.265
90	9	2		0.161	0.257		0.115	0.256
90	9	3		0.193	0.264		0.118	0.254
50	1	2	0.051	0.161	0.240	0.037	0.119	0.243
50	1	3	0.055	0.154	0.248	0.034	0.127	0.233
50	2	1	0.055	0.161	0.216	0.050	0.133	0.254

**Table A.2.4 (continued)** Experimental results of films thickness

Gly (%)	Sample	Measure	Thickness (mm)					
			Experiment 1			Experiment 2		
			<i>Chit 1</i>	<i>Chit 2</i>	<i>Chit 3</i>	<i>Chit 1</i>	<i>Chit 2</i>	<i>Chit 3</i>
50	2	2	0.056	0.161	0.231	0.041	0.121	0.241
50	2	3	0.048	0.158	0.253	0.058	0.114	0.243
50	3	1	0.042	0.163	0.234	0.066	0.187	0.239
50	3	2	0.046	0.160	0.249	0.052	0.119	0.234
50	3	3	0.069	0.149	0.232	0.062	0.116	0.221
50	4	1	0.056	0.145	0.231	0.046	0.120	0.237
50	4	2	0.055	0.154	0.228	0.041	0.105	0.236
50	4	3	0.061	0.165	0.244	0.080	0.113	0.225
50	5	1	0.086	0.151	0.242	0.051	0.115	0.225
50	5	2	0.072	0.155	0.223	0.037	0.102	0.235
50	5	3	0.072	0.130	0.219	0.034	0.101	0.227
50	6	1	0.061	0.145	0.224	0.050	0.106	0.229
50	6	2	0.058	0.186	0.230	0.041	0.099	0.229
50	6	3	0.059	0.128	0.239	0.058	0.103	0.227
50	7	1	0.056	0.146	0.248	0.066	0.115	0.224
50	7	2	0.059	0.153	0.227	0.052	0.133	0.226
50	7	3	0.059	0.147	0.250	0.062	0.114	0.230
50	8	1	0.059	0.162	0.244	0.046	0.120	0.221
50	8	2	0.060	0.131	0.241	0.041	0.118	0.252
50	8	3	0.059	0.173	0.238	0.080	0.126	0.224
50	9	1	0.065	0.148	0.235		0.140	0.223
50	9	2	0.058	0.154	0.245		0.136	0.225
50	9	3	0.073	0.148	0.236		0.157	0.229
10	1	1	0.069	0.114	0.343	0.059	0.123	0.243
10	1	2	0.053	0.137	0.504	0.048	0.135	0.197
10	1	3	0.054	0.151	0.454	0.040	0.125	0.235
10	2	1	0.081	0.120	0.437	0.053	0.122	0.240
10	2	2	0.078	0.125	0.383	0.054	0.107	0.268
10	2	3	0.081	0.127	0.446	0.053	0.137	0.261
10	3	1	0.095	0.128	0.371	0.046	0.125	0.243
10	3	2	0.085	0.131	0.363	0.046	0.134	0.213
10	3	3	0.077	0.109	0.499	0.045	0.127	0.240

**Table A.2.4 (continued)** Experimental results of films thickness

Gly (%)	Sample	Measure	Thickness (mm)					
			Experiment 1			Experiment 2		
			<i>Chit 1</i>	<i>Chit 2</i>	<i>Chit 3</i>	<i>Chit 1</i>	<i>Chit 2</i>	<i>Chit 3</i>
10	4	1	0.094	0.130		0.052	0.126	0.212
10	4	2	0.087	0.139		0.045	0.135	0.245
10	4	3	0.096	0.158		0.040	0.140	0.254
10	5	1	0.069	0.138		0.044	0.134	0.231
10	5	2	0.058	0.142		0.048	0.138	0.362
10	5	3	0.071	0.146		0.036	0.153	0.207
10	6	1	0.070	0.155		0.033	0.133	0.232
10	6	2	0.084	0.138		0.036	0.166	0.212
10	6	3	0.062	0.126		0.043	0.125	0.222
10	7	1	0.077	0.135		0.040	0.134	0.222
10	7	2	0.061	0.178		0.038	0.137	0.242
10	7	3	0.067	0.137		0.032	0.132	0.251
10	8	1	0.132	0.145		0.045	0.105	0.270
10	8	2	0.179	0.144		0.040	0.107	0.243
10	8	3	0.072	0.125		0.034	0.141	0.210
10	9	1	0.127			0.040		0.238
10	9	2	0.132			0.044		0.223
10	9	3	0.084			0.040		0.222

**Table A.2.5** Experimental results of films mechanical properties. EB (elongation at break) and TS (tensile strength)

Chit (%)	Gly (%)	Sample	Experiment 1		Experiment 2	
			EB (%)	TS (MPa)	EB (%)	TS (MPa)
1	90	1	31.79		74.20	
1	90	2	76.56	1.12	92.33	1.86
1	90	3	52.30		124.42	2.39
1	90	4	85.85	1.52	75.52	3.49
1	90	5	41.85	0.81		
1	90	6	44.91	1.57		
1	90	7	31.86			
1	50	1	68.43	2.82	53.93	7.65
1	50	2	89.97	3.00	57.70	
1	50	3	18.29		48.85	7.12
1	50	4	83.62	3.21	50.08	
1	50	6	86.15	3.13	60.93	7.02
1	50	7	72.18		74.02	
1	50	8	76.97	2.86	34.27	2.82
1	50	9	89.50	3.20	63.91	6.66
1	10	1	48.41	10.82	49.98	6.91
1	10	2	48.73	12.13	47.41	3.97
1	10	3	48.19	8.40	57.27	10.48
1	10	4	19.31	3.34	44.83	7.15
1	10	5	57.32	14.46	49.36	8.67
1	10	6	46.29	6.63	33.22	7.19
1	10	7	50.26	7.05	48.86	9.63
1	10	8	32.45	4.50	49.96	10.46
1	10	9	44.25	5.76	53.64	10.88
2	90	1	39.08	0.28	27.01	0.27
2	90	2	36.67	0.21	23.62	0.28
2	90	3	39.70	0.28	17.37	0.15
2	90	4	43.19	0.27	20.65	0.30
2	90	5	35.81	0.23	27.48	0.38
2	90	6	36.42	0.29	28.10	0.47
2	90	7	35.68	0.26		
2	90	8	33.08	0.23		
2	90	9	36.43	0.33		
2	50	1	43.02	0.84	26.93	0.85
2	50	2	36.69	0.84	28.18	0.59
2	50	3	40.75	0.81	31.92	1.01

**Table A.2.5 (continued)** Experimental results of films mechanical properties. EB (elongation at break) and TS (tensile strength)

Chit (%)	Gly (%)	Sample	Experiment 1		Experiment 2	
			EB (%)	TS (MPa)	EB (%)	TS (MPa)
2	50	4	37.70	0.66	30.66	1.17
2	50	5	39.00	0.83	34.54	1.51
2	50	6	36.52	0.75	35.75	1.65
2	50	7	37.31	0.76	35.99	1.99
2	50	8	30.86	0.73	28.44	0.70
2	50	9	40.19	0.73	26.14	0.71
2	10	1	19.28	14.12	9.60	5.76
2	10	2	24.39	9.01	27.82	13.53
2	10	3	10.95	7.51	35.21	13.30
2	10	4	15.88	4.60	9.75	9.64
2	10	5	22.83	11.89	36.63	20.39
2	10	6	8.44	9.59	37.38	22.67
2	10	7	7.74	9.31	20.30	13.78
2	10	8	16.83	15.05	30.72	16.19
2	10	9			6.18	10.15
3	90	1	22.23	0.38	15.61	0.65
3	90	2	26.66	0.39	14.95	0.60
3	90	3	27.54	0.51	17.28	0.61
3	90	4	18.82	0.40	12.05	0.44
3	90	5	34.03	0.50	13.86	0.53
3	90	6	28.72	0.54	16.45	0.60
3	90	7	29.03	0.51	15.28	0.51
3	90	8	24.48	0.45	11.80	0.31
3	90	9	21.30	0.43	9.18	0.22
3	50	1	29.61	1.87	26.00	1.15
3	50	2	22.78	1.62	21.24	0.99
3	50	3	31.49	1.94	22.69	1.09
3	50	4	30.55	1.97	26.54	1.29
3	50	5	24.94	1.62	24.63	1.19
3	50	6	26.84	1.70	24.17	1.28
3	50	7	28.19	1.77	24.91	1.30
3	50	8	22.45	1.52	26.66	1.30
3	50	9	21.15	1.41		
3	10	1	24.83	10.04	7.78	3.85
3	10	2	21.70	8.15	6.34	5.80
3	10	3	19.35	8.58	4.62	4.29

**Table A.2.5** Experimental results of films mechanical properties. EB (elongation at break) and TS (tensile strength)

			Experiment 1		Experiment 2	
Chit (%)	Gly (%)	Sample	EB (%)	TS (MPa)	EB (%)	TS (MPa)
3	10	4	10.31	2.51	4.98	5.98
3	10	5			3.21	5.41
3	10	6			2.35	4.96
3	10	7			3.64	5.81
3	10	8			5.83	7.01
3	10	9			4.59	6.02

**Table A.2.6** Experimental results of films thermal properties.  $T_g$  (glass transition temperature).  $\Delta h$  (melting enthalpy) and  $T_m$  (melting temperature)

Chit (%)	Gly (%)	Sample	Experiment 1			Experiment 2		
			$T_g$ ( $^{\circ}\text{C}$ )	$\Delta h$ ( $\text{J g}^{-1}$ )	$T_m$ ( $^{\circ}\text{C}$ )	$T_g$ ( $^{\circ}\text{C}$ )	$\Delta h$ ( $\text{J g}^{-1}$ )	$T_m$ ( $^{\circ}\text{C}$ )
1	90	1	-70.57	-221.41	135.85	-73.75	-133.31	144.99
1	90	2	-73.22	-273.78	137.19	-71.81	-108.51	152.79
1	50	1	-56.32	-132.78	127.20	-69.70	-168.30	138.25
1	50	2	-42.86	-155.11	126.74	-74.37	-150.33	141.95
1	10	1	-26.60	-98.18	131.32	-33.52	-82.46	126.60
1	10	2	-15.43	-36.89	137.34	-4.53	-62.48	94.04
2	90	1	-65.20	-265.43	126.28	-66.40	-197.65	134.32
2	90	2	-60.48	-137.90	132.50	-68.25	-214.02	132.81
2	50	1	-54.28	-236.59	129.58	-39.38	-198.73	129.77
2	50	2	-67.60	-198.16	124.70	-44.88	-181.97	129.97
2	10	1	-5.20	-186.13	127.28	1.57	-203.23	109.19
2	10	2	-17.65	-177.96	126.88	0.80	-93.55	119.23
3	90	1	-78.32	-237.54	122.99	-86.10	-299.68	125.54
3	90	2	-83.91	-390.58	124.96	-83.35	-324.69	124.99
3	50	1	-62.25	-248.30	120.61	-63.58	-222.27	117.61
3	50	2	-65.77	-260.68	115.78	-66.88	-265.54	122.15
3	10	1	18.19	-132.38	89.97	36.11	-214.11	120.87
3	10	2	17.70	-156.64	106.26	33.56	-200.33	121.59



**A.3** Post hoc multi comparison tests (Tukey's test). to conclude on the isolated effect of chitosan and glycerol addition.

**Table A.3.1** Tukey's test to conclude on the effect of glycerol

<b>Post Hoc Tukey HSD test</b>									
<b>Include condition: Chit=1 %</b>									
Variable: $a_w$ solution			Variable: Thickness (mm)			Variable: $a_w$ film			
Gly	(1)	(2)	(3)	(1)	(2)	(3)	(1)	(2)	(3)
(%)	<b>1.0020</b>	<b>1.0013</b>	<b>0.99900</b>	<b>0.06550</b>	<b>0.05233</b>	<b>0.06050</b>	<b>0.54525</b>	<b>0.56600</b>	<b>0.5570</b>
<b>10</b>		0.897	0.253406		0.309805	0.854521		0.284275	0.088586
<b>90</b>	0.896705		0.438257	0.309805		0.694734	0.284275		0.566966
<b>50</b>	0.253406	0.438257		0.854521	0.694734		0.088586	0.566966	

<b>Post Hoc Tukey HSD test</b>									
<b>Include condition: Chit=1 %</b>									
Variable: Elongation at break (%)			Variable: Tensile strength (MPa)			Variable: Moisture content (%)			
Gly	(1)	(2)	(3)	(1)	(2)	(3)	(1)	(2)	(3)
(%)	<b>48.633</b>	<b>70.773</b>	<b>84.448</b>	<b>8.4588</b>	<b>4.4873</b>	<b>1.4900</b>	<b>26.187</b>	<b>38.536</b>	<b>52.657</b>
<b>10</b>		0.097969	0.026095		0.284275	0.088586		0.056291	0.003421
<b>90</b>	0.097969		0.441057	0.284275		0.566966	0.056291		0.066061
<b>50</b>	0.026095	0.441057		0.088586	0.566966		0.003421	0.066061	

<b>Post Hoc Tukey HSD test</b>									
<b>Include condition: Chit=1 %</b>									
Variable: Solubility (%)			Variable: Oxygen permeability ( $\text{g Pa}^{-1} \text{m}^{-1} \text{s}^{-1}$ )			Variable: Glass transition temperature ( $^{\circ}\text{C}$ )			
Gly	(1)	(2)	(3)	(1)	(2)	(3)	(1)	(2)	(3)
(%)	<b>48.556</b>	<b>54.110</b>	<b>71.121</b>	<b>0.000</b>	<b>0.000</b>	<b>0.000</b>	<b>-20.02</b>	<b>-56.29</b>	<b>-72.52</b>
<b>10</b>		0.459923	0.009393		0.834916	0.934683		0.016945	0.005476
<b>90</b>	0.459923		0.039929	0.834916		0.987449	0.016945		0.357640
<b>50</b>	0.009393	0.039929		0.934683	0.987448		0.005476	0.357640	

<b>Post Hoc Tukey HSD test</b>						
<b>Include condition: Chit=1 %</b>						
Variable: Melting enthalpy ( $\text{Jg}^{-1}$ )			Variable: Melting temperature ( $^{\circ}\text{C}$ )			
Gly	(1)	(2)	(3)	(1)	(2)	(3)
(%)	<b>-70.00</b>	<b>-152.1</b>	<b>-191.1</b>	<b>122.33</b>	<b>130.73</b>	<b>144.99</b>
<b>10</b>		0.180148	0.081831		0.751085	0.261404
<b>90</b>	0.180148		0.706202	0.751085		0.576495
<b>50</b>	0.081831	0.706202		0.261404	0.576495	

<b>Post Hoc Tukey HSD test</b>									
<b>Include condition: Chit=2 %</b>									
Variable: $a_w$ solution			Variable: Thickness (mm)			Variable: $a_w$ film			
Gly	(1)	(2)	(3)	(1)	(2)	(3)	(1)	(2)	(3)
(%)	<b>1.0010</b>	<b>1.0008</b>	<b>0.99750</b>	<b>0.12425</b>	<b>0.13550</b>	<b>0.15150</b>	<b>0.52125</b>	<b>0.50900</b>	<b>0.550375</b>
10		0.980783	0.063946		0.560718	0.071131		0.336148	0.136054
90	0.980783		0.085570	0.560718		0.332819	0.336148		0.801124
50	0.063946	0.085570		0.071131	0.332819		0.136054	0.801124	

<b>Post Hoc Tukey HSD test</b>									
<b>Include condition: Chit=2 %</b>									
Variable: Elongation at break (%)			Variable: Tensile strength (MPa)			Variable: Moisture content (%)			
Gly	(1)	(2)	(3)	(1)	(2)	(3)	(1)	(2)	(3)
(%)	<b>20.273</b>	<b>33.703</b>	<b>31.593</b>	<b>10.606</b>	<b>0.77850</b>	<b>0.25850</b>	<b>17.842</b>	<b>37.173</b>	<b>51.659</b>
10		0.081157	0.146693		0.000635	0.000492		0.000572	0.000184
90	0.081157		0.920416	0.000635		0.944888	0.000572		0.003200
50	0.146693	0.920416		0.000492	0.944888		0.000184	0.003200	

<b>Post Hoc Tukey HSD test</b>									
<b>Include condition: Chit=2 %</b>									
Variable: Solubility (%)			Variable: Oxygen permeability ( $\text{g Pa}^{-1} \text{m}^{-1} \text{s}^{-1}$ )			Variable: Glass transition temperature ( $^{\circ}\text{C}$ )			
Gly	(1)	(2)	(3)	(1)	(2)	(3)	(1)	(2)	(3)
(%)	<b>36.229</b>	<b>50.000</b>	<b>61.030</b>	<b>0.000</b>	<b>0.000</b>	<b>0.000</b>	<b>-5.120</b>	<b>-51.53</b>	<b>-65.08</b>
10		0.001813	0.000192		0.455588	0.247950		0.000292	0.000189
90	0.001813		0.007069	0.455588		0.884011	0.000292		0.138291
50	0.000192	0.007069		0.247950	0.884011		0.000189	0.138291	

<b>Post Hoc Tukey HSD test</b>						
<b>Include condition: Chit=2 %</b>						
Variable: Melting enthalpy ( $\text{Jg}^{-1}$ )			Variable: Melting temperature ( $^{\circ}\text{C}$ )			
Gly (%)	(1)	(2)	(3)	(1)	(2)	(3)
	<b>-165.2</b>	<b>-203.9</b>	<b>-203.8</b>	<b>120.65</b>	<b>128.51</b>	<b>131.48</b>
10		0.453386	0.455296		0.163846	0.051127
90	0.453386		0.999993	0.163846		0.733996
50	0.455296	0.999993		0.051127	0.733996	

<b>Post Hoc Tukey HSD test</b>									
<b>Include condition: Chit=3 %</b>									
Variable: $a_w$ solution				Variable: Thickness (mm)			Variable: $a_w$ film		
Gly	(1)	(2)	(3)	(1)	(2)	(3)	(1)	(2)	(3)
(%)	<b>1.0020</b>	<b>0.99975</b>	<b>0.99600</b>	<b>0.31575</b>	<b>0.24250</b>	<b>0.22800</b>	<b>0.50725</b>	<b>0.51450</b>	<b>0.52700</b>
<b>10</b>		0.227304	0.005388		0.274949	0.215208		0.261966	0.006704
<b>90</b>	0.227304		0.055220	0.274949		0.950255	0.261966		0.061370
<b>50</b>	0.005388	0.055220		0.215208	0.950255		0.006704	0.061370	

<b>Post Hoc Tukey HSD test</b>									
<b>Include condition: Chit=3 %</b>									
Variable: Elongation at break (%)				Variable: Tensile strength (MPa)			Variable: Moisture content (%)		
Gly	(1)	(2)	(3)	(1)	(2)	(3)	(1)	(2)	(3)
(%)	<b>15.162</b>	<b>24.905</b>	<b>21.279</b>	<b>6.9595</b>	<b>1.14035</b>	<b>0.45433</b>	<b>16.530</b>	<b>38.668</b>	<b>54.516</b>
<b>10</b>		0.174551	0.506194		0.004061	0.002537		0.000201	0.000201
<b>90</b>	0.174551		0.776505	0.004061		0.746592	0.000201		0.000201
<b>50</b>	0.506194	0.776505		0.002537	0.746592		0.000201	0.000201	

<b>Post Hoc Tukey HSD test</b>									
<b>Include condition: Chit=3 %</b>									
Variable: Solubility (%)				Variable: Oxygen permeability (g Pa <sup>-1</sup> m <sup>-1</sup> s <sup>-1</sup> )			Variable: Glass transition temperature (°C)		
Gly	(1)	(2)	(3)	(1)	(2)	(3)	(1)	(2)	(3)
(%)	<b>29.891</b>	<b>49.543</b>	<b>63.233</b>	<b>0.000</b>	<b>0.000</b>	<b>0.000</b>	<b>26.390</b>	<b>-64.62</b>	<b>-81.86</b>
<b>10</b>		0.000201	0.000201		0.209689	0.141834		0.000201	0.000201
<b>90</b>	0.000201		0.000201	0.209689		0.910109	0.000201		0.018066
<b>50</b>	0.000201	0.000201		0.141834	0.910109		0.000201	0.018066	

<b>Post Hoc Tukey HSD test</b>						
<b>Include condition: Chit=3 %</b>						
Variable: Melting enthalpy (Jg <sup>-1</sup> )				Variable: Melting temperature (°C)		
Gly	(1)	(2)	(3)	(1)	(2)	(3)
(%)	<b>-175.9</b>	<b>-249.2</b>	<b>-317.6</b>	<b>109.67</b>	<b>117.04</b>	<b>124.31</b>
<b>10</b>		0.124734	0.009939		0.375803	0.160845
<b>90</b>	0.124734		0.192408	0.375803		0.747134
<b>50</b>	0.009939	0.192408		0.160845	0.747134	

**Table A.3.12** Tukey's test to conclude on the effect of chitosan

<b>Post Hoc Tukey HSD test</b>										
<b>Include condition: Gly=90 %</b>										
Variable: $a_w$ solution			Variable: Thickness (mm)			Variable: $a_w$ film				
<b>Chit</b>	<b>(1)</b>	<b>(2)</b>	<b>(3)</b>	<b>(1)</b>	<b>(2)</b>	<b>(3)</b>	<b>(1)</b>	<b>(2)</b>	<b>(3)</b>	
<b>(%)</b>	<b>0.99900</b>	<b>0.99750</b>	<b>0.99600</b>	<b>0.6050</b>	<b>0.15150</b>	<b>0.22800</b>	<b>0.5570</b>	<b>0.50375</b>	<b>0.52700</b>	
<b>1</b>		0.800930	0.481430		0.014423	0.001044		0.000443	0.007040	
<b>2</b>	0.800930		0.753943	0.014423		0.017836	0.000443		0.010086	
<b>3</b>	0.481430	0.753943		0.001044	0.017836		0.007040	0.010086		

<b>Post Hoc Tukey HSD test</b>										
<b>Include condition: Gly=90 %</b>										
Variable: Elongation at break (%)			Variable: Tensile strength (MPa)			Variable: Moisture content (%)				
<b>Chit</b>	<b>(1)</b>	<b>(2)</b>	<b>(3)</b>	<b>(1)</b>	<b>(2)</b>	<b>(3)</b>	<b>(1)</b>	<b>(2)</b>	<b>(3)</b>	
<b>(%)</b>	<b>84.448</b>	<b>31.593</b>	<b>21.279</b>	<b>1.490</b>	<b>0.25850</b>	<b>0.45433</b>	<b>52.657</b>	<b>51.569</b>	<b>54.516</b>	
<b>1</b>		0.000725	0.000462		0.002083	0.006150		0.951047	0.856938	
<b>2</b>	0.000725		0.266436	0.002083		0.535074	0.951047		0.611927	
<b>3</b>	0.000462	0.266436		0.006150	0.535074		0.856938	0.611927		

<b>Post Hoc Tukey HSD test</b>										
<b>Include condition: Gly=90 %</b>										
Variable: Solubility (%)			Variable: Oxygen permeability ( $\text{g Pa}^{-1} \text{m}^{-1} \text{s}^{-1}$ )			Variable: Glass transition temperature ( $^{\circ}\text{C}$ )				
<b>Chit</b>	<b>(1)</b>	<b>(2)</b>	<b>(3)</b>	<b>(1)</b>	<b>(2)</b>	<b>(3)</b>	<b>(1)</b>	<b>(2)</b>	<b>(3)</b>	
<b>(%)</b>	<b>71.121</b>	<b>61.030</b>	<b>63.233</b>	<b>0.000</b>	<b>0.000</b>	<b>0.000</b>	<b>-72.52</b>	<b>-65.08</b>	<b>-81.86</b>	
<b>1</b>		0.201606	0.373363		0.986175	0.702910		0.062487	0.031745	
<b>2</b>	0.201606		0.880241	0.986175		0.714235	0.062487		0.000944	
<b>3</b>	0.373363	0.880241		0.702910	0.714235		0.031745	0.000944		

<b>Post Hoc Tukey HSD test</b>						
<b>Include condition: Gly=90 %</b>						
Variable: Melting enthalpy ( $\text{Jg}^{-1}$ )			Variable: Melting temperature ( $^{\circ}\text{C}$ )			
<b>Chit</b>	<b>(1)</b>	<b>(2)</b>	<b>(3)</b>	<b>(1)</b>	<b>(2)</b>	<b>(3)</b>
<b>(%)</b>	<b>-191.1</b>	<b>-203.8</b>	<b>-317.6</b>	<b>144.99</b>	<b>131.48</b>	<b>1124.31</b>
<b>1</b>		0.979600	0.233660		0.054470	0.011498
<b>2</b>	0.979600		0.195940	0.054470		0.246719
<b>3</b>	0.233660	0.195940		0.011498	0.246719	

<b>Post Hoc Tukey HSD test</b>									
<b>Include condition: Gly=50 %</b>									
Variable: $a_w$ solution			Variable: Thickness (mm)			Variable: $a_w$ film			
<b>Chit</b>	<b>(1)</b>	<b>(2)</b>	<b>(3)</b>	<b>(1)</b>	<b>(2)</b>	<b>(3)</b>	<b>(1)</b>	<b>(2)</b>	<b>(3)</b>
<b>(%)</b>	<b>1.003</b>	<b>1.008</b>	<b>0.9975</b>	<b>0.05233</b>	<b>0.13550</b>	<b>0.24250</b>	<b>0.56600</b>	<b>0.50900</b>	<b>0.51450</b>
<b>1</b>		0.782717	0.218213		0.000811	0.000201		0.020698	0.033469
<b>2</b>	0.782717		0.457225	0.000811		0.000249	0.020698		0.931186
<b>3</b>	0.218213	0.457225		0.000201	0.000249		0.033469	0.931186	

<b>Post Hoc Tukey HSD test</b>									
<b>Include condition: Gly=50 %</b>									
Variable: Elongation at break (%)			Variable: Tensile strength (MPa)			Variable: Moisture content (%)			
<b>Chit</b>	<b>(1)</b>	<b>(2)</b>	<b>(3)</b>	<b>(1)</b>	<b>(2)</b>	<b>(3)</b>	<b>(1)</b>	<b>(2)</b>	<b>(3)</b>
<b>(%)</b>	<b>70.773</b>	<b>33.703</b>	<b>24.903</b>	<b>4.4873</b>	<b>0.77850</b>	<b>1.4035</b>	<b>38.536</b>	<b>37.173</b>	<b>38.668</b>
<b>1</b>		0.004274	0.001245		0.020200	0.047188		0.943738	0.999507
<b>2</b>	0.004274		0.489878	0.020200		0.805971	0.943738		0.922093
<b>3</b>	0.001245	0.489878		0.047188	0.805971		0.999507	0.922093	

<b>Post Hoc Tukey HSD test</b>									
<b>Include condition: Gly=50 %</b>									
Variable: Solubility (%)			Variable: Oxygen permeability ( $\text{g Pa}^{-1} \text{m}^{-1} \text{s}^{-1}$ )			Variable: Glass transition temperature ( $^{\circ}\text{C}$ )			
<b>Chit</b>	<b>(1)</b>	<b>(2)</b>	<b>(3)</b>	<b>(1)</b>	<b>(2)</b>	<b>(3)</b>	<b>(1)</b>	<b>(2)</b>	<b>(3)</b>
<b>(%)</b>	<b>54.110</b>	<b>50.000</b>	<b>49.543</b>	<b>0.000</b>	<b>0.000</b>	<b>0.000</b>	<b>-56.29</b>	<b>-51.53</b>	<b>-64.62</b>
<b>1</b>		0.353369	0.286873		0.613565	0.170282		0.818246	0.557530
<b>2</b>	0.353369		0.983071	0.613565		0.524589	0.818246		0.225265
<b>3</b>	0.286873	0.983071		0.170282	0.524589		0.557530	0.225265	

<b>Post Hoc Tukey HSD test</b>						
<b>Include condition: Gly=50 %</b>						
Variable: Melting enthalpy ( $\text{Jg}^{-1}$ )			Variable: Melting temperature ( $^{\circ}\text{C}$ )			
<b>Chit</b>	<b>(1)</b>	<b>(2)</b>	<b>(3)</b>	<b>(1)</b>	<b>(2)</b>	<b>(3)</b>
<b>(%)</b>	<b>-152.1</b>	<b>-203.9</b>	<b>-249.2</b>	<b>130.73</b>	<b>128.51</b>	<b>119.04</b>
<b>1</b>		0.026328	0.000843		0.756250	0.012830
<b>2</b>	0.026328		0.034183	0.756250		0.025126
<b>3</b>	0.000843	0.034183		0.012830	0.025126	



## **Appendix B**

---

*Appendix to Chapter 3*





## B.1 Experimental results of films chemical composition

**Table B.1.1** Experiment results of films chemical composition, produced with different film forming solutions (FFS)

FFS composition				Experiment 1		Experiment 2	
Chit (%)	Gly (%)	Sample	Measure	Chit (mg g <sup>-1</sup> film)	Gly (mg g <sup>-1</sup> film)	Chit (mg g <sup>-1</sup> film)	Gly (mg g <sup>-1</sup> film)
1	90	1	1	121.0	33.2	150.9	50.5
1	90	1	2	130.1	33.3	179.8	55.4
1	90	2	1	138.2	33.0	164.6	
1	90	2	2			179.5	46.2
1	90	3	1	128.1		205.4	47.0
1	90	3	2	130.9		211.2	
1	50	1	1	134.9	25.8	261.3	37.3
1	50	1	2	139.1	25.4	264.7	25.9
1	50	2	1	141.2	26.1	237.4	
1	50	2	2	176.1		224.7	31.8
1	50	3	1	146.8		244.4	57.2
1	50	3	2	140.1		243.0	
1	10	1	1	408.0	10.9	372.3	9.8
1	10	1	2	401.3	12.8	367.2	11.4
1	10	2	1	403.9	8.2	340.0	
1	10	2	2	403.1		338.8	14.3
1	10	3	1	408.0		403.4	12.8
1	10	3	2	410.0		401.6	
2	90	1	1	41.8	36.2	150.5	36.1
2	90	1	2	47.5	38.6	174.7	37.6
2	90	2	1	45.1	40.7	160.5	
2	90	2	2	45.6		172.0	31.4
2	90	3	1	49.3		167.1	41.8
2	90	3	2	38.8		161.7	
2	50	1	1	221.2	16.1	119.2	35.0
2	50	1	2	187.6	18.5	119.6	29.7
2	50	2	1	188.8	19.1	115.0	
2	50	2	2	271.0		100.5	25.4
2	50	3	1	252.5		120.0	88.1
2	50	3	2	244.5		122.4	
2	10	1	1	359.0	11.5	382.2	10.9
2	10	1	2	367.7	12.0	380.9	12.9

**Table B.1.1 (continued)** Experiment results of films chemical composition, produced with different film forming solutions (FFS)

FFS composition				Experiment 1		Experiment 2	
Chit (%)	Gly (%)	Sample	Measure	Chit (mg g <sup>-1</sup> film)	Gly (mg g <sup>-1</sup> film)	Chit (mg g <sup>-1</sup> film)	Gly (mg g <sup>-1</sup> film)
2	10	2	2	385.2		360.4	16.9
2	10	3	1	388.0		335.6	18.3
2	10	3	2	386.5		342.5	
3	90	1	1	168.9	31.5	189.5	58.0
3	90	1	2	144.9	28.5	210.6	46.1
3	90	2	1			336.0	
3	90	2	2	152.3		336.3	53.3
3	90	3	1	184.1		270.8	56.0
3	90	3	2	162.5		277.9	
3	50	1	1	140.8	29.7	167.5	43.2
3	50	1	2	145.9	30.3	166.4	48.5
3	50	2	1		25.3	214.8	
3	50	2	2	162.8		303.3	47.9
3	50	3	1	167.8		171.1	45.2
3	50	3	2	171.7		185.7	
3	10	1	1	416.5	11.8	364.7	10.5
3	10	1	2	416.2	9.9	355.4	23.1
3	10	2	1	413.6	10.3	345.2	
3	10	2	2	416.2		344.4	17.9
3	10	3	1	426.1		369.3	19.6
3	10	3	2	417.9		372.2	
2	10	2	2	385.2		360.4	16.9
2	10	3	1	388.0		335.6	18.3
2	10	3	2	386.5		342.5	
3	90	1	1	168.9	31.5	189.5	58.0
3	90	1	2	144.9	28.5	210.6	46.1
3	90	2	1			336.0	
3	90	2	2	152.3		336.3	53.3
3	90	3	1	184.1		270.8	56.0
3	90	3	2	162.5		277.9	

**B.2 Experimental results of films relaxation time****Table B.2.1** Experiment results of films water and glycerol relaxation time

Chit (%)	Gly (%)	$T_2$ (ms)	
		Glycerol	Water
1	90	264.3	2545.2
1	50	107.0	367.0
1	10	7.7	59.7
2	90	83.5	1402.0
2	50	5.1	51.3
2	10	6.8	76.2
3	90	69.3	1197.5
3	50	40.3	688.1
3	10	5.4	41.7



## Appendix C



*Appendix to Chapter 5*



### C.1 NMR experimental results of fresh-cut fruit relaxation times ( $T_2$ ) distribution as function of water population (A)

**Table C.1.1** Results of fresh-cut fruit relaxation time during storage period

Experiment 1					Experiment 2				
Day	Melon		Pear		Day	Melon		Pear	
	$T_2$ (ms)	A	$T_2$ (ms)	A		$T_2$ (ms)	A	$T_2$ (ms)	A
0	100000	0.0000	100000	0.0002	0	10000	0.0001	100000	0.0001
0	86207	0.0000	86207	0.0007	0	86207	0.0002	86207	0.0002
0	74627	0.0000	74627	0.0014	0	74627	0.0005	74627	0.0005
0	64516	0.0000	64516	0.0023	0	64516	0.0009	64516	0.0009
0	55556	0.0000	55556	0.0035	0	55556	0.0014	55556	0.0014
0	48077	0.0000	48077	0.0049	0	48077	0.0020	48077	0.0020
0	41494	0.0000	41494	0.0064	0	41494	0.0027	41494	0.0027
0	35842	0.0000	35842	0.0083	0	35842	0.0036	35842	0.0036
0	30960	0.0000	30960	0.0103	0	30960	0.0046	30960	0.0046
0	26738	0.0000	26738	0.0125	0	26738	0.0057	26738	0.0057
0	23095	0.0000	23095	0.0149	0	23095	0.0070	23095	0.0070
0	19960	0.0000	19960	0.0176	0	19960	0.0084	19960	0.0084
0	17241	0.0001	17241	0.0204	0	17241	0.0100	17241	0.0100
0	14881	0.0003	14881	0.0233	0	14881	0.0118	14881	0.0118
0	12854	0.0006	12854	0.0265	0	12854	0.0137	12854	0.0137
0	11099	0.0011	11099	0.0298	0	11099	0.0158	11099	0.0158
0	9615	0.0017	9615	0.0332	0	9615	0.0180	9615	0.0180
0	8264	0.0024	8264	0.0368	0	8264	0.0204	8264	0.0204
0	7143	0.0034	7143	0.0405	0	7143	0.0230	7143	0.0230
0	6173	0.0046	6173	0.0443	0	6173	0.0257	6173	0.0257
0	5348	0.0059	5348	0.0481	0	5348	0.0285	5348	0.0285
0	4608	0.0076	4608	0.0520	0	4608	0.0314	4608	0.0314
0	3984	0.0094	3984	0.0559	0	3984	0.0344	3984	0.0344
0	3436	0.0115	3436	0.0597	0	3436	0.0376	3436	0.0376
0	2967	0.0138	2967	0.0635	0	2967	0.0408	2967	0.0408

**Table C.1.1 (continued)** Results of fresh-cut fruit relaxation time ( $T_2$ ), during storage period

Experiment 1					Experiment 2				
Day	Melon		Pear		Day	Melon		Pear	
	$T_2$ (ms)	A	$T_2$ (ms)	A		$T_2$ (ms)	A	$T_2$ (ms)	A
0	2564	0.0163	2564	0.0673	0	2564	0.0440	2564	0.0440
0	2212	0.0191	2212	0.0708	0	2212	0.0472	2212	0.0472
0	1912	0.0220	1912	0.0742	0	1912	0.0504	1912	0.0504
0	1653	0.0250	1653	0.0773	0	1653	0.0535	1653	0.0535
0	1427	0.0282	1427	0.0801	0	1427	0.0565	1427	0.0565
0	1232	0.0315	1232	0.0825	0	1232	0.0593	1232	0.0593
0	1064	0.0348	1064	0.0845	0	1064	0.0619	1064	0.0619
0	917	0.0380	917	0.0860	0	917	0.0642	917	0.0642
0	794	0.0412	794	0.0868	0	794	0.0661	794	0.0661
0	685	0.0441	685	0.0870	0	685	0.0676	685	0.0676
0	592	0.0468	592	0.0865	0	592	0.0686	592	0.0686
0	510	0.0491	510	0.0851	0	510	0.0689	510	0.0689
0	442	0.0509	442	0.0829	0	442	0.0686	442	0.0686
0	382	0.0522	382	0.0798	0	382	0.0676	382	0.0676
0	329	0.0528	329	0.0758	0	329	0.0657	329	0.0657
0	285	0.0526	285	0.0709	0	285	0.0631	285	0.0631
0	246	0.0517	246	0.0652	0	246	0.0596	246	0.0596
0	212	0.0499	212	0.0587	0	212	0.0553	212	0.0553
0	183	0.0472	183	0.0516	0	183	0.0502	183	0.0502
0	158	0.0437	158	0.0440	0	158	0.0445	158	0.0445
0	137	0.0393	137	0.0362	0	137	0.0382	137	0.0382
0	118	0.0343	118	0.0284	0	118	0.0316	118	0.0316
0	102	0.0288	102	0.0211	0	102	0.0249	102	0.0249
0	88	0.0230	88	0.0145	0	88	0.0185	88	0.0185
0	76	0.0173	76	0.0088	0	76	0.0126	76	0.0126



**Table C.1.1 (continued)** Results of fresh-cut fruit relaxation time ( $T_2$ ), during storage period

Experiment 1					Experiment 2				
Day	Melon		Pear		Day	Melon		Pear	
	$T_2$ (ms)	A	$T_2$ (ms)	A		$T_2$ (ms)	A	$T_2$ (ms)	A
0	66	0.0119	66	0.0046	0	66	0.0076	66	0.0076
0	57	0.0073	57	0.0017	0	57	0.0038	57	0.0038
0	49	0.0037	49	0.0003	0	49	0.0013	49	0.0013
0	42	0.0013	42	0.0000	0	42	0.0001	42	0.0001
0	37	0.0002	37	0.0000	0	37	0.0000	37	0.0000
0	32	0.0000	32	0.0000	0	32	0.0000	32	0.0000
0	27	0.0000	27	0.0000	0	27	0.0000	27	0.0000
0	24	0.0000	24	0.0000	0	24	0.0000	24	0.0000
0	20	0.0000	20	0.0000	0	20	0.0000	20	0.0000
0	18	0.0000	18	0.0000	0	18	0.0000	18	0.0000
0	15	0.0000	15	0.0000	0	15	0.0000	15	0.0000
0	13	0.0000	13	0.0000	0	13	0.0000	13	0.0000
0	11	0.0000	11	0.0000	0	11	0.0000	11	0.0000
0	10	0.0000	10	0.0000	0	10	0.0000	10	0.0000
0	8	0.0000	8	0.0000	0	8	0.0000	8	0.0000
0	7	0.0000	7	0.0000	0	7	0.0000	7	0.0000
0	6	0.0000	6	0.0000	0	6	0.0000	6	0.0000
0	5	0.0000	5	0.0000	0	5	0.0000	5	0.0000
0	5	0.0000	5	0.0000	0	5	0.0000	5	0.0000
0	4	0.0000	4	0.0000	0	6504	0.0000	4	0.0000
0	4	0.0000	4	0.0000	0	4	0.0000	4	0.0000
0	3	0.0000	3	0.0000	0	3	0.0000	3	0.0000
0	3	0.0000	3	0.0000	0	3	0.0000	3	0.0000
0	2	0.0000	2	0.0000	0	2	0.0000	2	0.0000
0	2	0.0000	2	0.0000	0	2	0.0000	2	0.0000



**Table C.1.1 (continued)** Results of fresh-cut fruit relaxation time ( $T_2$ ), during storage period

Experiment 1					Experiment 2				
Day	Melon		Pear		Day	Melon		Pear	
	$T_2$ (ms)	A	$T_2$ (ms)	A		$T_2$ (ms)	A	$T_2$ (ms)	A
3	100000	0.0001	100000	0.0001	1	100000	0.0000	100000	0.0000
3	86207	0.0003	86207	0.0004	1	86207	0.0000	86207	0.0000
3	74627	0.0007	74627	0.0009	1	74627	0.0000	74627	0.0000
3	64516	0.0011	64516	0.0015	1	64516	0.0000	64516	0.0000
3	55556	0.0017	55556	0.0022	1	55556	0.0000	55556	0.0000
3	48077	0.0024	48077	0.0031	1	48077	0.0000	48077	0.0000
3	41494	0.0031	41494	0.0042	1	41494	0.0000	41494	0.0000
3	35842	0.0040	35842	0.0055	1	35842	0.0000	35842	0.0000
3	30960	0.0049	30960	0.0069	1	30960	0.0000	30960	0.0000
3	26738	0.0060	26738	0.0085	1	26738	0.0000	26738	0.0000
3	23095	0.0071	23095	0.0103	1	23095	0.0001	23095	0.0001
3	19960	0.0083	19960	0.0123	1	19960	0.0002	19960	0.0002
3	17241	0.0096	17241	0.0144	1	17241	0.0004	17241	0.0004
3	14881	0.0109	14881	0.0167	1	14881	0.0008	14881	0.0008
3	12854	0.0124	12854	0.0192	1	12854	0.0013	12854	0.0013
3	11099	0.0138	11099	0.0218	1	11099	0.0019	11099	0.0019
3	9615	0.0154	9615	0.0246	1	9615	0.0027	9615	0.0027
3	8264	0.0170	8264	0.0276	1	8264	0.0038	8264	0.0038
3	7143	0.0187	7143	0.0306	1	7143	0.0050	7143	0.0050
3	6173	0.0204	6173	0.0338	1	6173	0.0064	6173	0.0064
3	5348	0.0221	5348	0.0372	1	5348	0.0081	5348	0.0081
3	4608	0.0239	4608	0.0406	1	4608	0.0101	4608	0.0101
3	3984	0.0257	3984	0.0441	1	3984	0.0122	3984	0.0122
3	3436	0.0275	3436	0.0476	1	3436	0.0146	3436	0.0146
3	2967	0.0293	2967	0.0511	1	2967	0.0173	2967	0.0173

**Table C.1.1 (continued)** Results of fresh-cut fruit relaxation time ( $T_2$ ), during storage period

Experiment 1					Experiment 2				
Day	Melon		Pear		Day	Melon		Pear	
	$T_2$ (ms)	A	$T_2$ (ms)	A		$T_2$ (ms)	A	$T_2$ (ms)	A
3	2564	0.0311	2564	0.0547	1	2564	0.0201	2564	0.0201
3	2212	0.0328	2212	0.0581	1	2212	0.0232	2212	0.0232
3	1912	0.0346	1912	0.0615	1	1912	0.0264	1912	0.0264
3	1653	0.0363	1653	0.0647	1	1653	0.0298	1653	0.0298
3	1427	0.0379	1427	0.0676	1	1427	0.0333	1427	0.0333
3	1232	0.0394	1232	0.0704	1	1232	0.0369	1232	0.0369
3	1064	0.0409	1064	0.0727	1	1064	0.0405	1064	0.0405
3	917	0.0422	917	0.0747	1	917	0.0440	917	0.0440
3	794	0.0434	794	0.0762	1	794	0.0474	794	0.0474
3	685	0.0444	685	0.0771	1	685	0.0506	685	0.0506
3	592	0.0452	592	0.0774	1	592	0.0536	592	0.0536
3	510	0.0458	510	0.0769	1	510	0.0561	510	0.0561
3	442	0.0462	442	0.0757	1	442	0.0582	442	0.0582
3	382	0.0462	382	0.0737	1	382	0.0597	382	0.0597
3	329	0.0460	329	0.0708	1	329	0.0605	329	0.0605
3	285	0.0455	285	0.0670	1	285	0.0606	285	0.0606
3	246	0.0446	246	0.0624	1	246	0.0599	246	0.0599
3	212	0.0434	212	0.0570	1	212	0.0582	212	0.0582
3	183	0.0418	183	0.0508	1	183	0.0557	183	0.0557
3	158	0.0398	158	0.0441	1	158	0.0523	158	0.0523
3	137	0.0374	137	0.0370	1	137	0.0480	137	0.0480
3	118	0.0347	118	0.0298	1	118	0.0430	118	0.0430
3	102	0.0316	102	0.0228	1	102	0.0373	102	0.0373
3	88	0.0283	88	0.0162	1	88	0.0312	88	0.0312
3	76	0.0248	76	0.0105	1	76	0.0250	76	0.0250

**Table C.1.1 (continued)** Results of fresh-cut fruit relaxation time ( $T_2$ ), during storage period

Experiment 1					Experiment 2				
Day	Melon		Pear		Day	Melon		Pear	
	$T_2$ (ms)	A	$T_2$ (ms)	A		$T_2$ (ms)	A	$T_2$ (ms)	A
3	66	0.0212	66	0.0059	1	66	0.0188	66	0.0188
3	57	0.0175	57	0.0026	1	57	0.0131	57	0.0131
3	49	0.0139	49	0.0007	1	49	0.0082	49	0.0082
3	42	0.0105	42	0.0000	1	42	0.0043	42	0.0043
3	37	0.0074	37	0.0000	1	37	0.0017	37	0.0017
3	32	0.0048	32	0.0000	1	32	0.0003	32	0.0003
3	27	0.0027	27	0.0000	1	27	0.0000	27	0.0000
3	24	0.0012	24	0.0000	1	24	0.0000	24	0.0000
3	20	0.0003	20	0.0000	1	20	0.0000	20	0.0000
3	18	0.0000	18	0.0000	1	18	0.0000	18	0.0000
3	15	0.0000	15	0.0000	1	15	0.0000	15	0.0000
3	13	0.0000	13	0.0000	1	13	0.0000	13	0.0000
3	11	0.0000	11	0.0000	1	11	0.0000	11	0.0000
3	10	0.0000	10	0.0000	1	10	0.0000	10	0.0000
3	8	0.0000	8	0.0000	1	8	0.0000	8	0.0000
3	7	0.0000	7	0.0000	1	7	0.0000	7	0.0000
3	6	0.0000	6	0.0000	1	6	0.0000	6	0.0000
3	5	0.0000	5	0.0000	1	5	0.0000	5	0.0000
3	5	0.0000	5	0.0000	1	5	0.0000	5	0.0000
3	4	0.0000	4	0.0000	1	4	0.0000	4	0.0000
3	4	0.0000	4	0.0000	1	4	0.0000	4	0.0000
3	3	0.0000	3	0.0000	1	3	0.0000	3	0.0000
3	3	0.0000	3	0.0000	1	3	0.0000	3	0.0000
3	2	0.0000	2	0.0000	1	2	0.0000	2	0.0000
3	2	0.0000	2	0.0000	1	2	0.0000	2	0.0000



**Table C.1.1 (continued)** Results of fresh-cut fruit relaxation time ( $T_2$ ), during storage period

Experiment 1					Experiment 2				
Day	Melon		Pear		Day	Melon		Pear	
	$T_2$ (ms)	A	$T_2$ (ms)	A		$T_2$ (ms)	A	$T_2$ (ms)	A
4	100000	0.0001	100000	0.0001	2	100000	0.0001	100000	0.0001
4	86207	0.0004	86207	0.0004	2	86207	0.0003	86207	0.0003
4	74627	0.0008	74627	0.0008	2	74627	0.0006	74627	0.0006
4	64516	0.0013	64516	0.0014	2	64516	0.0010	64516	0.0010
4	55556	0.0019	55556	0.0021	2	55556	0.0015	55556	0.0015
4	48077	0.0026	48077	0.0030	2	48077	0.0021	48077	0.0021
4	41494	0.0035	41494	0.0040	2	41494	0.0028	41494	0.0028
4	35842	0.0044	35842	0.0052	2	35842	0.0036	35842	0.0036
4	30960	0.0054	30960	0.0066	2	30960	0.0044	30960	0.0044
4	26738	0.0066	26738	0.0082	2	26738	0.0054	26738	0.0054
4	23095	0.0078	23095	0.0099	2	23095	0.0064	23095	0.0064
4	19960	0.0091	19960	0.0118	2	19960	0.0075	19960	0.0075
4	17241	0.0105	17241	0.0138	2	17241	0.0087	17241	0.0087
4	14881	0.0120	14881	0.0161	2	14881	0.0100	14881	0.0100
4	12854	0.0135	12854	0.0185	2	12854	0.0114	12854	0.0114
4	11099	0.0151	11099	0.0210	2	11099	0.0128	11099	0.0128
4	9615	0.0168	9615	0.0238	2	9615	0.0142	9615	0.0142
4	8264	0.0185	8264	0.0266	2	8264	0.0158	8264	0.0158
4	7143	0.0202	7143	0.0296	2	7143	0.0173	7143	0.0173
4	6173	0.0220	6173	0.0328	2	6173	0.0190	6173	0.0190
4	5348	0.0239	5348	0.0361	2	5348	0.0207	5348	0.0207
4	4608	0.0257	4608	0.0394	2	4608	0.0224	4608	0.0224
4	3984	0.0276	3984	0.0428	2	3984	0.0241	3984	0.0241
4	3436	0.0295	3436	0.0463	2	3436	0.0259	3436	0.0259
4	2967	0.0313	2967	0.0498	2	2967	0.0276	2967	0.0276

**Table C.1.1 (continued)** Results of fresh-cut fruit relaxation time ( $T_2$ ), during storage period

Experiment 1					Experiment 2				
Day	Melon		Pear		Day	Melon		Pear	
	$T_2$ (ms)	A	$T_2$ (ms)	A		$T_2$ (ms)	A	$T_2$ (ms)	A
4	2564	0.0332	2564	0.0533	2	2564	0.0294	2564	0.0294
4	2212	0.0350	2212	0.0567	2	2212	0.0312	2212	0.0312
4	1912	0.0368	1912	0.0601	2	1912	0.0329	1912	0.0329
4	1653	0.0385	1653	0.0633	2	1653	0.0346	1653	0.0346
4	1427	0.0401	1427	0.0662	2	1427	0.0363	1427	0.0363
4	1232	0.0417	1232	0.0690	2	1232	0.0379	1232	0.0379
4	1064	0.0431	1064	0.0714	2	1064	0.0394	1064	0.0394
4	917	0.0444	917	0.0734	2	917	0.0407	917	0.0407
4	794	0.0455	794	0.0749	2	794	0.0420	794	0.0420
4	685	0.0464	685	0.0758	2	685	0.0431	685	0.0431
4	592	0.0472	592	0.0762	2	592	0.0440	592	0.0440
4	510	0.0477	510	0.0759	2	510	0.0447	510	0.0447
4	442	0.0479	442	0.0747	2	442	0.0451	442	0.0451
4	382	0.0478	382	0.0728	2	382	0.0453	382	0.0453
4	329	0.0475	329	0.0700	2	329	0.0452	329	0.0452
4	285	0.0468	285	0.0664	2	285	0.0448	285	0.0448
4	246	0.0457	246	0.0619	2	246	0.0440	246	0.0440
4	212	0.0443	212	0.0566	2	212	0.0429	212	0.0429
4	183	0.0425	183	0.0505	2	183	0.0414	183	0.0414
4	158	0.0403	158	0.0439	2	158	0.0395	158	0.0395
4	137	0.0377	137	0.0370	2	137	0.0373	137	0.0373
4	118	0.0348	118	0.0298	2	118	0.0346	118	0.0346
4	102	0.0316	102	0.0229	2	102	0.0317	102	0.0317
4	88	0.0281	88	0.0163	2	88	0.0284	88	0.0284
4	76	0.0245	76	0.0106	2	76	0.0249	76	0.0249



**Table C.1.1 (continued)** Results of fresh-cut fruit relaxation time ( $T_2$ ), during storage period

Experiment 1					Experiment 2				
Day	Melon		Pear		Day	Melon		Pear	
	$T_2$ (ms)	A	$T_2$ (ms)	A		$T_2$ (ms)	A	$T_2$ (ms)	A
4	66	0.0207	66	0.0060	2	66	0.0213	66	0.0213
4	57	0.0170	57	0.0026	2	57	0.0177	57	0.0177
4	49	0.0133	49	0.0007	2	49	0.0141	49	0.0141
4	42	0.0099	42	0.0000	2	42	0.0106	42	0.0106
4	37	0.0069	37	0.0000	2	37	0.0076	37	0.0076
4	32	0.0044	32	0.0000	2	32	0.0049	32	0.0049
4	27	0.0024	27	0.0000	2	27	0.0028	27	0.0028
4	24	0.0010	24	0.0000	2	24	0.0013	24	0.0013
4	20	0.0003	20	0.0000	2	20	0.0004	20	0.0004
4	18	0.0000	18	0.0000	2	18	0.0000	18	0.0000
4	15		15	0.0000	2	15	0.0000	15	0.0000
4	13	0.0000	13	0.0000	2	13	0.0000	13	0.0000
4	11	0.0000	11	0.0000	2	11	0.0000	11	0.0000
4	10	0.0000	10	0.0000	2	10	0.0000	10	0.0000
4	8	0.0000	8	0.0000	2	8	0.0000	8	0.0000
4	7	0.0000	7	0.0000	2	7	0.0000	7	0.0000
4	6	0.0000	6	0.0000	2	6	0.0000	6	0.0000
4	5	0.0000	5	0.0000	2	5	0.0000	5	0.0000
4	5	0.0000	5	0.0000	2	5	0.0000	5	0.0000
4	4	0.0000	4	0.0000	2	4	0.0000	4	0.0000
4	4	0.0000	4	0.0000	2	4	0.0000	4	0.0000
4	3	0.0000	3	0.0000	2	3	0.0000	3	0.0000
4	3	0.0000	3	0.0000	2	3	0.0000	3	0.0000
4	2	0.0000	2	0.0000	2	2	0.0000	2	0.0000
4	2	0.0000	2	0.0000	2	2	0.0000	2	0.0000



**Table C.1.1 (continued)** Results of fresh-cut fruit relaxation time ( $T_2$ ), during storage period

Experiment 1					Experiment 2				
Day	Melon		Pear		Day	Melon		Pear	
	$T_2$ (ms)	A	$T_2$ (ms)	A		$T_2$ (ms)	A	$T_2$ (ms)	A
5	100000	0.0002	100000	0.0000	3	100000	0.0001	100000	0.0001
5	86207	0.0005	86207	0.0000	3	86207	0.0004	86207	0.0004
5	74627	0.0009	74627	0.0001	3	74627	0.0008	74627	0.0008
5	64516	0.0015	64516	0.0002	3	64516	0.0014	64516	0.0014
5	55556	0.0022	55556	0.0004	3	55556	0.0020	55556	0.0020
5	48077	0.0030	48077	0.0007	3	48077	0.0028	48077	0.0028
5	41494	0.0040	41494	0.0011	3	41494	0.0037	41494	0.0037
5	35842	0.0051	35842	0.0016	3	35842	0.0047	35842	0.0047
5	30960	0.0063	30960	0.0022	3	30960	0.0058	30960	0.0058
5	26738	0.0076	26738	0.0030	3	26738	0.0070	26738	0.0070
5	23095	0.0090	23095	0.0040	3	23095	0.0083	23095	0.0083
5	19960	0.0104	19960	0.0051	3	19960	0.0097	19960	0.0097
5	17241	0.0120	17241	0.0065	3	17241	0.0112	17241	0.0112
5	14881	0.0136	14881	0.0080	3	14881	0.0128	14881	0.0128
5	12854	0.0154	12854	0.0097	3	12854	0.0144	12854	0.0144
5	11099	0.0171	11099	0.0117	3	11099	0.0161	11099	0.0161
5	9615	0.0190	9615	0.0138	3	9615	0.0179	9615	0.0179
5	8264	0.0209	8264	0.0162	3	8264	0.0197	8264	0.0197
5	7143	0.0228	7143	0.0188	3	7143	0.0215	7143	0.0215
5	6173	0.0247	6173	0.0217	3	6173	0.0234	6173	0.0234
5	5348	0.0267	5348	0.0247	3	5348	0.0253	5348	0.0253
5	4608	0.0287	4608	0.0280	3	4608	0.0272	4608	0.0272
5	3984	0.0307	3984	0.0314	3	3984	0.0292	3984	0.0292
5	3436	0.0327	3436	0.0350	3	3436	0.0311	3436	0.0311
5	2967	0.0346	2967	0.0387	3	2967	0.0331	2967	0.0331

**Table C.1.1 (continued)** Results of fresh-cut fruit relaxation time ( $T_2$ ), during storage period

Experiment 1					Experiment 2				
Day	Melon		Pear		Day	Melon		Pear	
	$T_2$ (ms)	A	$T_2$ (ms)	A		$T_2$ (ms)	A	$T_2$ (ms)	A
5	2564	0.0366	2564	0.0426	3	2564	0.0350	2564	0.0350
5	2212	0.0385	2212	0.0465	3	2212	0.0368	2212	0.0368
5	1912	0.0403	1912	0.0505	3	1912	0.0387	1912	0.0387
5	1653	0.0420	1653	0.0544	3	1653	0.0404	1653	0.0404
5	1427	0.0436	1427	0.0583	3	1427	0.0421	1427	0.0421
5	1232	0.0452	1232	0.0620	3	1232	0.0436	1232	0.0436
5	1064	0.0466	1064	0.0656	3	1064	0.0450	1064	0.0450
5	917	0.0478	917	0.0688	3	917	0.0463	917	0.0463
5	794	0.0488	794	0.0717	3	794	0.0474	794	0.0474
5	685	0.0497	685	0.0741	3	685	0.0484	685	0.0484
5	592	0.0503	592	0.0760	3	592	0.0491	592	0.0491
5	510	0.0506	510	0.0772	3	510	0.0495	510	0.0495
5	442	0.0507	442	0.0777	3	442	0.0497	442	0.0497
5	382	0.0505	382	0.0773	3	382	0.0496	382	0.0496
5	329	0.0499	329	0.0761	3	329	0.0491	329	0.0491
5	285	0.0490	285	0.0739	3	285	0.0483	285	0.0483
5	246	0.0477	246	0.0708	3	246	0.0472	246	0.0472
5	212	0.0460	212	0.0668	3	212	0.0456	212	0.0456
5	183	0.0439	183	0.0618	3	183	0.0437	183	0.0437
5	158	0.0415	158	0.0559	3	158	0.0414	158	0.0414
5	137	0.0387	137	0.0494	3	137	0.0387	137	0.0387
5	118	0.0356	118	0.0423	3	118	0.0356	118	0.0356
5	102	0.0321	102	0.0350	3	102	0.0323	102	0.0323
5	88	0.0284	88	0.0277	3	88	0.0287	88	0.0287
5	76	0.0246	76	0.0207	3	76	0.0249	76	0.0249

**Table C.1.1 (continued)** Results of fresh-cut fruit relaxation time ( $T_2$ ), during storage period

Experiment 1					Experiment 2				
Day	Melon		Pear		Day	Melon		Pear	
	$T_2$ (ms)	A	$T_2$ (ms)	A		$T_2$ (ms)	A	$T_2$ (ms)	A
5	66	0.0207	66	0.0143	3	66	0.0210	66	0.0210
5	57	0.0168	57	0.0089	3	57	0.0172	57	0.0172
5	49	0.0131	49	0.0047	3	49	0.0134	49	0.0134
5	42	0.0097	42	0.0019	3	42	0.0100	42	0.0100
5	37	0.0067	37	0.0004	3	37	0.0069	37	0.0069
5	32	0.0041	32	0.0000	3	32	0.0043	32	0.0043
5	27	0.0022	27	0.0000	3	27	0.0023	27	0.0023
5	24	0.0009	24	0.0000	3	24	0.0010	24	0.0010
5	20	0.0002	20	0.0000	3	20	0.0003	20	0.0003
5	18	0.0000	18	0.0000	3	18	0.0000	18	0.0000
5	15	0.0000	15	0.0000	3	15	0.0000	15	0.0000
5	13	0.0000	13	0.0000	3	13	0.0000	13	0.0000
5	11	0.0000	11	0.0000	3	11	0.0000	11	0.0000
5	10	0.0000	10	0.0000	3	10	0.0000	10	0.0000
5	8	0.0000	8	0.0000	3	8	0.0000	8	0.0000
5	7	0.0000	7	0.0000	3	7	0.0000	7	0.0000
5	6	0.0000	6	0.0000	3	6	0.0000	6	0.0000
5	5	0.0000	5	0.0000	3	5	0.0000	5	0.0000
5	5	0.0000	5	0.0000	3	5	0.0000	5	0.0000
5	4	0.0000	4	0.0000	3	4	0.0000	4	0.0000
5	4	0.0000	4	0.0000	3	4	0.0000	4	0.0000
5	3	0.0000	3	0.0000	3	3	0.0000	3	0.0000
5	3	0.0000	3	0.0000	3	3	0.0000	3	0.0000
5	2	0.0000	2	0.0000	3	2	0.0000	2	0.0000
5	2	0.0000	2	0.0000	3	2	0.0000	2	0.0000



**Table C.1.1 (continued)** Results of fresh-cut fruit relaxation time ( $T_2$ ), during storage period

Experiment 1					Experiment 2				
Day	Melon		Pear		Day	Melon		Pear	
	$T_2$ (ms)	A	$T_2$ (ms)	A		$T_2$ (ms)	A	$T_2$ (ms)	A
6	10000 0	0.0000	10000 0	0.0002	4	10000 0	0.0000	10000 0	0.0000
6	86207	0.0000	86207	0.0005	4	86207	0.0000	86207	0.0000
6	74627	0.0000	74627	0.0011	4	74627	0.0000	74627	0.0000
6	64516	0.0000	64516	0.0018	4	64516	0.0000	64516	0.0000
6	55556	0.0000	55556	0.0027	4	55556	0.0000	55556	0.0000
6	48077	0.0000	48077	0.0038	4	48077	0.0000	48077	0.0000
6	41494	0.0000	41494	0.0050	4	41494	0.0000	41494	0.0000
6	35842	0.0000	35842	0.0065	4	35842	0.0000	35842	0.0000
6	30960	0.0000	30960	0.0081	4	30960	0.0000	30960	0.0000
6	26738	0.0000	26738	0.0099	4	26738	0.0000	26738	0.0000
6	23095	0.0000	23095	0.0119	4	23095	0.0000	23095	0.0000
6	19960	0.0001	19960	0.0140	4	19960	0.0000	19960	0.0000
6	17241	0.0002	17241	0.0163	4	17241	0.0001	17241	0.0001
6	14881	0.0004	14881	0.0188	4	14881	0.0002	14881	0.0002
6	12854	0.0007	12854	0.0214	4	12854	0.0005	12854	0.0005
6	11099	0.0012	11099	0.0242	4	11099	0.0009	11099	0.0009
6	9615	0.0019	9615	0.0271	4	9615	0.0015	9615	0.0015
6	8264	0.0028	8264	0.0302	4	8264	0.0022	8264	0.0022
6	7143	0.0039	7143	0.0333	4	7143	0.0032	7143	0.0032
6	6173	0.0052	6173	0.0366	4	6173	0.0044	6173	0.0044
6	5348	0.0068	5348	0.0399	4	5348	0.0058	5348	0.0058
6	4608	0.0086	4608	0.0433	4	4608	0.0075	4608	0.0075
6	3984	0.0107	3984	0.0467	4	3984	0.0094	3984	0.0094
6	3436	0.0131	3436	0.0502	4	3436	0.0117	3436	0.0117
6	2967	0.0157	2967	0.0536	4	2967	0.0142	2967	0.0142

**Table C.1.1 (continued)** Results of fresh-cut fruit relaxation time ( $T_2$ ), during storage period

Experiment 1					Experiment 2				
Day	Melon		Pear		Day	Melon		Pear	
	$T_2$ (ms)	A	$T_2$ (ms)	A		$T_2$ (ms)	A	$T_2$ (ms)	A
6	2564	0.0186	2564	0.0570	4	2564	0.0169	2564	0.0169
6	2212	0.0217	2212	0.0602	4	2212	0.0199	212	0.0199
6	1912	0.0251	1912	0.0634	4	1912	0.0231	1912	0.0231
6	1653	0.0286	1653	0.0664	4	1653	0.0266	1653	0.0266
6	1427	0.0322	1427	0.0691	4	1427	0.0301	1427	0.0301
6	1232	0.0360	1232	0.0715	4	1232	0.0338	1232	0.0338
6	1064	0.0398	1064	0.0736	4	1064	0.0376	1064	0.0376
6	917	0.0436	917	0.0753	4	917	0.0414	917	0.0414
6	794	0.0472	794	0.0765	4	794	0.0451	794	0.0451
6	685	0.0507	685	0.0771	4	685	0.0486	685	0.0486
6	592	0.0539	592	0.0772	4	592	0.0519	592	0.0519
6	510	0.0568	510	0.0765	4	510	0.0548	510	0.0548
6	442	0.0591	442	0.0751	4	442	0.0573	442	0.0573
6	382	0.0609	382	0.0729	4	382	0.0592	382	0.0592
6	329	0.0619	329	0.0699	4	329	0.0605	329	0.0605
6	285	0.0622	285	0.0660	4	285	0.0610	285	0.0610
6	246	0.0616	246	0.0614	4	246	0.0607	246	0.0607
6	212	0.0601	212	0.0559	4	212	0.0595	212	0.0595
6	183	0.0577	183	0.0499	4	183	0.0573	183	0.0573
6	158	0.0543	158	0.0433	4	158	0.0541	158	0.0541
6	137	0.0499	137	0.0363	4	137	0.0500	137	0.0500
6	118	0.0447	118	0.0293	4	118	0.0450	118	0.0450
6	102	0.0389	102	0.0224	4	102	0.0394	102	0.0394
6	88	0.0326	88	0.0160	4	88	0.0332	88	0.0332
6	76	0.0261	76	0.0104	4	76	0.0267	76	0.0267



**Table C.1.1 (continued)** Results of fresh-cut fruit relaxation time ( $T_2$ ), during storage period

Experiment 1					Experiment 2				
Day	Melon		Pear		Day	Melon		Pear	
	$T_2$ (ms)	A	$T_2$ (ms)	A		$T_2$ (ms)	A	$T_2$ (ms)	A
6	66	0.0197	66	0.0059	4	66	0.0204	66	0.0204
6	57	0.0138	57	0.0026	4	57	0.0144	57	0.0144
6	49	0.0086	49	0.0007	4	49	0.0091	49	0.0091
6	42	0.0046	42	0.0000	4	42	0.0049	42	0.0049
6	37	0.0018	37	0.0000	4	37	0.0020	37	0.0020
6	32	0.0004	32	0.0000	4	32	0.0004	32	0.0004
6	27	0.0000	27	0.0000	4	27	0.0000	27	0.0000
6	24	0.0000	24	0.0000	4	24	0.0000	24	0.0000
6	20	0.0000	20	0.0000	4	20	0.0000	20	0.0000
6	18	0.0000	18	0.0000	4	18	0.0000	18	0.0000
6	15	0.0000	15	0.0000	4	15	0.0000	15	0.0000
6	13	0.0000	13	0.0000	4	13	0.0000	13	0.0000
6	11	0.0000	11	0.0000	4	11	0.0000	11	0.0000
6	10	0.0000	10	0.0000	4	10	0.0000	10	0.0000
6	8	0.0000	8	0.0000	4	8	0.0000	8	0.0000
6	7	0.0000	7	0.0000	4	7	0.0000	7	0.0000
6	6	0.0000	6	0.0000	4	6	0.0000	6	0.0000
6	5	0.0000	5	0.0000	4	5	0.0000	5	0.0000
6	5	0.0000	5	0.0000	4	5	0.0000	5	0.0000
6	4	0.0000	4	0.0000	4	4	0.0000	4	0.0000
6	4	0.0000	4	0.0000	4	4	0.0000	4	0.0000
6	3	0.0000	3	0.0000	4	3	0.0000	3	0.0000
6	3	0.0000	3	0.0000	4	3	0.0000	3	0.0000
6	2	0.0000	2	0.0000	4	2	0.0000	2	0.0000
6	2	0.0000	2	0.0000	4	2	0.0000	2	0.0000



**Table C.1.1 (continued)** Results of fresh-cut fruit relaxation time ( $T_2$ ), during storage period

Experiment 1					Experiment 2				
Day	Melon		Pear		Day	Melon		Pear	
	$T_2$ (ms)	A	$T_2$ (ms)	A		$T_2$ (ms)	A	$T_2$ (ms)	A
7	100000	0.0001	100000	0.0001	7	100000	0.0000	100000	0.0000
7	86207	0.0004	86207	0.0004	7	86207	0.0000	86207	0.0000
7	74627	0.0008	74627	0.0008	7	74627	0.0000	74627	0.0000
7	64516	0.0013	64516	0.0014	7	64516	0.0000	64516	0.0000
7	55556	0.0019	55556	0.0021	7	55556	0.0000	55556	0.0000
7	48077	0.0026	48077	0.0030	7	48077	0.0000	48077	0.0000
7	41494	0.0034	41494	0.0040	7	41494	0.0000	41494	0.0000
7	35842	0.0043	35842	0.0052	7	35842	0.0000	35842	0.0000
7	30960	0.0053	30960	0.0066	7	30960	0.0000	30960	0.0000
7	26738	0.0064	26738	0.0081	7	26738	0.0000	26738	0.0000
7	23095	0.0076	23095	0.0098	7	23095	0.0000	23095	0.0000
7	19960	0.0089	19960	0.0116	7	19960	0.0000	19960	0.0000
7	17241	0.0103	17241	0.0136	7	17241	0.0000	17241	0.0000
7	14881	0.0117	14881	0.0158	7	14881	0.0000	14881	0.0000
7	12854	0.0132	12854	0.0181	7	12854	0.0000	12854	0.0000
7	11099	0.0147	11099	0.0206	7	11099	0.0000	11099	0.0000
7	9615	0.0163	9615	0.0232	7	9615	0.0000	9615	0.0000
7	8264	0.0180	8264	0.0260	7	8264	0.0000	8264	0.0000
7	7143	0.0197	7143	0.0289	7	7143	0.0000	7143	0.0000
7	6173	0.0214	6173	0.0319	7	6173	0.0000	6173	0.0000
7	5348	0.0232	5348	0.0350	7	5348	0.0000	5348	0.0000
7	4608	0.0249	4608	0.0382	7	4608	0.0000	4608	0.0000
7	3984	0.0267	3984	0.0414	7	3984	0.0000	3984	0.0000
7	3436	0.0285	3436	0.0447	7	3436	0.0000	3436	0.0000
7	2967	0.0303	2967	0.0480	7	2967	0.0000	2967	0.0000

**Table C.1.1 (continued)** Results of fresh-cut fruit relaxation time ( $T_2$ ), during storage period

Experiment 1					Experiment 2				
Day	Melon		Pear		Day	Melon		Pear	
	$T_2$ (ms)	A	$T_2$ (ms)	A		$T_2$ (ms)	A	$T_2$ (ms)	A
7	2564	0.0320	2564	0.0513	7	2564	0.0000	2564	0.0000
7	2212	0.0337	2212	0.0546	7	2212	0.0000	2212	0.0000
7	1912	0.0354	1912	0.0577	7	1912	0.0000	1912	0.0000
7	1653	0.0370	1653	0.0607	7	1653	0.0000	1653	0.0000
7	1427	0.0386	1427	0.0635	7	1427	0.0002	1427	0.0002
7	1232	0.0400	1232	0.0661	7	1232	0.0013	1232	0.0013
7	1064	0.0413	1064	0.0683	7	1064	0.0040	1064	0.0040
7	917	0.0425	917	0.0702	7	917	0.0087	917	0.0087
7	794	0.0436	794	0.0716	7	794	0.0154	794	0.0154
7	685	0.0445	685	0.0726	7	685	0.0243	685	0.0243
7	592	0.0452	592	0.0729	7	592	0.0348	592	0.0348
7	510	0.0456	510	0.0726	7	510	0.0467	510	0.0467
7	442	0.0459	442	0.0716	7	442	0.0591	442	0.0591
7	382	0.0458	382	0.0699	7	382	0.0712	382	0.0712
7	329	0.0455	329	0.0673	7	329	0.0820	329	0.0820
7	285	0.0449	285	0.0639	7	285	0.0906	285	0.0906
7	246	0.0439	246	0.0598	7	246	0.0960	246	0.0960
7	212	0.0426	212	0.0548	7	212	0.0975	212	0.0975
7	183	0.0409	183	0.0492	7	183	0.0944	183	0.0944
7	158	0.0389	158	0.0430	7	158	0.0868	158	0.0868
7	137	0.0365	137	0.0364	7	137	0.0751	137	0.0751
7	118	0.0338	118	0.0297	7	118	0.0601	118	0.0601
7	102	0.0308	102	0.0230	7	102	0.0435	102	0.0435
7	88	0.0276	88	0.0167	7	88	0.0272	88	0.0272
7	76	0.0241	76	0.0110	7	76	0.0134	76	0.0134

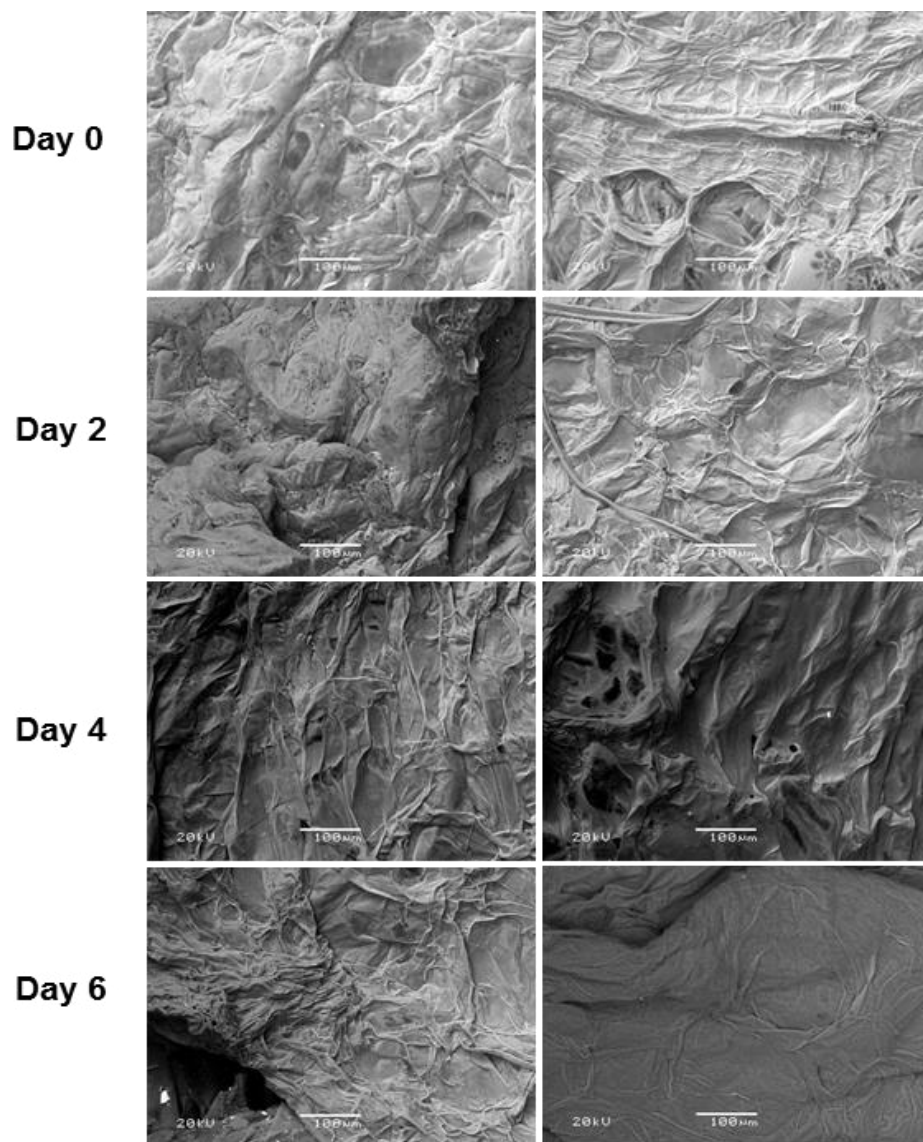
**Table C.1.1 (continued)** Results of fresh-cut fruit relaxation time ( $T_2$ ), during storage period

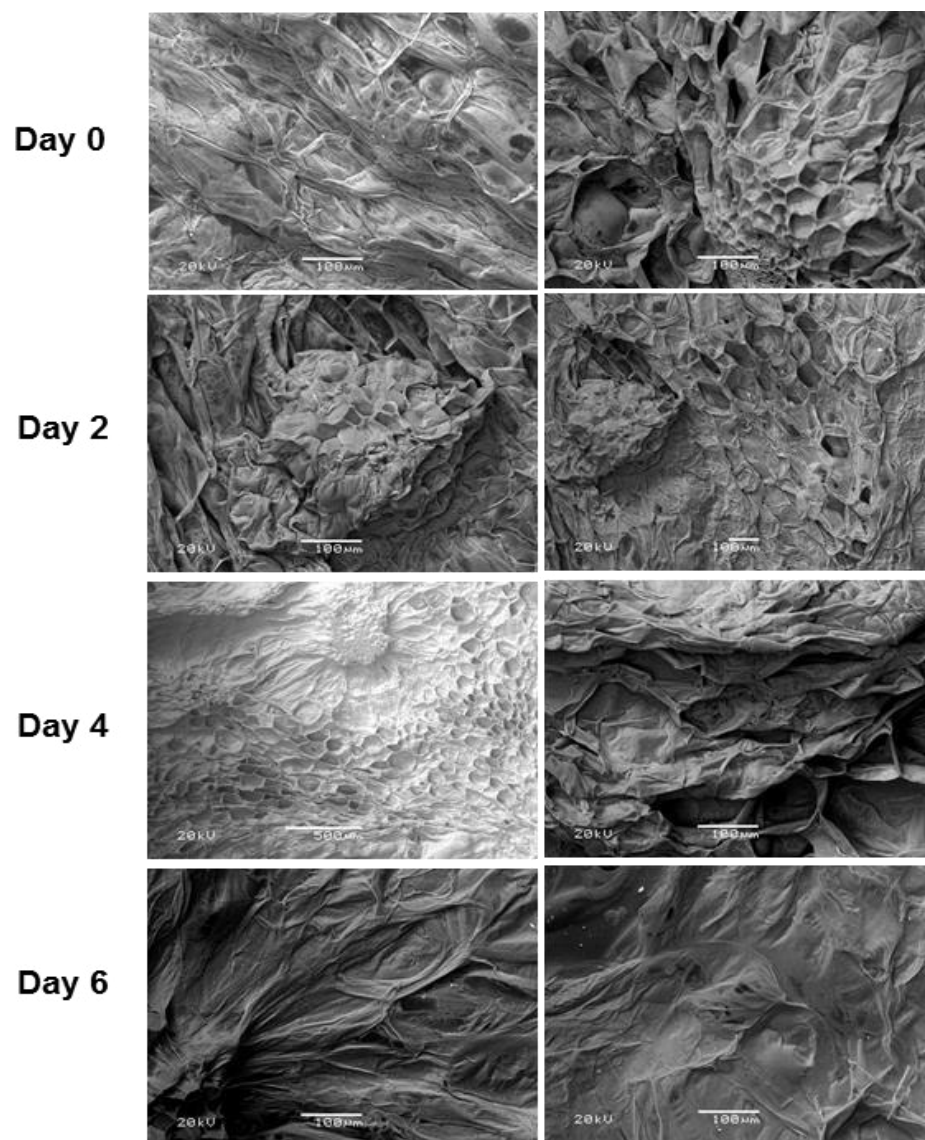
Experiment 1					Experiment 2				
Day	Melon		Pear		Day	Melon		Pear	
	$T_2$ (ms)	A	$T_2$ (ms)	A		$T_2$ (ms)	A	$T_2$ (ms)	A
7	66	0.0206	66	0.0064	7	66	0.0041	66	0.0041
7	57	0.0170	57	0.0029	7	57	0.0000	57	0.0000
7	49	0.0135	49	0.0009	7	49	0.0000	49	0.0000
7	42	0.0102	42	0.0000	7	42	0.0000	42	0.0000
7	37	0.0073	37	0.0000	7	37	0.0000	37	0.0000
7	32	0.0047	32	0.0000	7	32	0.0000	32	0.0000
7	27	0.0027	27	0.0000	7	27	0.0000	27	0.0000
7	24	0.0012	24	0.0000	7	24	0.0000	24	0.0000
7	20	0.0003	20	0.0000	7	20	0.0000	20	0.0000
7	18	0.0000	18	0.0000	7	18	0.0000	18	0.0000
7	15	0.0000	15	0.0000	7	15	0.0000	15	0.0000
7	13	0.0000	13	0.0000	7	13	0.0000	13	0.0000
7	11	0.0000	11	0.0000	7	11	0.0000	11	0.0000
7	10	0.0000	10	0.0000	7	10	0.0000	10	0.0000
7	8	0.0000	8	0.0000	7	8	0.0000	8	0.0000
7	7	0.0000	7	0.0000	7	7	0.0000	7	0.0000
7	6	0.0000	6	0.0000	7	6	0.0000	6	0.0000
7	5	0.0000	5	0.0000	7	5	0.0000	5	0.0000
7	5	0.0000	5	0.0000	7	5	0.0000	5	0.0000
7	4	0.0000	4	0.0000	7	4	0.0000	4	0.0000
7	4	0.0000	4	0.0000	7	4	0.0000	4	0.0000
7	3	0.0000	3	0.0000	7	3	0.0000	3	0.0000
7	3	0.0000	3	0.0000	7	3	0.0000	3	0.0000
7	2	0.0000	2	0.0000	7	2	0.0000	2	0.0000
7	2	0.0000	2	0.0000	7	2	0.0000	2	0.0000



## C.2 Scanning electron microscope (SEM) images of fresh-cut fruit, at different days of storage

### C.2.1 SEM images of fresh-cut melon during storage period



**C.2.2 SEM images of fresh-cut pear during storage period**



### C.3 Experimental results of fresh-cut fruit quality parameters

**Table C.3.1** Colour, firmness and  $a_w$  of fresh-cut melon, during storage period at refrigerated conditions

Exp	Day	Sample	Measure	Colour			Firmness (N)	$a_w$
				L*	a*	b*		
1	0	1	1	73.69	1.58	5.60	2.59	1.000
1	0	1	2	71.35	1.79	4.09	2.97	1.000
1	0	1	3	71.50	1.36	6.15	3.40	
1	0	1	4	68.89	1.18	6.71	2.61	
1	0	1	5	69.87	1.20	6.59	3.07	
1	0	1	6	73.90	1.75	4.86		
1	0	2	1	70.29	0.49	7.13	3.14	1.000
1	0	2	2	69.53	0.96	7.04	3.92	1.000
1	0	2	3	69.50	0.92	7.07	3.32	
1	0	2	4	74.15	1.32	5.81	4.91	
1	0	2	5	71.30	0.62	6.66	5.03	
1	0	2	6	72.31	0.76	6.68	5.13	
1	0	3	1	70.46	1.82	4.01	6.82	0.999
1	0	3	2	71.12	1.50	5.43	4.85	1.000
1	0	3	3	72.20	1.67	4.91	3.62	
1	0	3	4	67.65	1.47	5.31	5.22	
1	0	3	5	64.09	1.40	5.48	4.43	
1	0	3	6	68.08	1.38	5.54	2.98	
1	3	1	1	71.21	0.93	7.22	2.70	1.000
1	3	1	2	67.50	1.30	6.17	3.21	0.998
1	3	1	3	73.20	1.66	5.07	2.66	
1	3	1	4	69.29	1.37	6.16	2.68	
1	3	1	5	60.74	1.62	5.42	2.37	
1	3	1	6	70.71	1.26	6.99		
1	3	2	1	70.60	1.34	5.32	3.22	1.000
1	3	2	2	69.58	1.30	6.18	4.42	0.996
1	3	2	3	68.94	0.28	8.84	3.83	
1	3	2	4	65.35	0.64	8.12	4.83	
1	3	2	5	69.64	1.05	6.79	3.83	
1	3	2	6	65.17	0.91	7.50		
1	3	3	1	71.31	1.51	5.86	3.58	0.998
1	3	3	2	71.56	1.55	5.50	3.49	0.996
1	3	3	3	71.82	1.79	4.05	3.97	

**Table C.3.1 (continued)** Colour, firmness and water activity ( $a_w$ ) of fresh-cut melon, during storage period at refrigerated conditions

Exp	Day	Sample	Measure	Colour			Firmness (N)	$a_w$
				L*	a*	b*		
1	3	3	4	68.85	1.66	4.61	3.99	
1	3	3	5	67.64	1.59	4.59	3.44	
1	3	3	6	69.46	1.33	5.46		
1	4	1	1	71.99	1.21	6.23	3.38	1.000
1	4	1	2	70.46	1.15	6.13	2.85	0.993
1	4	1	3	68.80	0.96	6.65	2.60	
1	4	1	4	71.35	1.32	5.19	2.64	
1	4	1	5	73.01	1.12	6.53		
1	4	1	6	68.39	1.30	5.21		
1	4	2	1	70.53	0.63	8.00	2.92	0.998
1	4	2	2	69.07	0.19	10.81	2.65	0.992
1	4	2	3	70.54	0.32	8.10	2.94	
1	4	2	4	73.03	0.94	7.28	5.15	
1	4	2	5	74.58	1.12	7.07	3.17	
1	4	2	6	72.75	1.13	6.76		
1	4	3	1	72.79	1.58	5.25	3.48	0.997
1	4	3	2	72.81	1.63	4.67	3.07	1.000
1	4	3	3	70.13	1.72	3.01	3.07	
1	4	3	4	71.49	1.67	4.14	3.25	
1	4	3	5	66.92	1.73	2.88	4.44	
1	4	3	6	73.53	1.60	4.41		
1	5	1	1	72.70	1.32	5.37	2.68	0.998
1	5	1	2	71.62	1.21	5.62	3.10	0.997
1	5	1	3	72.17	1.54	4.48	2.71	
1	5	1	4	71.89	1.52	4.26	3.16	
1	5	1	5	71.08	1.37	4.99	2.53	
1	5	1	6	71.28	1.57	4.52		
1	5	2	1	69.96	1.22	4.70	3.73	0.994
1	5	2	2	75.19	1.27	5.75	3.41	0.994
1	5	2	3	74.17	0.32	7.37	3.36	
1	5	2	4	74.66	1.21	5.61	4.78	
1	5	2	5	73.39	0.62	7.57	3.63	
1	5	2	6	71.13	0.61	6.06		
1	5	3	1	73.53	2.05	3.20	2.94	0.994
1	5	3	2	74.18	1.94	3.52	2.90	0.995
1	5	3	3	69.94	1.54	4.26	3.38	

**Table C.3.1 (continued)** Colour firmness and water activity ( $a_w$ ) of fresh-cut melon, during storage period at refrigerated conditions

Exp	Day	Sample	Measure	Colour			Firmness (N)	$a_w$
				L*	a*	b*		
1	5	3	4	66.14	1.37	4.01	2.59	
1	5	3	5	65.50	1.49	3.74	2.32	
1	5	3	6	70.63	1.61	4.44		
1	6	1	1	72.26	1.70	4.01	2.98	0.998
1	6	1	2	63.21	0.97	5.87	3.17	0.998
1	6	1	3	70.51	1.09	6.65	2.34	
1	6	1	4	66.55	1.37	4.55	3.28	
1	6	1	5	75.17	1.21	6.58	2.61	
1	6	1	6	70.59	1.38	4.68	0.00	
1	6	2	1	70.77	0.73	6.70	3.66	0.989
1	6	2	2	73.41	1.18	5.70	2.94	0.994
1	6	2	3	70.77	0.55	6.56	3.05	
1	6	2	4	71.36	1.32	4.64	3.75	
1	6	2	5	73.34	1.44	4.47	4.50	
1	6	2	6	69.51	1.27	4.51		
1	6	3	1	68.89	1.63	3.84	2.97	0.997
1	6	3	2	70.43	1.75	4.02	3.77	1.000
1	6	3	3	73.46	1.87	3.45	2.66	
1	6	3	4	70.76	1.76	3.50	2.53	
1	6	3	5	70.81	1.85	3.29	3.91	
1	6	3	6	71.64	1.88	2.81		
1	7	1	1	72.10	1.41	6.15	2.40	0.997
1	7	1	2	72.94	1.30	5.78	3.24	0.997
1	7	1	3	71.59	1.06	6.46	3.25	
1	7	1	4	71.12	1.35	4.78	2.59	
1	7	1	5	72.50	1.51	4.69	3.31	
1	7	1	6	68.39	1.45	5.11	3.87	
1	7	2	1	70.85	1.24	6.24	3.00	0.995
1	7	2	2	68.68	0.53	6.28	3.28	0.996
1	7	2	3	72.13	1.28	5.38	2.31	
1	7	2	4	72.42	1.17	4.96	3.72	
1	7	2	5	70.82	1.36	5.68	2.68	
1	7	2	6	70.06	0.54	7.67	3.09	
1	7	3	1	72.03	2.00	3.43	3.05	0.995
1	7	3	2	72.60	1.91	4.60	2.58	0.998
1	7	3	3	72.96	1.94	3.62	3.68	

**Table C.3.1 (continued)** Colour, firmness and water activity ( $a_w$ ) of fresh-cut melon, during storage period at refrigerated conditions

Exp	Day	Sample	Measure	Colour			Firmness (N)	$a_w$
				L*	a*	b*		
1	7	3	4	69.70	1.51	5.53	2.20	
1	7	3	5	75.22	2.14	3.27		
1	7	3	6	71.14	1.97	3.68		
2	0	1	1	77.95	2.85	10.38	10.75	0.999
2	0	1	2	74.32	4.40	13.50	6.93	0.999
2	0	1	3	74.79	3.27	12.73	6.71	
2	0	1	4	77.29	2.73	11.76	8.71	
2	0	1	5	76.41	4.13	12.94	5.95	
2	0	1	6	76.85	2.65	12.79		
2	0	2	1	74.73	3.09	13.96	12.51	0.998
2	0	2	2	76.03	2.87	11.49	8.25	1.000
2	0	2	3	79.12	3.53	7.32	7.13	
2	0	2	4	76.54	4.06	14.95	8.65	
2	0	2	5	76.93	4.19	15.51	6.29	
2	0	2	6	73.39	3.99	12.55		
2	0	3	1	79.25	3.60	13.09	12.41	0.999
2	0	3	2	76.59	4.44	12.73	8.73	0.999
2	0	3	3	77.51	3.37	11.25	10.78	
2	0	3	4	78.33	3.49	14.32	8.66	
2	0	3	5	79.07	3.20	14.19	9.58	
2	0	3	6	75.32	3.21	12.04		
2	1	1	1	78.57	3.66	11.52	5.89	0.991
2	1	1	2	75.07	4.43	13.46	10.94	0.996
2	1	1	3	78.18	3.48	10.15	10.37	
2	1	1	4	79.81	3.20	9.10	8.00	
2	1	1	5	78.75	3.26	9.23	7.73	
2	1	1	6	80.01	3.42	8.45		
2	1	2	1	76.53	3.67	11.61	9.30	0.993
2	1	2	2	76.46	3.80	12.36	10.68	0.994
2	1	2	3	79.22	3.73	8.80	10.73	
2	1	2	4	78.43	4.50	14.75	9.11	
2	1	2	5	76.42	4.46	12.71	7.05	
2	1	2	6	80.27	3.88	9.71		
2	1	3	1	75.57	4.21	16.61	14.70	0.997
2	1	3	2	72.66	5.34	16.53	6.84	0.993
2	1	3	3	77.30	4.48	15.25	10.02	

**Table C.3.1 (continued)** Colour, firmness and water activity ( $a_w$ ) of fresh-cut melon, during storage period at refrigerated conditions

Exp	Day	Sample	Measure	Colour			Firmness (N)	$a_w$
				L*	a*	b*		
2	1	3	4	70.15	5.20	21.43	10.93	
2	1	3	5	79.56	3.20	11.49	7.56	
2	1	3	6	67.65	7.75	23.26		
2	2	1	1	80.04	3.88	9.45	7.17	0.982
2	2	1	2	76.79	4.51	12.61	10.96	0.989
2	2	1	3	79.54	3.30	11.32	10.57	
2	2	1	4	80.03	3.93	9.59	11.85	
2	2	1	5	77.38	3.76	11.22	11.60	
2	2	1	6	77.34	3.59	12.26		
2	2	2	1	76.18	2.87	7.72	6.91	0.984
2	2	2	2	78.27	4.11	12.26	11.72	0.982
2	2	2	3	80.06	3.60	9.73	10.13	
2	2	2	4	74.21	5.77	19.96	10.60	
2	2	2	5	79.43	4.18	10.61	9.98	
2	2	2	6	77.43	4.37	13.51		
2	2	3	1	77.43	3.25	12.54	6.61	0.984
2	2	3	2	73.05	4.04	14.26	10.55	0.995
2	2	3	3	71.97	5.85	22.02	8.52	
2	2	3	4	74.55	4.62	13.24	7.54	
2	2	3	5	77.80	4.17	13.50	8.42	
2	2	3	6	77.60	5.35	14.22		
2	3	1	1	77.17	2.96	10.48	5.72	0.989
2	3	1	2	78.45	3.94	10.54	10.73	0.995
2	3	1	3	78.40	3.47	11.44	7.22	
2	3	1	4	78.42	3.18	11.82	7.64	
2	3	1	5	75.29	4.29	12.28	11.36	
2	3	1	6	76.00	2.78	12.14		
2	3	2	1	76.40	4.07	15.98	8.07	0.976
2	3	2	2	79.30	3.70	9.77	10.56	0.998
2	3	2	3	75.47	3.67	11.75	9.20	
2	3	2	4	77.76	4.44	15.10	11.59	
2	3	2	5	74.90	5.01	16.60	9.31	
2	3	2	6	79.83	3.84	10.25		
2	3	3	1	78.48	3.98	14.20	6.76	0.987
2	3	3	2	78.35	3.82	10.26	7.51	0.995
2	3	3	3	74.37	3.85	14.35	16.49	
2	3	3	4	75.36	4.06	14.26	10.47	
2	3	3	5	78.27	4.92	13.87	12.02	

**Table C.3.1 (continued)** Colour, firmness and water activity ( $a_w$ ) of fresh-cut melon, during storage period at refrigerated conditions

Exp	Day	Sample	Measure	Colour			Firmness (N)	$a_w$
				L*	a*	b*		
2	3	3	6	78.34	3.84	12.84		
2	4	1	1	74.73	3.10	11.71	8.35	0.987
2	4	1	2	79.96	3.40	9.73	9.35	0.993
2	4	1	3	78.66	3.96	12.26	12.51	
2	4	1	4	78.85	3.64	11.51	4.59	
2	4	1	5	79.11	3.06	9.61	7.47	
2	4	1	6	78.56	4.04	11.54	10.67	
2	4	2	1	79.93	3.70	10.52	7.99	0.956
2	4	2	2	78.26	5.16	14.43	12.83	0.974
2	4	2	3	72.86	4.84	10.45	7.46	
2	4	2	4	77.26	3.52	9.92	13.42	
2	4	2	5	78.93	3.92	12.48	11.10	
2	4	2	6	78.29	4.92	15.92	7.24	
2	4	3	1	64.87	7.43	21.99	11.28	0.975
2	4	3	2	72.24	5.07	16.09	12.99	0.996
2	4	3	3	77.82	3.60	11.08	18.16	
2	4	3	4	77.68	4.65	14.68	11.58	
2	4	3	5	68.05	6.15	20.28	12.27	
2	4	3	6	77.24	4.21	15.03	7.83	
2	7	1	1	81.35	3.76	10.17	12.68	0.991
2	7	1	2	78.91	3.93	11.96	10.84	0.990
2	7	1	3	79.66	4.07	11.16	9.06	
2	7	1	4	77.82	3.17	11.13	10.60	
2	7	1	5	76.01	4.05	15.11	10.33	
2	7	1	6	78.20	4.57	11.14		
2	7	2	1	78.40	4.47	11.18	11.54	0.957
2	7	2	2	78.62	3.86	10.45	12.76	0.979
2	7	2	3	69.11	5.40	16.15	11.93	
2	7	2	4	76.21	5.63	17.36	8.89	
2	7	2	5	74.53	3.56	11.81	8.33	
2	7	2	6	74.76	3.41	11.61		
2	7	3	1	77.45	4.48	13.98	13.92	0.979
2	7	3	2	76.67	4.84	17.87	13.43	0.980
2	7	3	3	74.97	5.90	15.14	11.58	
2	7	3	4	76.72	3.90	13.42	13.12	
2	7	3	5	79.38	3.60	12.27	9.55	
2	7	3	6	72.38	5.50	16.50		

**Table C.3.2** Colour, firmness and water activity ( $a_w$ ) of fresh-cut pear, during storage period at refrigerated conditions

Exp	Day	Sample	Measure	Colour			Firmness (N)	$a_w$
				L*	a*	b*		
1	0	1	1	74.37	3.27	15.00	12.24	0.985
1	0	1	2	76.83	3.14	14.89	7.26	0.999
1	0	1	3	79.24	2.90	12.01	6.34	
1	0	1	4	76.38	3.57	9.53	10.36	
1	0	1	5	78.96	2.34	8.75	8.66	
1	0	1	6	78.14	3.39	14.32		
1	0	2	1	77.66	2.94	8.27	13.32	0.999
1	0	2	2	79.01	2.47	11.62	9.92	0.999
1	0	2	3	78.69	3.09	6.66	11.13	
1	0	2	4	78.54	2.88	9.89	8.92	
1	0	2	5	79.32	1.84	12.75	12.48	
1	0	2	6	76.64	3.37	10.37	9.57	
1	0	3	1	77.28	2.52	11.60	14.44	0.999
1	0	3	2	73.45	4.71	18.51	9.78	0.999
1	0	3	3	75.93	4.22	14.88	12.56	
1	0	3	4	75.26	1.82	11.38	6.12	
1	0	3	5	74.21	2.72	13.25	7.67	
1	0	3	6	75.24	2.28	13.48	10.37	
1	3	1	1	73.80	3.03	14.44	9.10	0.995
1	3	1	2	76.02	3.43	12.54	6.94	0.995
1	3	1	3	75.22	3.34	13.39	8.43	
1	3	1	4	79.25	2.19	10.90	8.50	
1	3	1	5	75.43	2.56	12.86	11.19	
1	3	1	6	79.22	2.27	10.53		
1	3	2	1	77.28	3.03	14.44	13.87	0.997
1	3	2	2	80.66	3.43	12.54	10.15	0.997
1	3	2	3	76.85	3.34	13.39	9.15	
1	3	2	4	74.00	2.19	10.90	10.87	
1	3	2	5	78.90	2.56	12.86	7.06	
1	3	2	6	73.71	2.27	10.53		
1	3	3	1	80.07	2.95	8.10	11.15	0.993
1	3	3	2	79.29	2.82	11.02	11.60	0.993
1	3	3	3	73.39	4.08	16.05	6.68	
1	3	3	4	79.76	2.90	9.68	8.71	
1	3	3	5	75.85	3.28	13.55	6.97	
1	3	3	6	78.16	2.50	11.68		

**Table C.3.2 (continued)** Colour, firmness and water activity ( $a_w$ ) of fresh-cut pear, during storage period at refrigerated conditions

Exp	Day	Sample	Measure	Colour			Firmness (N)	$a_w$
				L*	a*	b*		
1	4	1	1	80.56	2.72	10.16	7.49	0.996
1	4	1	2	80.20	2.01	13.42	9.77	0.978
1	4	1	3	76.16	3.16	11.36	13.40	
1	4	1	4	76.36	4.92	15.40	13.92	
1	4	1	5	75.24	3.67	13.79	5.94	
1	4	1	6	77.83	2.65	11.63		
1	4	2	1	74.15	2.95	13.58	14.93	0.996
1	4	2	2	77.09	3.48	13.25	11.90	0.988
1	4	2	3	77.72	2.53	9.50	7.65	
1	4	2	4	77.15	1.64	15.30	9.07	
1	4	2	5	75.80	2.12	13.47	7.88	
1	4	2	6	78.44	3.15	13.28		
1	4	3	1	79.58	2.75	10.33	11.16	0.984
1	4	3	2	77.84	3.40	15.77	11.59	0.993
1	4	3	3	74.47	3.18	13.41	9.55	
1	4	3	4	81.78	3.16	8.99	12.16	
1	4	3	5	80.75	2.79	8.34	7.94	
1	4	3	6	77.82	3.31	11.46		
1	5	1	1	79.96	3.18	11.53	11.27	0.983
1	5	1	3	78.74	3.60	11.90	13.66	
1	5	1	4	80.00	3.54	12.53	8.51	
1	5	1	5	73.76	4.86	16.48	7.39	
1	5	1	6	78.59	2.44	12.63		
1	5	2	1	78.77	3.49	6.75	12.75	0.988
1	5	2	2	77.67	3.74	15.69	11.52	0.994
1	5	2	3	78.06	3.18	11.65	9.64	
1	5	2	4	79.52	4.11	10.73	15.67	
1	5	2	5	78.59	3.38	13.50	9.56	
1	5	2	6	76.96	3.46	10.34		
1	5	3	1	77.48	3.19	10.38	9.55	0.981
1	5	3	2	80.65	3.51	10.32	13.53	0.998
1	5	3	3	73.92	4.36	17.00	10.82	
1	5	3	4	79.86	2.78	9.60	9.55	
1	5	3	5	79.17	3.40	10.80	10.94	
1	5	3	6	78.88	3.22	12.01		
1	6	1	1	75.10	3.45	13.46	15.44	0.976
1	6	1	2	78.98	3.62	13.97	6.84	0.995
1	6	1	3	79.14	3.39	11.89	7.79	
1	6	1	4	78.71	2.89	11.86	5.20	



**Table C.3.2 (continued)** Colour, firmness and water activity ( $a_w$ ) of fresh-cut pear, during storage period at refrigerated conditions

Exp	Day	Sample	Measure	Colour			Firmness (N)	$a_w$
				L*	a*	b*		
1	6	1	5	75.59	3.76	15.60	6.67	
1	6	1	6	79.05	3.10	13.73	4.92	
1	6	2	1	75.88	2.87	12.51	8.70	0.978
1	6	2	2	77.64	3.43	10.40	10.04	0.989
1	6	1	5	75.59	3.76	15.60	6.67	
1	6	1	6	79.05	3.10	13.73	4.92	
1	6	2	1	75.88	2.87	12.51	8.70	0.978
1	6	2	3	79.78	3.41	13.05	11.89	
1	6	2	4	80.01	3.12	6.58	13.05	
1	6	2	5	80.12	2.97	14.01	13.35	
1	6	2	6	77.92	3.69	13.92		
1	6	3	1	79.12	3.43	10.53	12.18	0.967
1	6	3	2	75.15	3.93	13.96	13.52	0.975
1	6	3	3	77.22	3.20	12.81	9.24	
1	6	3	4	75.74	4.91	18.30	11.79	
1	6	3	5	76.56	3.19	16.51	13.58	
1	6	3	6	77.59	2.81	10.37		
1	7	1	1	78.11	3.69	11.88	10.06	0.989
1	7	1	2	78.32	3.24	9.28	17.32	0.956
1	7	1	3	73.90	5.65	18.46	11.63	
1	7	1	4	79.86	3.30	12.65	14.74	
1	7	1	5	77.45	3.58	14.18	12.96	
1	7	1	6	79.51	3.42	11.98	7.32	
1	7	2	1	76.36	3.55	8.94	18.11	0.988
1	7	2	2	79.53	3.60	12.23	12.38	0.989
1	7	2	3	80.37	3.55	8.69	9.02	
1	7	2	4	75.24	4.76	16.45	11.43	
1	7	2	5	78.67	3.74	17.17	12.16	
1	7	2	6	76.78	3.32	13.26	9.55	
2	0	1	1	79.59	3.46	12.94	14.87	
2	0	1	2	77.95	2.85	10.38	10.75	0.999
2	0	1	3	74.32	4.4	13.5	6.93	0.999
2	0	1	4	74.79	3.27	12.73	6.71	
2	0	1	5	77.29	2.73	11.76	8.71	
2	0	1	6	76.41	4.13	12.94	5.95	
2	0	2	1	76.85	2.65	12.79		

**Table C.3.2 (continued)** Colour, firmness and water activity ( $a_w$ ) of fresh-cut pear, during storage period at refrigerated conditions

Exp	Day	Sample	Measure	Colour			Firmness (N)	$a_w$
				L*	a*	b*		
2	0	2	2	74.73	3.09	13.96	12.51	0.998
2	0	2	3	76.03	2.87	11.49	8.25	1.000
2	0	2	4	79.12	3.53	7.32	7.13	
2	0	2	5	76.54	4.06	14.95	8.65	
2	0	2	6	76.93	4.19	15.51	6.29	
2	0	3	1	73.39	3.99	12.55		
2	0	3	2	79.25	3.6	13.09	12.41	0.999
2	0	3	3	76.59	4.44	12.73	8.73	0.999
2	0	3	4	77.51	3.37	11.25	10.78	
2	0	3	5	78.33	3.49	14.32	8.66	
2	0	3	6	79.07	3.2	14.19	9.58	
2	1	1	1	75.32	3.21	12.04		
2	1	1	2	78.57	3.66	11.52	5.89	0.991
2	1	1	3	75.07	4.43	13.46	10.94	0.996
2	1	1	4	78.18	3.48	10.15	10.37	
2	1	1	5	79.81	3.2	9.1	8.00	
2	1	1	6	78.75	3.26	9.23	7.73	
2	1	2	1	80.01	3.42	8.45		
2	1	2	2	76.53	3.67	11.61	9.30	0.993
2	1	2	3	79.22	3.73	8.8	10.73	
2	1	2	4	78.43	4.5	14.75	9.11	
2	1	2	5	76.42	4.46	12.71	7.05	
2	1	2	6	80.27	3.88	9.71		
2	1	3	1	75.57	4.21	16.61	14.70	0.997
2	1	3	2	72.66	5.34	16.53	6.84	0.993
2	1	3	3	77.30	4.48	15.25	10.02	
2	1	3	4	70.15	5.2	21.43	10.93	
2	1	3	5	79.56	3.2	11.49	7.56	
2	1	3	6	67.65	7.75	23.26		
2	2	1	1	80.04	3.88	9.45	7.17	0.982
2	2	1	2	76.79	4.51	12.61	10.96	0.989
2	2	1	3	79.54	3.3	11.32	10.57	
2	2	1	4	80.03	3.93	9.59	11.85	
2	2	1	5	77.38	3.76	11.22	11.60	
2	2	1	6	77.34	3.59	12.26		
2	2	2	1	76.18	2.87	7.72	6.91	0.984

**Table C.3.2 (continued)** Colour, firmness and water activity ( $a_w$ ) of fresh-cut pear, during storage period at refrigerated conditions

Exp	Day	Sample	Measure	Colour			Firmness (N)	$a_w$
				L*	a*	b*		
2	0	2	2	74.73	3.09	13.96	12.51	0.998
2	0	2	3	76.03	2.87	11.49	8.25	1.000
2	0	2	4	79.12	3.53	7.32	7.13	
2	0	2	5	76.54	4.06	14.95	8.65	
2	0	2	6	76.93	4.19	15.51	6.29	
2	0	3	1	73.39	3.99	12.55		
2	0	3	2	79.25	3.6	13.09	12.41	0.999
2	0	3	3	76.59	4.44	12.73	8.73	0.999
2	0	3	4	77.51	3.37	11.25	10.78	
2	0	3	5	78.33	3.49	14.32	8.66	
2	0	3	6	79.07	3.2	14.19	9.58	
2	1	1	1	75.32	3.21	12.04		
2	1	1	2	78.57	3.66	11.52	5.89	0.991
2	1	1	3	75.07	4.43	13.46	10.94	0.996
2	1	1	4	78.18	3.48	10.15	10.37	
2	1	1	5	79.81	3.2	9.1	8.00	
2	1	1	6	78.75	3.26	9.23	7.73	
2	1	2	1	80.01	3.42	8.45		
2	1	2	2	76.53	3.67	11.61	9.30	0.993
2	1	2	3	79.22	3.73	8.8	10.73	
2	1	2	4	78.43	4.5	14.75	9.11	
2	1	2	5	76.42	4.46	12.71	7.05	
2	1	2	6	80.27	3.88	9.71		
2	1	3	1	75.57	4.21	16.61	14.70	0.997
2	1	3	2	72.66	5.34	16.53	6.84	0.993
2	1	3	3	77.30	4.48	15.25	10.02	
2	1	3	4	70.15	5.2	21.43	10.93	
2	1	3	5	79.56	3.2	11.49	7.56	
2	1	3	6	67.65	7.75	23.26		
2	2	1	1	80.04	3.88	9.45	7.17	0.982
2	2	1	2	76.79	4.51	12.61	10.96	0.989
2	2	1	3	79.54	3.3	11.32	10.57	
2	2	1	4	80.03	3.93	9.59	11.85	
2	2	1	5	77.38	3.76	11.22	11.60	
2	2	1	6	77.34	3.59	12.26		
2	2	2	1	76.18	2.87	7.72	6.91	0.984

**Table C.3.2 (continued)** Colour, firmness and water activity ( $a_w$ ) of fresh-cut pear, during storage period at refrigerated conditions

Exp	Day	Sample	Measure	Colour			Firmness (N)	$a_w$
				L*	a*	b*		
2	3	1	1	77.17	2.96	10.48	5.72	0.989
2	3	1	2	78.45	3.94	10.54	10.73	0.995
2	3	1	3	78.4	3.47	11.44	7.22	
2	3	1	4	78.42	3.18	11.82	7.64	
2	3	1	5	75.29	4.29	12.28	11.36	
2	3	1	6	76.00	2.78	12.14		
2	3	2	1	76.40	4.07	15.98	8.07	0.976
2	3	2	2	79.30	3.00	9.77	10.56	0.998
2	3	2	3	75.47	3.67	11.75	9.20	
2	3	2	4	77.76	4.44	15.1	11.59	
2	3	2	5	74.90	5.01	16.6	9.31	
2	3	2	6	79.83	3.84	10.25		
2	3	3	1	78.48	3.98	14.2	6.76	0.987
2	3	3	2	78.35	3.82	10.26	7.51	0.995
2	3	3	3	74.37	3.85	14.35	16.49	
2	3	3	4	75.36	4.06	14.26	10.47	
2	3	3	5	78.27	4.92	13.87	12.02	
2	3	3	6	78.34	3.84	12.84		
2	4	1	1	74.73	3.10	11.71	8.35	0.987
2	4	1	2	79.96	3.4	9.73	9.35	0.993
2	4	1	3	78.66	3.96	12.26	12.51	
2	4	1	4	78.85	3.64	11.51	4.59	
2	4	1	5	79.11	3.06	9.61	7.47	
2	4	1	6	78.56	4.004	11.54	10.67	
2	4	2	1	79.93	3.7	10.52	7.99	0.956
2	4	2	2	78.26	5.16	14.43	12.83	0.974
2	4	2	3	72.86	4.84	10.45	7.46	
2	4	2	4	77.26	3.52	9.92	13.42	
2	4	2	5	78.93	3.92	12.48	11.10	
2	4	2	6	78.29	4.92	15.92	7.24	
2	4	3	1	64.87	7.43	21.99	11.28	0.975
2	4	3	2	72.24	5.07	16.09	12.99	0.996
2	4	3	3	77.82	3.60	11.08	18.16	
2	4	3	4	77.68	4.65	14.68	11.58	
2	4	3	5	68.05	6.15	20.28	12.27	
2	4	3	6	77.24	4.21	15.03	7.83	

**Table C.3.2 (continued)** Colour, firmness and water activity ( $a_w$ ) of fresh-cut pear, during storage period at refrigerated conditions

Exp	Day	Sample	Measure	Colour			Firmness (N)	$a_w$
				L*	a*	b*		
2	7	1	1	81.35	3.76	10.17	12.68	0.991
2	7	1	2	78.91	3.93	11.96	10.84	0.990
2	7	1	3	79.66	4.07	11.16	9.06	
2	7	1	4	77.82	3.17	11.13	10.60	
2	7	1	5	76.01	4.05	15.11	10.33	
2	7	1	6	78.2	4.57	11.14		
2	7	2	1	78.4	4.47	11.18	11.54	0.957
2	7	2	2	78.62	3.86	10.45	12.76	0.979
2	7	2	3	69.11	5.4	16.15	11.93	
2	7	2	4	76.21	5.63	17.36	8.89	
2	7	2	5	74.53	3.56	11.81	8.33	
2	7	2	6	74.76	3.41	11.61		
2	7	3	1	77.45	4.48	13.98	13.92	0.979
2	7	3	2	76.67	4.84	17.87	13.43	0.980
2	7	3	3	74.97	5.90	15.14	11.58	
2	7	3	4	76.72	3.90	13.42	13.12	
2	7	3	5	79.38	3.60	12.27	9.55	
2	7	3	6	72.38	5.50	16.50		